THESIS

ASSESSMENT OF POTENTIAL IMPACTS OF CLIMATE CHANGE ON THE INTEGRITY AND MAINTENANCE COSTS OF SIMPLY SUPPORTED STEEL GIRDER BRIDGES IN THE UNITED STATES

Submitted by

Susan Mayumi Kock Palu

Department of Civil and Environmental Engineering

In partial fulfillment of the requirements

For the Degree of Master of Science

Colorado State University

Fort Collins, Colorado

Fall 2019

Master's Committee:

Advisor: Hussam Mahmoud

Rebecca Atadero
Bolivar Senior

ABSTRACT

ASSESSMENT OF POTENTIAL IMPACTS OF CLIMATE CHANGE
ON THE INTEGRITY AND MAINTENANCE COSTS
OF SIMPLY SUPPORTED STEEL GIRDER BRIDGES IN THE UNITED STATES

Bridges in America are aging and deteriorating, causing substantial financial strain on federal resources and taxpayers' money. Amid several deterioration issues affecting bridges one of the most common and costly is malfunction and deterioration of expansion joints, due to accumulation of road debris between joints, traffic, and weather. Clogged joints in particular prevent the superstructure from expanding when subject to a temperature increase, giving rise to thermal stresses that are not accounted for during the design phase. These additional demands, in the form of combined axial loads and moments, are expected to even worsen considering potential future changes in climate. Herein, a new framework is developed to assess structural vulnerability and estimate maintenance costs for approximately 80,000 simply supported steel girder bridges across the U.S. The approach aims to aid in establishing a priority order for bridge maintenance and offer insights on how to better allocate funds for a large inventory of bridges. The structural vulnerability is quantified in terms of the reduced capacity resulting from axial load and moment interaction on the girder-slab composite. The projected daily maximum temperatures for future years of 2040, 2060, 2080 and 2100 were processed from the coupled climate model GFDL CM3 under three climate scenarios: RCP 2.6, RCP 6.0 and RCP 8.5. The results showed that the most critical regions for all climate scenarios are: Northern Rockies & Plains, Northwest, Upper Midwest and West. In contrast, the less susceptible regions are the Southeast followed by the Northeast. In addition to vulnerability, life cycle cost analysis was conducted considering the evolution of structural condition of each asset along the years through the interaction equation.

The results showed that savings on the order of $4.5 billion could be attained when vulnerability-informed maintenance practice is followed as opposed to its conventional counterpart. It was observed that the climate scenario RCP 2.6, which represents greater efforts to reduce anthropogenic climate change, resulted in the smallest maintenance cost. Moderate efforts over emissions RCP 6.0 implies a $600 million increase, while no intervention under RCP 8.5 results in an additional $2 billion cost over the long term.

ACKNOWLEDGEMENTS

I am grateful to God for giving me life, and life to the full, faith, strength, perseverance, peace, joy and hope through his son Jesus Christ; and blessing me with so amazing people in my way, making my experiences much more meaningful and special.

I would like to thank Dr. Hussam Mahmoud for the opportunity of coursing the master program at CSU, the financial supporting through the unique experience as graduate research and teaching assistant, and the outstanding advising. I am thankful for all his support, teachings, and inspiring enthusiasm during my studies. I am grateful to my committee members Dr. Rebecca Atadero and Dr. Bolivar Senior for the valuable contribution to my research. I thank Mr. Akshat Chulahwat for sharing his talent and time in developing figures utilized in this work, most by his extraordinary hand drawings. Also, I thank Dr. Thomas Siller for the great opportunity to work as teaching assistant in his class during my master program; my thank also for the TA's Katherine Sitler and Sydney Doidge.

I am immensely grateful to Marcos, my wonderful husband for his love and care, unceasing support, for encouraging me always, patience and understanding and his immeasurable efforts to help me. I love you so much and my deepest thank to you!

I would like to thank our whole family in Brazil, specially my parents (and outstanding engineers) Luiza Kiyoko Fujita Kock and Carlos Alfredo Kock for their love and support all the time. I also thank my brothers Marcel Eiji Kock and Rafael Junji Kock, my great-aunt Tia Nina (*in memoriam*), and my parents-in-law Maria Ilda Palu and José Carlos Palu. Thank you so much for your constant care, support and patience during our absence, we missed you so much!

Thank you so much our friends Carol, Wade, Shanni, Cameron, and all the Pacheco family for their love, friendship and assistance. My sincerely thanks to Mr. Lee and LoraLee, Brenda and all the Carter family, Steve and Edie Eckles, Tim and Lorna Green, Randy and Jan Babcock, Mel and Bonnie Crane, Deborah Artzer and Will (*in memoriam*), Jeane Foster, John and Susan Morse, Phyllis and Dick Peterson (*in memoriam*), Sue Clark, Marcie Stewart, Pastor Bill and Priscilla Prather, Mr. Bill Prater (*in memoriam*), John and Diana Finley, Don and Fran Lambert, Jeff and Sandy Lindberg, Joe and Sandy Martinez, Jan and Carroll Morony, Betty and all the Moseley family, Bruce Nuttall, Rev. Kimberly Salico-Diehl, and Pastor Brad and Thea Jensen for all their support along our journey in U.S. and the amazing moments we spend together. I thank very much Lubna Al-Ani, Janeth and Chun-Yao for their friendship and all their help.

DEDICATION

To Marcos, my beloved husband

TABLE OF CONTENTS

LIST OF TABLES

LIST OF FIGURES

1. INTRODUCTION

1.1 Bridge Infrastructure in the U.S. and Management Challenges

The United States possess approximately 600,000 highway bridges to serve the extensive National Highway System as vital links to carry the main passenger traffic and freight of the country (FHWA, 2017). Figure 1.1 shows the distribution of every highway bridge in the U.S. It is not a surprise that bridge infrastructure in America is aging and deteriorating as result of traffic demand due to population growth and limitations in resources required for proper maintenance and rehabilitation. In addition, since weather is also a key factor that affects deterioration in bridges, current deterioration rates may be even exacerbated in the future due to changes in climate. According to the National Academy of Engineering (2018), urban infrastructure restoration and improvement is ranked among the greatest challenges for the Engineers of the 21st century.

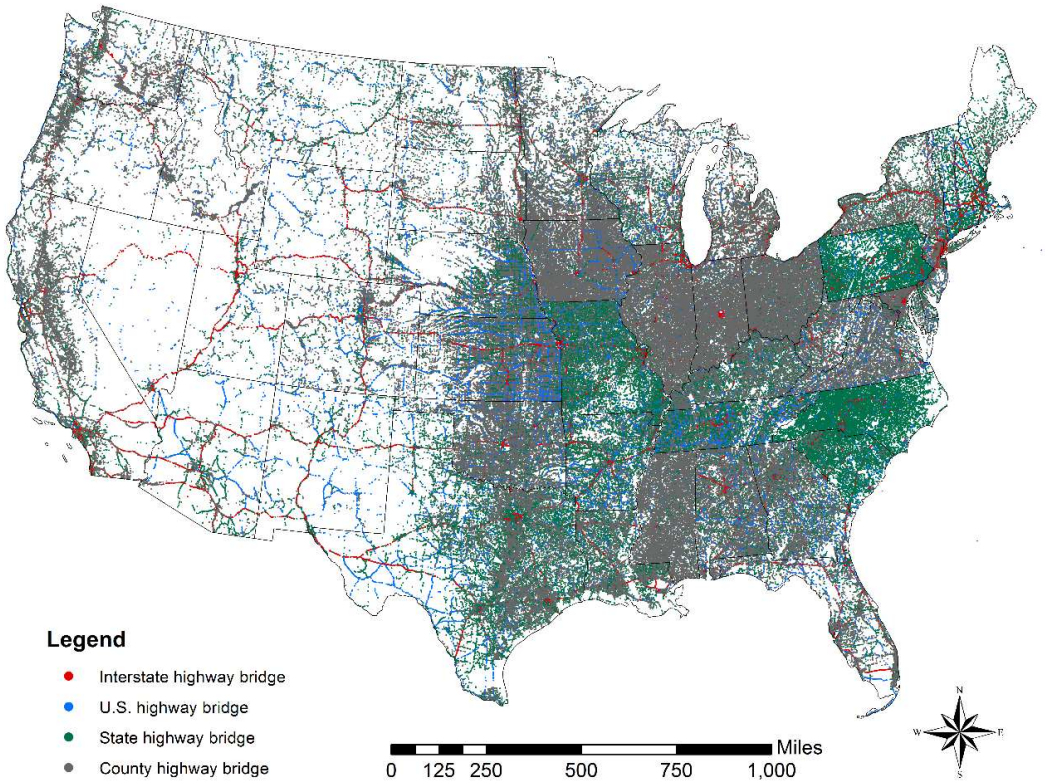

Figure 1.1 – Highways bridges in USA

The state of infrastructure in the U.S. is reported by the American Society of Civil Engineers (ASCE) every four years. In 2017, the bridge infrastructure in the U.S. received a grade C+ by the ASCE (2017a) as a reflection of their current condition. About 40% of the bridges are 50 years or older, some reaching or even exceeding their service life (FHWA, 2017). More than 50,000 bridges in America are identified as structurally deficient, implying that elements of the bridge structure were found in poor conditions due to deterioration or damage (FHWA, 2017; ASCE, 2017a). Despite the poor conditions of these bridges, there were approximately 188 million trips across them each day in 2016 (ASCE, 2017a). Furthermore, more than 80,000 bridges are classified as functionally obsolete, meaning that they do not attend the current engineering standards anymore to serve their intended purpose (e.g. narrow lanes or low load-carrying capacity for the present traffic demand) (FHWA, 2017; ASCE, 2017a). Figure 1.2 shows the amount of structurally deficient and functionally obsolete bridges for some main types of design. One can also note that the girder type, which consists of two or more longitudinal beams that span over the piers to support the superstructure weight and the traffic load, is by far the most common design type of bridges built in the U.S.

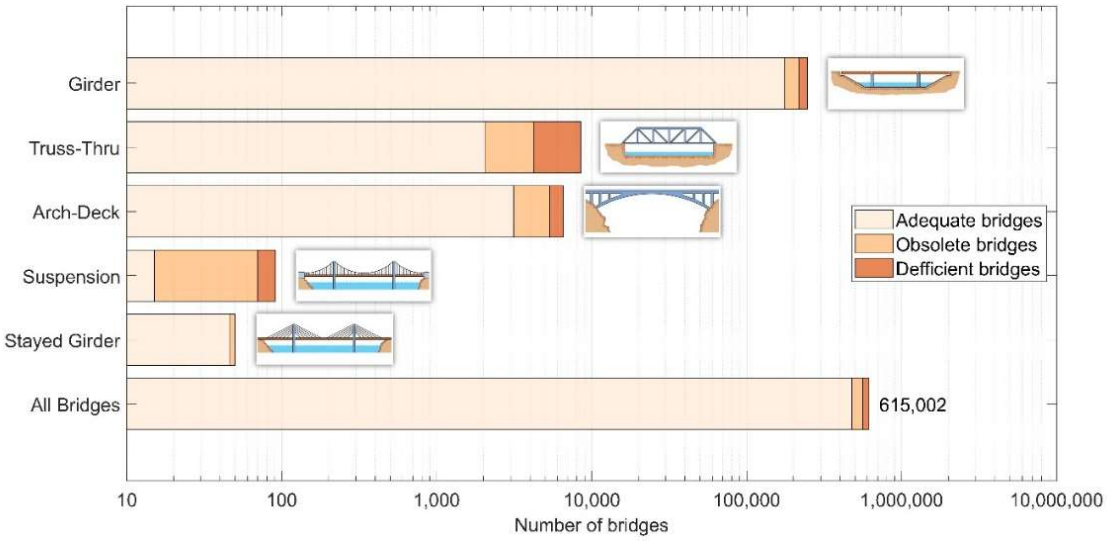

Figure 1.2 – Distribution of bridges built in USA by type of design

There are innumerous deterioration issues in bridges that require maintenance and rehabilitation. This included for example degradation of expansion joints and bearings, corrosion of steel (e.g. main girders), spalling and delamination of deck, degradation of piers, scour of foundation, to mention a few. If not properly addressed, those problems can affect the serviceability of the structure, or even escalate to a level that can compromise public safety. Therefore, considering the already established poor condition of many bridges, the several deterioration issues that develop especially with aging and the limitation of financial funds, it is crucial for transportation agencies implement strategic management plans that promote cost savings and the sustainability for long-term budgets, yet ensuring the serviceability and safety of the structures.

1.2 Adaption of Bridge Infrastructure and Engineering Practices to a Changing Climate

Engineering practices are usually based on the assumption of a stationary weather and climate. Nevertheless, the observation of unprecedent changes in climate has prompted infrastructure vulnerability (which is designed to remain functional and safe for long service lives) to climate change to be a topic of concern and debate among officials, researches and practitioners. Figure 1.3 shows extreme weather metrics for the U.S. in recent decades, including for instance the increase in the number of record high monthly temperatures (red).

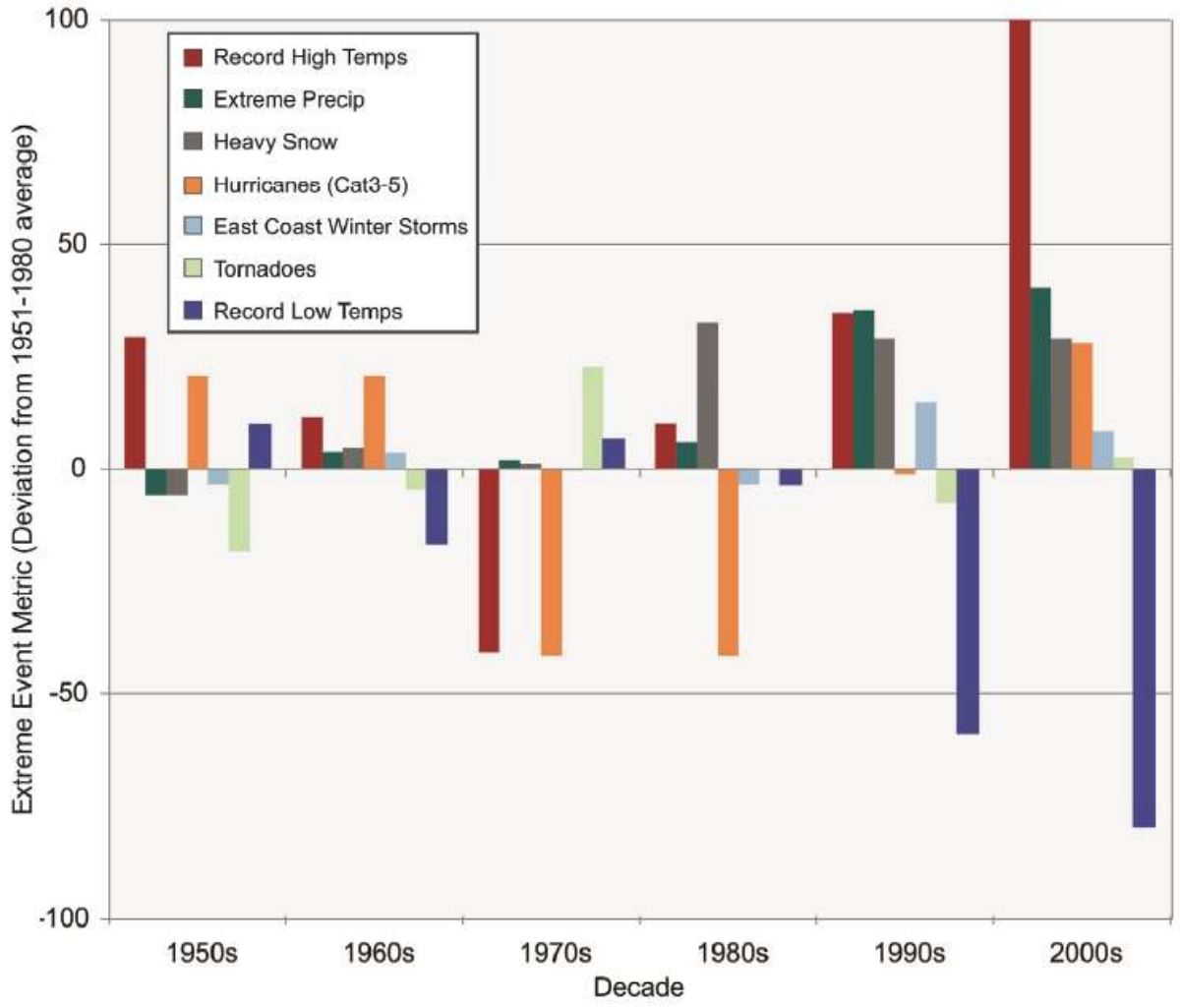

Figure 1.3 – Extreme weather metrics for the U.S. in recent decades, showing the number of record high monthly temperatures (red); the number of daily precipitation events exceeding the threshold for a 1-in-20 year recurrence (dark green); the sum of the number of top 50 snowstorms for the U.S. regions east of the Rocky Mountains (gray); the number of category 3, 4, or 5 hurricanes in the North Atlantic (orange); the number of strong East Coast winter storms (light blue); the number of tornadoes of EF1 intensity or higher (light green); and the number of record low monthly temperatures (dark blue) (Olsen, 2015).

This discussion has been informed by government agencies and research communities due the fact that changes in climate may require different maintenance and rehabilitation approaches for existing infrastructure as well as adaption of new engineering practices.

As an example, in 2011 the ASCE created a Committee on Adaption to a Changing Climate (CACC) to report technical requirements and challenges associated with infrastructure to a changing climate. Specifically with respect to transportation infrastructure, ASCE urged that an increase in the number of hot days may result in deterioration in roadways and expansion joints of bridges (Olsen, 2015). Figure 1.4 illustrates two different approaches to incorporate climate science into engineering practice and assess the vulnerability of a system to climate changes. According to ASCE (2015), the "top-down" technique uses the projections of Global Climate Models under certain emission scenarios which are downscaled to evaluate the effects on the system. On the contrary, in a "bottom-up", the thresholds for which the system fails are defined first, then climate data are applied to evaluate the acceptability of the threshold exceedance and develop the necessary design provisions.

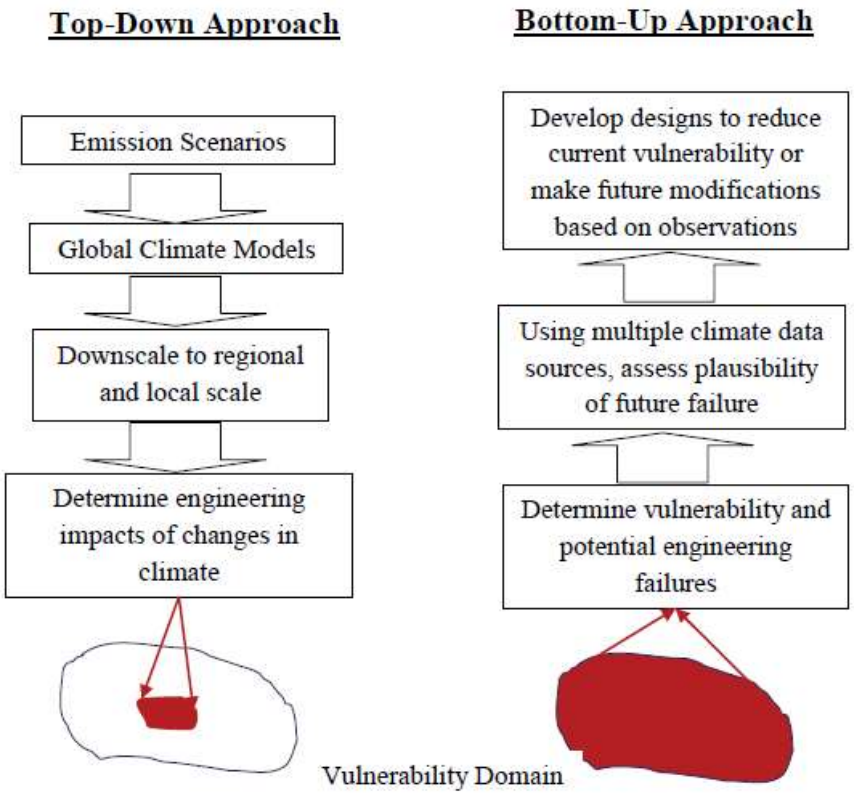

Figure 1.4 – Top-down and bottom-up approaches to climate change adaption (Olsen, 2015)

Likewise, the Federal Highway Administration published the Climate Change Adaption Guide for Transportation Systems Management, Operations, and Maintenance to aid departments of transportation (DOTs) to understand potential climate change risks and required actions to minimize them. For instance, FHWA draws attentions for bridges with joints, which may require earlier or different maintenance approaches (Asam et al., 2015). Moreover, the Transportation Research Board (TRB) issued the report "Potential Impacts of Climate Change on U.S. Transportation" with focus on the consequences of climate change on infrastructure and operations of U.S. transportation, highlighting that longer periods of extreme heat may affect the operation and increase maintenance costs of bridge with expansion joints (TRB, 2008).

Given the recent focus and interest of various federal agencies in understanding the effect of climate change on civil infrastructure, the overarching goal of this present study is to evaluate the effect of variability in temperature, in future years and throughout the U.S. main territory, on existing bridges in the country. A Global Climate Model (GCM), which mathematically represents the interactions between main climate system components – atmosphere, ocean, land surface and sea ice, in response to an anthropogenic forcing scenario, is utilized to obtain the projected temperatures. The anthropogenic forcing scenario is attributed to human activities and the consequent greenhouse gas concentrations. Herein, three distinct forcing scenarios, known as Representative Concentration Pathways (RPCs) are simulated. Each RCP is identified as a number correspondent to the change in radiative forcing at the tropopause by 2100 relative to preindustrial levels: 2.6 (lower forcing), 6.0 and 8.5 (higher forcing) Watts per square meter (W/m^2), leading to a distinct trend in global temperature (Olsen, 2015; Wuebbles et al., 2017).

1.3 Statement of the Problem

Amid several deterioration issues affecting bridges, one of the most common problem is clogging and deterioration of expansion joints due to road debris, and traffic and weather, respectively, requiring periodic maintenance and replacement. This problem becomes even more significant given the abundance of bridge deck joints throughout the country. The widespread adoption of simply supported spans (that utilize expansion joints at the superstructure discontinuities), a straightforward structural concept, facilitated the construction of a large quantity of bridges in the U.S. during the “Interstate Era”. Nevertheless, at that time, potential issues and costs associated with maintenance of deck joints were overlooked (Rager, 2016; Kelly, 2017). As a result, maintenance cost to keep expansion joints clean and functional has been a burden to the American transportation agencies (Rogers et al., 2012).

The main purpose of expansion joints is to allow for bridges to accommodate thermal movements. However, road debris readily build up into the joint and prevent the superstructure from expanding when subject to a temperature rise. As a result, thermal stresses not accounted for during the original design are induced into the structure. The consequences can be even worsened considering larger temperature amplitudes due to climate changes. Figure 1.5 shows what is typically known as major potential damages to structural elements of simply supported bridges due to the combined effect of temperature rise and malfunction of expansion joints. These include for example local buckling of the main steel girder flanges, spalling of concrete of the abutments, and cracking and crushing of the roadway deck, which could compromise the functionality and structural integrity of the bridge.

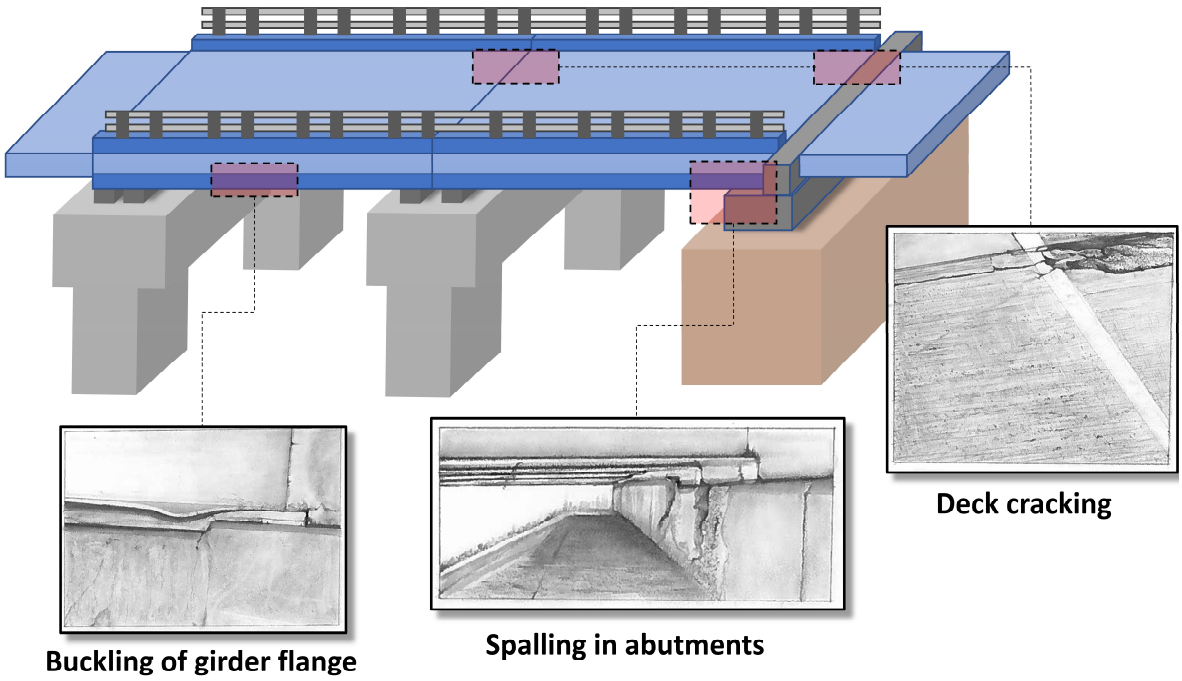

Figure 1.5 – Potential bridge damages caused by the combination of clogged joint condition and unpredicted thermal stresses

Another function of many types of expansion joints is to work as a barrier to protect structural elements and components located below the deck. However, as they are subjected to the action of traffic and weather, they deteriorate and leak, allowing debris, water and deicing chemicals to pass through, leading to the degradation of bearings, deck and beams ends, and pier caps. This is why frequent replacement of expansion joints is considered a necessity to avoid deterioration of bridges.

Herein, this study presents a new inventory-level approach for the assessment of potential impacts of climate change (including future years up to 2100) and malfunction of expansion joints on vulnerability as well as maintenance cost of approximately 80,000 U.S. simply supported steel girder bridges (hereinafter called SSSG bridges). The reason for choosing to examine SSSG bridges in this study is because besides the fact that girder bridges are the most abundant design type of bridges built in the U.S., more than half of them are structurally deficient, being mostly SSSG bridges.

Moreover, steel girder bridges deserves attention since from all bridges that failed between 1989 and 2000 in the U.S., they corresponded to about one-third of failures (Wardhana & Hadipriono, 2003).

Initially, a procedure to carry out a comprehensive data collection and process, related to bridges structural parameters and other pertinent information from the National Bridge Inventory (NBI), historical temperatures from National Oceanic and Atmospheric Administration (NOAA) database, and projected temperatures from GFDL CM3 climate model is presented. Next, an analytical method is proposed to quantify the vulnerability of each bridge for future years under three different climate scenarios referred as Representative Concentration Pathway (RCP) – RCP 2.6 (lower forcing scenario), 6.0 (moderate) and 8.5 (higher), with focus on the capacity of the steel girder-concrete slab composite, that is the main load carrying element of the superstructure. Further, a life cycle cost analysis is conducted, considering climate change scenarios and the respective effect on the structural condition of each bridge. The presented framework and the results obtained allow for the most critical bridges to be identified and for a priority order of bridge maintenance to be established. Ultimately this can result in cost savings and a better allocation of financial resources for feature years in which the bridges are in service. The proposed framework is schematically shown in Figure 1.6.

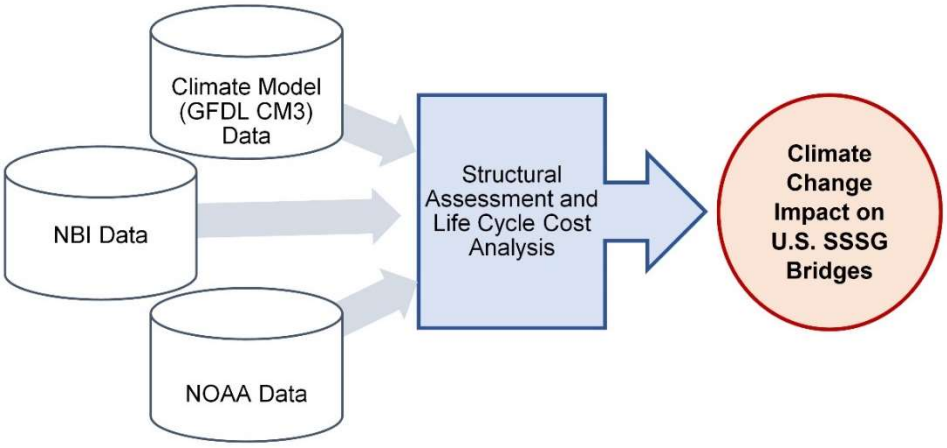

Figure 1.6 – Proposed inventory-level approach for the assessment of potential climate change impacts over U.S. SSSG bridges

1.4 Research Objectives and Tasks

The research aims to develop a framework to assess structural vulnerability and quantify maintenance cost over approximately 80,000 SSSG bridges in the U.S. over future years. Specifically, vulnerability of the main load carrying slab-girders composite is evaluated while considering the compound effects of malfunction of expansion joints and climate change. The overarching objective is to provide an overview of the most affected regions and states if no intervention is made and the benefits associated with conducting proper maintenance based on life cycle cost. Finally, this work purposes to contribute with insights for establishing a priority order of SSSG bridges maintenance and optimizing funds allocation. Figure 1.7 illustrates the principal steps of the proposed framework.

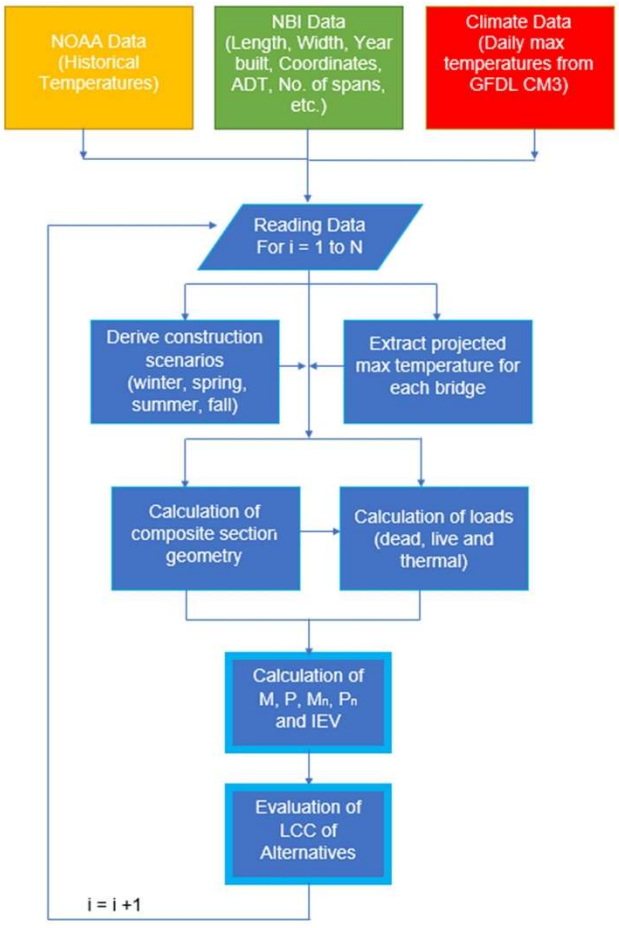

Figure 1.7 – Flow chart of principal process for structural and life cycle cost analysis of U.S. SSSG bridges

The main tasks to accomplish the objectives of the research are:

1) Task 1: Conduct comprehensive literature review.
2) Task 2: Collect pertinent U.S. bridge and temperature data.
    a) Data from the National Bridge Inventory (NBI) (FHWA, 2017): these data are related to the physical parameters of the bridge (e.g. length, width, number of spans) and other pertinent information (e.g. year built, coordinates, average daily traffic);
    b) Data from NOAA Regional Time Series (NOAA, 2018): these data comprise the seasonal historical temperatures for the nine U.S. climate regions (Northwest, Northern Plains and Rockies, Upper Midwest, Ohio Valley, Northeast, West, Southwest, South, and Southeast) recorded since 1895;
    c) Data from GFDL CM3 coupled climate model from NOAA Geophysical Fluid Dynamics Laboratory (GFDL, 2019): these data consists of the projected daily maximum temperature throughout the U.S. provided in blocks of 5 years: 2036-2040, 2056-2060, 2076-2080 and 2096-2100. The data of three different RCP's: 2.6, 6.0 and 8.5, are collected for each year.
3) Task 3: Process and analyze the collected data described in Task 2.
    a) Data from National Bridge Inventory (NBI):
        i. Investigate the main characteristics and obtain pertinent information of the entire U.S. bridges inventory and SSSG bridges;
        ii. Prepare data to be utilized as input for structural and economic assessment.
    b) Data from NOAA Regional Time Series (NOAA, 2018): develop construction temperature scenarios for each bridge;

c) Data from GFDL CM3 coupled climate model from NOAA Geophysical Fluid Dynamics Laboratory (GFDL, 2019): extract the projected daily maximum temperature for each bridge for 2040, 2060, 2080 and 2100, under three different RCP's: 2.6, 6.0 and 8.5 separately.

4) Task 4: Develop a framework to assess the structural vulnerability and the life cycle cost of SSSG bridges considering the effects of climate change and expansion restriction due to joint malfunction. The two subsets of the framework consist of:
    a) Analytical method to quantify the structural vulnerability in terms of the interaction equation, focusing on the load carrying capacity of the girder-slab composite;
    b) Analytical method to quantify the life cycle cost of SSSG bridges that accounts for the effects of climate change on the structural performance of the assets.
5) Task 5: Apply the proposed framework for approximately 80,000 U.S. SSSG bridges and analyze the results.
    a) Examine the influence of different construction temperature scenarios, type of debris materials and climate scenarios on the structural response of bridges;
    b) Conduct geographic analysis to illustrate the variability in the bridges' susceptibility to climate change among U.S. climate regions and states;
    c) Determine the life cycle cost for different maintenance alternatives;
    d) Compare maintenance alternatives and obtain the most cost-effective one;
    e) Quantify and compare the economic impact of different climate change scenarios for the most cost-effective alternative;
    f) Calculate the life cycle cost by state for the most cost-effective alternative.

2. LITERATURE REVIEW

2.1 Overview of U.S. Bridges Infrastructure

According to the National Academy of Engineering, urban infrastructure restoration and improvement is ranked among the greatest challenges for the Engineers of the 21st century (National Academy of Engineering, 2018). In order to keep track of the infrastructure condition in the U.S., every four years the ASCE evaluates sixteen fundamental infrastructure sectors such as energy, drinking water, schools, roads, dams, bridges, among others, and issues a report card, assigning a grade to each category based on the physical conditions and investments needed for improvement (ASCE, 2017a). In 2017, bridges in the U.S. received a grade C+ (ASCE, 2017a), as a reflection of their current condition. Undeniably, since the first report card was issued in 1998, the grade for U.S. bridges has been incrementally increasing but hovering around the C range for the last twenty years (ASCE, 2017b).

Right after a bridge is constructed (or rehabilitated), it is in good condition, providing the service for which it was designed. However, traffic load, weather, age and other factors act as deterioration agents, causing the level of service performance of the asset to fall. Periodic maintenance and rehabilitation will slow down deterioration while providing acceptable levels of service and safety. Another concept in transportation management to combat deterioration in a different manner is preservation. In contrast to traditional maintenance and rehabilitation activities that address existing deficiencies in bridges, preservation activities are conducted before deficiencies occur; thereby delaying the onset of deterioration. The economic effectiveness of extending the service life claimed by preservation can be compared with the traditional maintenance and rehabilitation practices by means of a life cycle cost analysis (FHWA, 2002).

Historically, since the collapse of the Silver Bridge over the Ohio River in December of 1967, which resulted in 46 casualties, more attention has been given to establishing sound procedures for inspection and management of U.S. bridges (Dunker & Rabbat, 1993; Lichtenstein, 1993). The Silver Bridge, structurally conceived as suspension type, was constructed in 1928 to link the cities of Point Pleasant, West Virginia and Gallipolis, Ohio. The collapse, that occurred during the rush hour, was attributed to a failure of a structural element and in part due to poor inspection (Dunker & Rabbat, 1993; Lichtenstein, 1993). As a consequence of this catastrophe, the Federal-Aid Highway Act of 1968 created the National Bridge Inspection Program and established a unified bridge proper safety inspection standard (FHWA, 2018b; Mahmoud, 2017). Despite such effort, in 1983 the Mianus River Bridge in Greenwich, Connecticut, collapsed due to insufficient maintenance, causing three fatalities and resulting in more stringent regulations regarding inspections and safety of bridges (Mahmoud, 2017). In 1987, another bridge failure occurred, this time linked to deteriorated substructure. The Schoharie Creek Bridge in NY collapsed due to scour of its foundation. After that catastrophe, states introduced under water inspection by scuba divers. If a diver detects damage, a cofferdam must be built to conduct the necessary repairs (Dunker & Rabbat, 1993).

Since 1968, the Federal Highway Administration (FHWA) has developed and maintained the National Bridge Inventory (NBI) – a substantial database that currently contains comprehensive information of every bridge longer than 6 m (20 feet) on all public roads. The inventory is annually updated with the aim of guaranteeing public safety through identification and evaluation of bridge deficiencies (FHWA, 2018b). According to the 2017 NBI (FHWA, 2017), the United States possess 615,002 highway bridges. These bridges are part of the National Highway System comprising of 76,564 km (47,575 miles) of Interstate Highways plus 289,119 km (179,650 miles) of major roads, which carries most of the highway passenger traffic and freight in U.S. (ARTBA, 2018).

The 2017 NBI shows that four in ten bridges are 50 years or older, reaching or even exceeding their service life with the average age of bridges in America being 45 years old (FHWA, 2017). In addition, in 2017 it was noted that 54,560 bridges in U.S. were characterized as being structurally deficient (FHWA, 2017) where 'deficient' implies that elements of the bridge structure were found in poor conditions due to deterioration or damage (ASCE, 2017a). Despite the poor conditions of these bridges, there were approximately 188 million trips across them each day in 2016 (ASCE, 2017a).

Bridges lose their functionality, also defined as their ability to serve their intended purpose, with aging. In the U.S., 14% of bridges were considered functionally obsolete in 2017 (FHWA, 2017). This reduction in functionality is defined for example on the basis of having narrow lanes or low load-carrying capacity for the present traffic demand. Consequently, they do not attend the current engineering standards anymore (ASCE, 2017a).

In the past years, the U.S. government has prioritized repairs of bridges throughout the country. The investment was boosted from $11.5 billion in 2006 to $18 billion in 2009 and 2010. In 2012, the amount spent was approximately $17.5 billion. While the spending is considered substantial, it is still insufficient. The most recent federal estimate of the required funds for rehabilitation projects for the nation's bridges is approximately $123 billion (ASCE, 2017a).

Undoubtedly the estimated spending is required to address a host of deterioration issues, especially in the case of older bridges. Deterioration in bridges includes: clogging of expansion joints with road debris that prevents thermal movements; corrosion and degradation of structural elements (e.g. main girders, pier caps) and components such as bearings due to improper drainage or leakage through damaged expansion joints; scour of foundations caused by water flow; deck deterioration and spalling due to standing water and deicers; decay or misalignment of bearings; cracks in bases due to uneven settling of foundation among others (Dunker & Rabbat, 1993). It is important to note that the effect of these listed problems on bridge performance will vary in terms of their level of impact.

For example, localized spalling over a bridge may cause discomfort to the user and damage to vehicles, generalized deck deterioration is expected to cause traffic delay, while large scour could threaten the integrity of the structure.

A study conducted by Wardhana and Hadipriono (2003) collected 503 cases of bridge failures in the U.S. from 1989 to 2000, in which 97% resulted in collapse (partial or complete) and 3% in distress (unserviceability that may or may not result in a collapse). Among the possible causes for such failures – design, detailing, construction, maintenance, use of materials and external events; improper maintenance was identified as the main cause for the distress cases and the second major cause for the collapses, being enlisted only behind the external events such as floods and scours.

Despite the limited funds available, neither proper assessment and inspection of structural elements and components of bridge infrastructure can be overlooked nor deteriorated problems be postponed. Therefore, it is even more essential to devise maintenance, operation and management strategies that minimize costs and maximize benefits of infrastructure in the future, while focusing on system preservation in the context of life cycle cost analysis (ASCE, 2014).

2.2 Deterioration of Bridges with Expansion Joints

2.2.1 Simply Supported Bridges

The present study focuses on issues regarding expansion joints in bridges. This is because even though innumerable components of the bridges throughout the country require maintenance or replacement, the deterioration of bridge deck expansion joints is one of the most common issues (Carroll Chris & Juneau Andrew, 2015; Rager, 2016; Kelly, 2017). Since they are integral components of a bridge, their malfunction can affect the serviceability of the structure (Wells et al., 2017; AASHTO, 2012; Chen & Duan, 2000; Dunker & Rabbat, 1993).

This problem becomes even more significant considering the abundance of deck joints bridges in the country.

Such frequency is the result of the widespread adoption of simply supported spans design type, which facilitated the construction of a large quantity of roadways in the U.S. after the 1956 Federal-Aid Highway Act. Nevertheless, at that time, potential issues and costs associated with maintenance of deck joints were unnoticed (Rager, 2016; Kelly, 2017). As a result, maintenance costs to keep expansion joints clean and functional have been a burden to transportation agencies (Rogers et al., 2012).

Simply supported bridges are classified in the NBI according to their design type and the material of the main elements of the superstructure. Herein, we evaluate approximately 80,000 simply supported steel girder (SSSG) bridges. The reason for choosing this particular class of bridges is because the design type “Girder” is the most recurrent among all the highway bridges built in the U.S. (approximately 40% of the total bridges) (FHWA, 2017). Furthermore, the girder design type presents the largest number of functionally obsolete and structurally deficient bridges (about 53%) identified in the country and most of them are steel girders (FHWA, 2017). In addition, it is important highlight that the three dominant material/design type of bridges that failed from 1989 to 2000 in U.S. were: steel girder (29% of failures), steel truss (21%) and concrete girder (6%) (Wardhana & Hadipriono, 2003).

2.2.2 Expansion Joints Systems

Expansion joint systems are integral components of a bridge that function to accommodate cyclic movements, without imposing significant secondary stresses on the superstructure (Chen & Duan, 2000). Moreover, bridge deck expansion joints consist of structural discontinuities between two elements, designed to allow movements (translation and rotation) of the deck and also the superstructure, at the joint, imposed by thermal changes, live loads and physical properties of materials (AASHTO, 2012; Wells et al., 2017).

There are two bridge deck joint systems: open or closed. Open joint systems allow for water and roadway debris to pass through the joint toward structural elements below the deck.

This system provides an economical solution; however, it is important to emphasize that AASHTO prescribes that “open joints should not be used where deicing chemicals are applied” (AASHTO, 2012). In the contrary, closed joint systems are sealed, and thus act as a barrier of protection to elements bellow the deck. In addition, expansion joints must provide a smooth ride for drivers (Chen & Duan, 2000; Wells et al., 2017).

Expansion joint systems are also classified based on the total movement range they need to accommodate - small, medium and large. Small movement range comprises of systems that allows for total movement up to approximately 45 mm. Some examples are sliding plates, compression seals, asphaltic plug and poured sealant joints. Medium movement range considers motion around 45 mm to 130 mm. Instances of medium movement range joints are strip seal and finger joints. Large movement range includes those that exceed approximately 130 mm. Modular joints belongs to this last category (Chen & Duan, 2000). Figure 2.1 illustrates some types of expansion joints.

The selection of the type of expansion joint will depend on a series of factors such as the magnitude and direction of the movement, type of structure, volumes of traffic, climatic conditions, skew angles, initial and life cycle cost analysis (Chen & Duan, 2000).

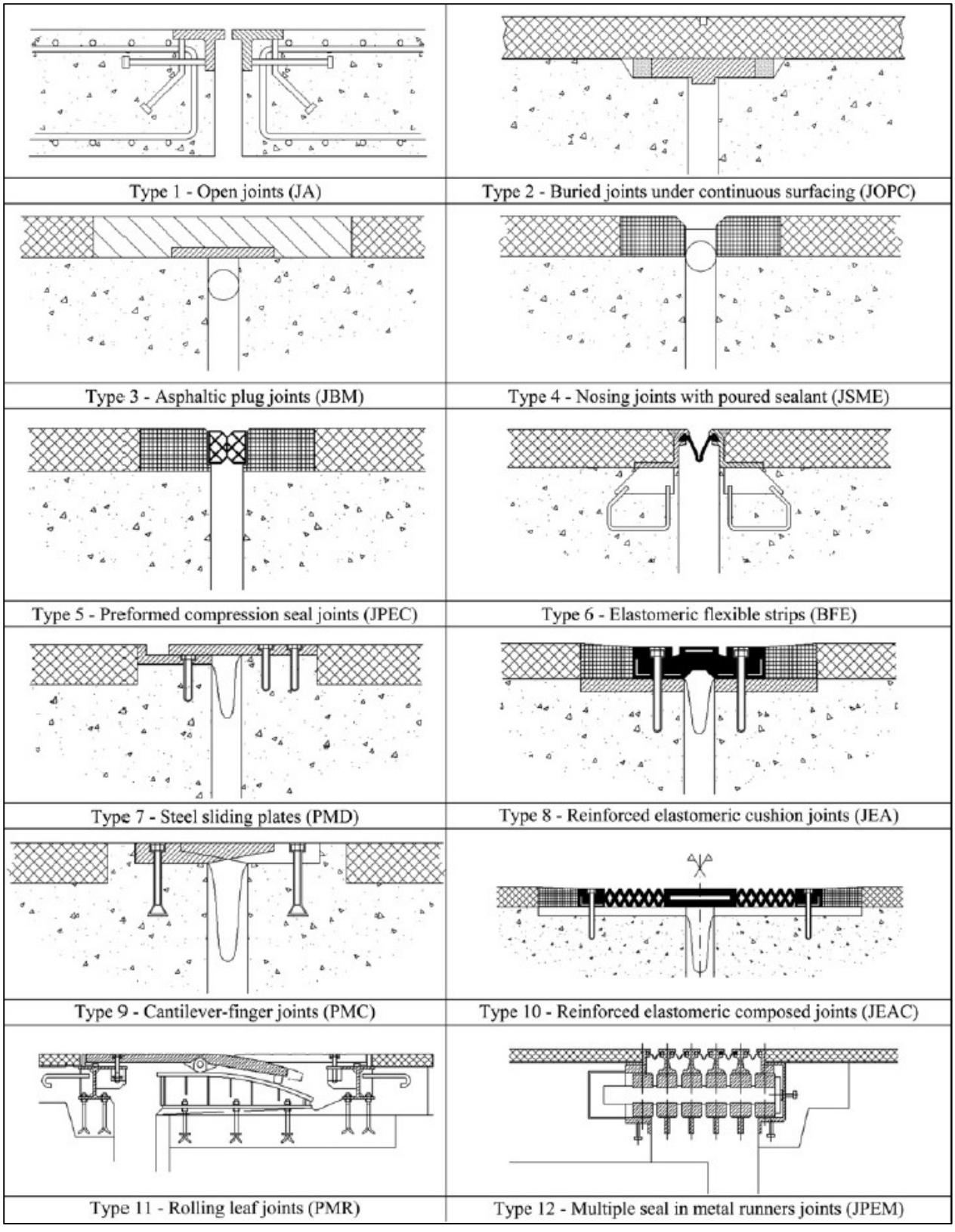

Figure 2.1 – Types of joints (Marques Lima & de Brito, 2009)

The design of expansion joints must consider movements generated by thermal variations, concrete shrinkage and creep, postensioning shortening, live and dead loads, wind and seismic loads, and structure settlements. Generally, thermal variations, concrete shrinkage and postensioning shortening (in the case of prestressed concrete) are explicitly accounted in the calculations. According to the AASHTO (2012), "If these movement are restrained, large horizontal forces may result". The thermal movement variation ΔL, which is the focus of this study, is calculated according to equation (2.1) (Chen & Duan, 2000).

$$\Delta L = \alpha L_o \Delta T \tag{2.1}$$

Where α is the coefficient of thermal expansion of the material; L_o is the original length of the structural element subject to thermal variation, and ΔT is the temperature variation. According to AASHTO, the temperature variation should be considered as the difference between the extreme maximum and minimum temperatures on the bridge (AASHTO, 2012).

The design and detailing of expansion joints also need to account for the impact of traffic load, effects of snowplow, avoidance of excessive noise and vibration, and accumulation of debris (AASHTO, 2012; Chen & Duan, 2000).

2.2.3 Drawbacks of Expansion Joints

Despite being small components, if expansion joints do not perform properly they can affect major structural elements of a bridge (Wells et al., 2017). Depending on the level of damage, the impact on bridge performance will range from driving discomfort or damage to vehicles, to traffic delays or bridge closures, and ultimately if not addressed appropriately, it can compromise safety of the bridge and the public.

Expansion joints easily become clogged with road debris. Figure 2.2 shows an image of an expansion joint clogged by gravel, dirt and other materials. If not cleaned periodically the expansion joints will not function as intended.

The impediment of thermal expansion of the superstructure will induce additional stress into the structural elements not accounted for in the original design. According to Chen (2008), this picture was taken before the bridge has completed 6 months of service.

Figure 2.2 – Debris in expansion joint (Chen, 2008)

Figure 2.3 shows another picture of this problematic widespread issue compromising the function of a finger joint of a bridge in Colorado. When the joint is not able to accommodate thermal movements, the deck, other elements of the bridge and the joint itself become overstressed (Wells et al., 2017).

Figure 2.3 – Finger joint clogged by debris on bridge B-16-FM (Rager, 2016)

If maintenance is not conducted, the accumulation of debris in expansion joints can cause pavement growth (Rager, 2016). According to the Michigan Department of Transportation (MDOT) pavement growth can results in calamitous damage to bridge components as guard rail concrete crushing, buckling of the main girder flanges, spalling of concrete of the abutments, crushing of deck concrete, among others (Rogers et al., 2012). The severity of the damage and consequently the time and cost to fix it will depend on how clogged the joints are and other factors as well such as temperature variation and volume of traffic. Moreover, those effects can be even exacerbated considering a potential climate warming in future (Olsen, 2015). Figure 2.4 illustrates the mechanism of pavement growth (Rogers et al., 2012).

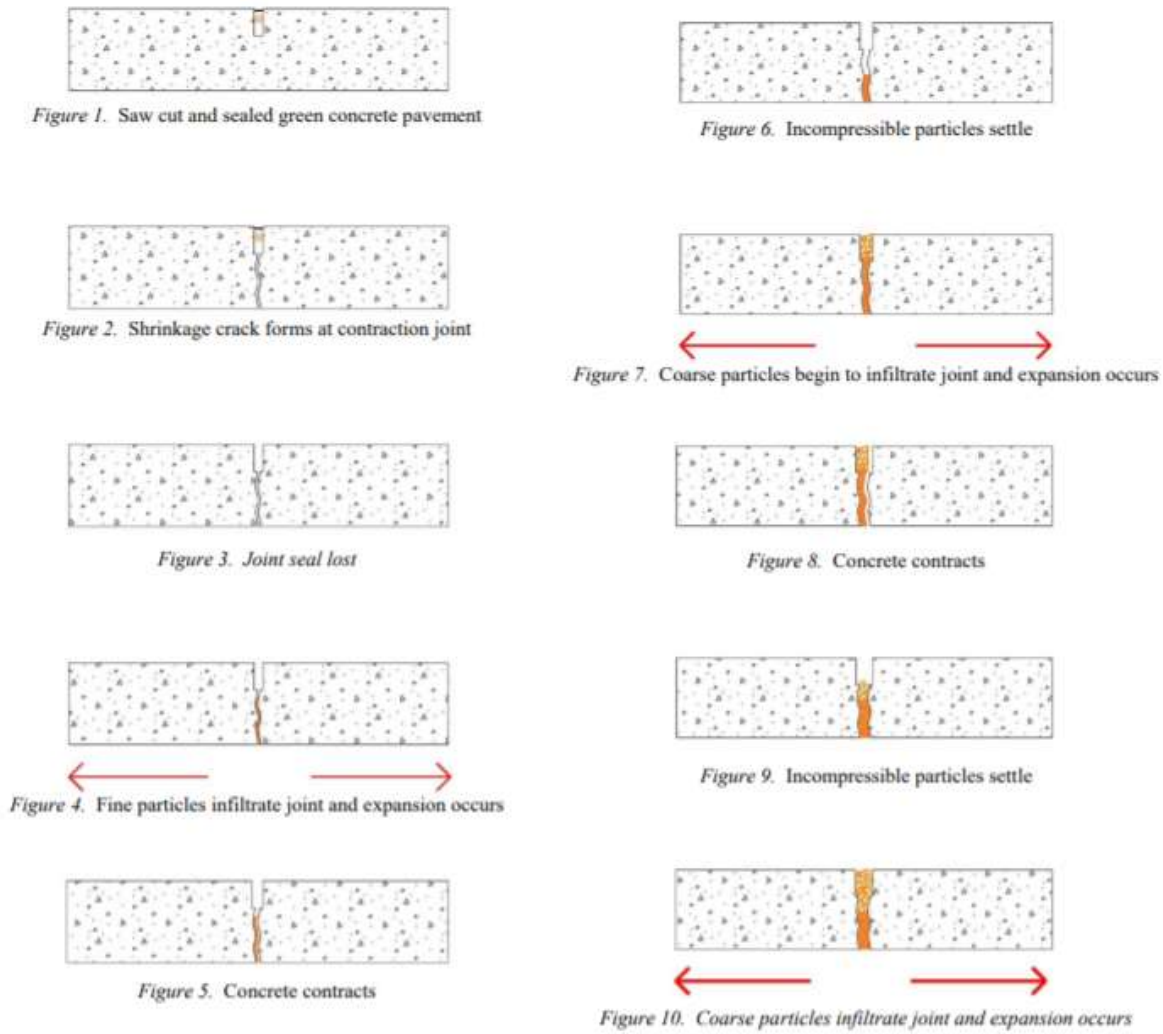

Figure 2.4 – Cycles of pavement growth mechanism (Rogers et al., 2012)

With temperature rise, the joint tends to close. However, since the joint is filled with debris, the superstructure of the bridge cannot freely expand as expected, inducing unpredicted thermal stresses into the structure. In contrast, when temperature drops, the superstructure contracts, incrementing the size of the joint gap. As the joint becomes wider, the debris, including incompressible materials, settle into the joint allowing for more debris fill up the joint. As a result, the joint is not able to close any further than this. When temperature rises again, there will be even more restriction to the expansion of the superstructure as the joint becomes more clogged with incompressible particles, increasing the thermal stresses. And the cycle repeats, every time the temperature decreases the joint gap enlarges allowing for the entrance of additional fine and coarser incompressible materials (Rogers et al., 2012).

Another concern is related to leakage of damaged and deteriorated expansion joints, that allows for debris, water and deicing chemicals to infiltrate underneath the bridge deck. Debris accumulates on top of piers caps around bearings and facilitates the retention of moisture and deicing chemicals, which can lead to significant degradation of bearings, deck and beam ends, pier caps and abutment seats as shown in Figure 2.5 (Wells et al., 2017). According to AASHTO "the failure of bridge bearings or joint seals may ultimately lead to deterioration or damage to the bridge."(AASHTO, 2012)

a **b**

Figure 2.5 – Corrosion of a) rocker bearing (Wells et al., 2017) and b) steel girders end (CTT, 2017)

If a bearing or sliding surfaces corrode as illustrate in Figure 2.5 a, the bearing can lock up and a member damage or failure can occur (Wells et al., 2017). Moreover, corroded structural members such as the girders of Figure 2.5 b have their load-carrying capacity reduced and become more susceptible to heavy traffic. Once the structure has started to deteriorate, the process of decay rushes (Dunker & Rabbat, 1993). The deterioration of bridge deck, bearing and substructure elements in extreme circumstances has resulted in premature, catastrophic failure (Chen & Duan, 2000). Deterioration of bridge components was the essential cause of 43 bridges failures between 1989 and 2000 (Wardhana & Hadipriono, 2003). Therefore, periodic and effective maintenance is vital to ensure the integrity of the bridges.

Herein, the vulnerability of the U.S. SSSG bridges subjected to temperature rise while joints are clogged is quantified in terms of the interaction equation. The interaction equation accounts for the demand-to-capacity ratio under axial loading and bending moment and it has long been recognized as a design limit state for main load carrying elements (Salmon & Johnson, 1996; AISC, 2017). As such, to ensure adequate structural performance of the bridge superstructure, this ratio should not exceed unity. The abovementioned axial loading component, not considered in the original design since a simply supported bridge is expected to resist to bending moment only, refers to the induced thermal load in response to the restriction to the superstructure expansion.

2.3 Climate Change

2.3.1 Climate Change and Engineering Practices

Engineering practices and standards are normally based on the assumption of stationary climate and weather, which is not an effective assumption in an era of climate change. The evident changes in climate have caused substantial impact on infrastructure (Underwood et al., 2017) and it is expected to further become even more vulnerable (Chinowsky et al., 2017; Peduzzi, 2017).

Thus, planning, designing, constructing, operating and maintaining the infrastructure should accommodate these changes (TRB, 2008). Therefore, better understanding of changes in climate, especially with respect to the respective magnitude, location and timing, which accounting for uncertainties, is fundamental to anticipate the potential impacts in infrastructure.

In 2011 the ASCE created a committee on Adaption to a Changing Climate (CACC) to "identify and communicate the technical requirements and civil engineering challenges for adaptation to climate change". In order to evaluate climate change effects on the safety, health and welfare of the public related to the use of civil infrastructure, the committee may establish recommendations for standards, loading criteria, evaluation and design procedures, research and monitoring needs for vital links of the U.S. infrastructure such as transportation, buildings, dams, energy generation, among others. The CACC draws attention to the transportation system, since changes in climate may affect its safety and operation. Very hot days can lead to rail track deformations, and increase in the number of hot days may cause deterioration in roadways and bridge expansion joints (ASCE, 2019; Olsen, 2015).

Similarly, the Federal Highway Administration issued the Climate Change Adaption Guide for Transportation Systems Management, Operations, and Maintenance (Asam et al., 2015) to assist departments of transportation (DOTs) and other transportation agencies to understand potential climate change risks and respective actions to reduce them. For instance, the report signalizes "determining future maintenance needs" of bridges with joints as an area of decision sensitive to climate change since those structures are chokepoints vulnerable to damage due to temperature. If changing in climate occurs, they may require earlier or different maintenance approaches. Another area of decision affected by climate change is budgeting for maintenance. The FHWA highlights that future change in climate may require resource allocations and budget planning other than todays' approach (Asam et al., 2015).

In the same way, the Transportation Research Board (TRB) released the report “Potential Impacts of Climate Change on U.S. Transportation” mainly focusing on the consequences of climate change on infrastructure and operations of U.S. transportation (TRB, 2008). Amid various risks to land, marine and air transportation modes, the report points out that longer periods of extreme heat “may cause thermal expansion of bridge joints, adversely affecting bridge operation and increasing maintenance costs”. The study emphasizes that current decisions taken considering potential effects of climate change can result in a more resilient performance of the transportation system and avoid higher investment in the future (TRB, 2008).

2.3.2 Global Climate Change and Drivers

Weather is defined as “the state of the atmosphere with respect to wind, temperature, cloudiness, moisture, pressure, etc.” (Olsen, 2015). This concept is related to short-term variations, on the order of minutes to around 15 days. On the other hand, climate, “is usually defined as the average weather, or more rigorously, as the statistical description in terms of the mean and variability of relevant quantities over a period of time ranging from months to thousands or millions of years” (Olsen, 2015).

Global climate change occurs when variations can be observed at global scale and continues over decades, generally at least 30 years. The Intergovernmental Panel on Climate Change (IPCC) concludes that “Warming of the climate system is unequivocal, and since the 1950s, many of the observed changes are unprecedented over decades to millennia.
The atmosphere and ocean have warmed, the amounts of snow and ice have diminished, sea level has risen, and the concentrations of greenhouse gases have increased.” (Olsen, 2015)

In addition, the IPCC in its Fifth Assessment Report (AR5) implies that human expansion of Earth’s natural greenhouse effect is extremely likely to has been the dominant cause of global warming trend.

Greenhouse gases, that naturally exists in atmosphere and trap part of the heat radiation from Earth toward space supporting life in the planet, have been increased by human activities since pre-industrial era due to economic and population growth (IPCC, 2014; NASA, 2019; Wuebbles et al., 2017). According to the Climate Science Special Report (Wuebbles et al., 2017) drivers of climate change over the industrial era comprise of both, natural and anthropogenic origin, yet a lesser degree of contribution is attributed to natural types. The substantial natural drivers are changes in solar irradiance, volcanic eruptions and El Nino-Southern Oscillation. Other minor contributors are natural emissions and sinks of greenhouse gases and tropospheric aerosols, effects of cosmic rays on cloud formation, changes in Earth's orbit, and variations in atmospheric CO_2 via chemical weathering of rock (Wuebbles et al., 2017).

Anthropogenic global climate change is referred to persistent variations observed at global scale attributed to human activities (Olsen, 2015). Well-mixed greenhouse gases (WMGHGs) as carbon dioxide (CO_2), methane (CH_4) and nitrous oxide (N_2O); short-lived climate forcers (SLCFs) which comprises of methane, some hydrofluorocarbons (HFCs), ozone and aerosols; contrails; and changes in albedo (land-use changes for instance) are examples of the main anthropogenic drivers in industrial era (Wuebbles et al., 2017). The contribution of natural and anthropogenic drivers for climate change over the industrial era is illustrated in Figure 2.6.

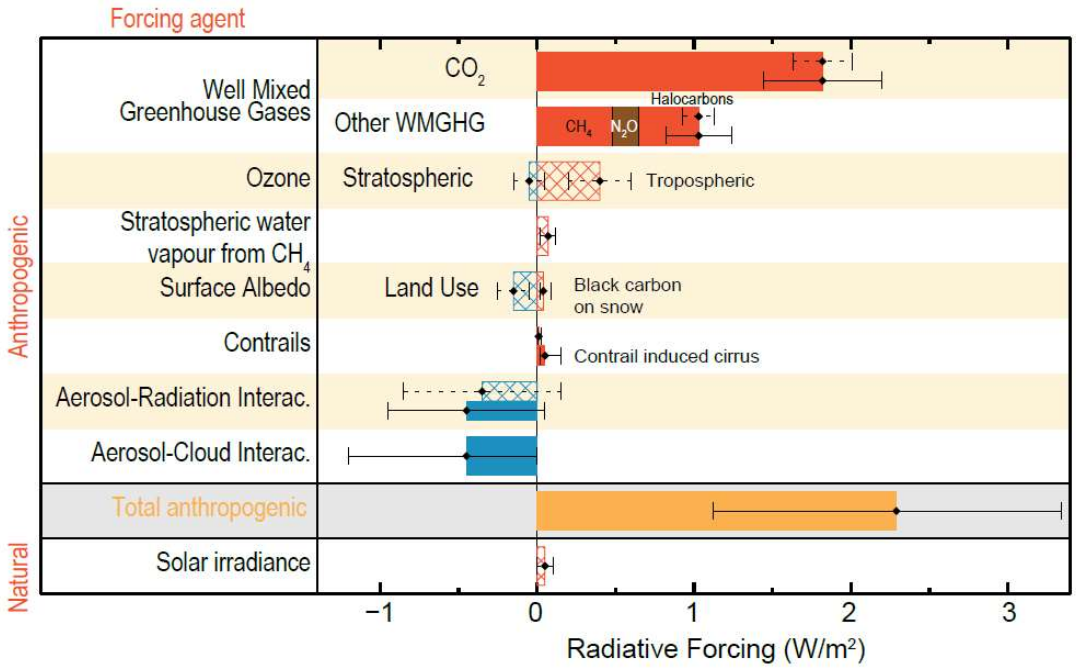

Figure 2.6 – Radiative forcing (RF; hatched) and effective radiative forcing (ERF; solid) in W/m² for the period 1750-2011. Uncertainties (5% to 95% confidence range) are given in dashed lines for RF and in solid lines for ERF (Wuebbles et al., 2017)

Some gases in the atmosphere prevent heat from escaping. “Long-lived gases that remain semi-permanently in the atmosphere and do not respond physically or chemically to changes in temperature are described as forcing climate change.” In contrast, those gases that responds are called “feedbacks” (e.g. water vapor) (NASA, 2019).

2.3.3 Climate Models and Scenarios

Climate Models are central tools to enhance the understanding and projectability of climate behavior on seasonal, annual, decadal and centennial time scales (NOAA, 2019). They involve scientific knowledge of a variety of disciplines as atmospheric sciences, oceanography, hydrology and others (Olsen, 2015). The two main classes of climate models are Global Climate Models (GCMs) and Earth System Models (ESMs). GCMs are mathematical representations of the interactions between principal climate system components: atmosphere, ocean, land surface and sea ice, in response to anthropogenic forcing.

These numerical models consider the Earth's energy balance between those four components to solve equations of thermodynamics and fluid mechanics for temperature and other variables of interests including pressure, winds, humidity, among others. (NOAA, 2019; Olsen, 2015).

ESMs have the same characteristics of GCMs and also accounts for carbon cycle and other chemical and biological cycles that influence the greenhouse gases concentrations in the atmosphere. Since ESMs are much newer and the assessment of their outputs have not been entirely consolidated, GCMs are usually utilized to assess climate impacts (Olsen, 2015).

GCMs has been evolved over the last 60 years with the inclusion of physical, chemical, biological and biogeochemical parameters in the numerical simulations. The combination of such climate system components can augment or diminish the effect of human emissions on the climate system. Thus, the response to external forcing, or climate sensitivity, depends on the extension of the components incorporated to the model (Wuebbles et al., 2017).

Climate models utilize three-dimensional grid of cells representing geographic locations (latitude and longitude) and elevations. The resolution of the model is defined by the size of the cells. The smaller the size of the cells, the higher the resolution. Moreover, the temporal resolution denotes the time steps adopted in the model. For spatial and temporal resolutions, the adoption of smaller resolution leads to more refined results, however, it is computationally more time-consuming (NOAA, 2019).

The most recent climate scenarios set by the IPCC to serve as inputs for global climate simulations are based on greenhouse gas concentration pathways (time-dependent values in the future). Defined as Representative Concentration Pathways (RPCs), they are radiative forcing scenarios. Each RCP is identified as a number correspondent to the change in radiative forcing at the tropopause by 2100 relative to preindustrial levels: 2.6, 4.5, 6.0 and 8.5 Watts per square meter (W/m^2) (Olsen, 2015; Wuebbles et al., 2017).

2.3.4 *Projections, Uncertainties and Probabilities of Future Climate*

A climate projection is generally founded on the outputs (e.g. temperature) of a single GCM with a particular configuration and forced by one scenario and it is expected to reproduce one possible future (Olsen, 2015).

According to Wuebbles et al. (2017), the uncertainty related to timing and magnitude of projected future climate change results from three components: 1) scientific uncertainty (limitations in the ability to model and understand the Earth's climate system), 2) scenario uncertainty (related to human activity) and 3) internal variability (variations in climate resulted from natural causes).

In Figure 2.7 one can observe that for short-term projection, the combination of scientific uncertainty and internal variability is the main contributor to uncertainty; though, as time progresses, the scenario uncertainty becomes more pronounced.

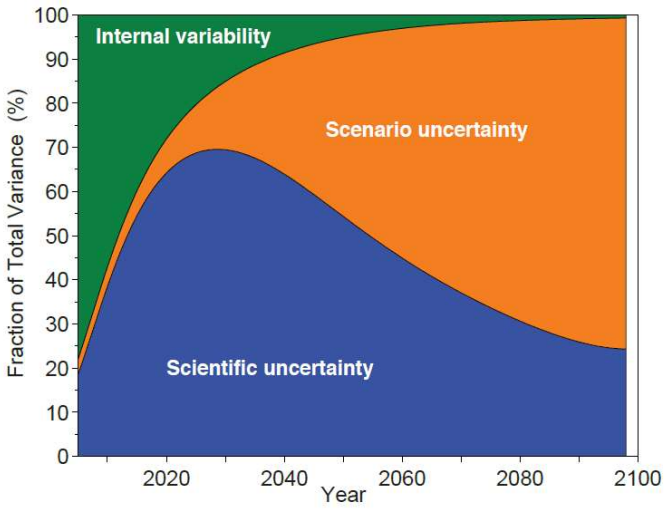

Figure 2.7 – Fraction of total variance in decadal mean surface air temperature prediction for U.S. (Alaska and Hawaii are not considered) and the sources of uncertainty (Wuebbles et al., 2017)

For engineering purposes, attempts in estimating the probability of future climate based on an ensemble of climate projections from different GCMs have been conducted (Olsen, 2015). However, one should be aware that this study does not intent to examine all existing climate models and scenarios.

Instead, the present study investigates the correlations between potential temperature rise with infrastructure vulnerability. Ultimately, it aims to offer insights into management approaches considering a massive bridge inventory.

2.4 Life Cycle Cost Analysis for the Transportation Sector

2.4.1 Definition and Purpose of Life Cycle Cost Analysis

Life Cycle Cost Analysis (LCCA) is an engineering economic analysis tool to compare competing alternatives for project implementation to assist officials in making economically, environmentally, and socially sound decisions. While monetizing environmental and social consequences is not always desired, the analytical process accounts for all relevant costs incurred during the service life of a certain asset – the life cycle cost (LCC) (FHWA, 2002). LCCA can be applied for instance to decide on the type of design (e.g. stayed or suspended) or material (steel or prestressed concrete) for bridge construction. According to ASCE, the use of LCCA leads to more precise and less biased comparisons (ASCE, 2014). Moreover, LCCA can be employed for the determination of inspection and maintenance intervals; thereby, ensuring structural safety while minimizing cost (Mahmoud et al., 2018).

The implementation of a transportation improvement generally involves several alternatives, each one associated with particular costs of construction, operation, maintenance and replacement. The initial costs tend to dominate the decision, especially under constrained budgets (ASCE, 2014). However, initial agency costs accounts for only part of the life cycle of the project. Actually, the selected option will also commit the agency to future costs as maintenance and replacement of components, which are essential to preserve the availability of the transportation asset to the public (FHWA, 2002). One example that illustrates the significance of future costs over the service life of infrastructure is the case of the U.S. SSSG bridges addressed in this research, where frequent maintenance, repair and replacement of expansion joints are crucial to maintain operability of the bridges.

ASCE emphasizes the importance of considering future inspection and maintenance activities in order to promote sustainable budgets and better management of vital infrastructure (ASCE, 2014). These types of future activities will undoubtedly result in costs to facility users. For example, work zones on transportation assets restricts the normal traffic capacity and reduces the traffic flow, causing user costs due to speed changes, stops, delays, detours and incidents. For this reason, LCCA is a valuable tool for investment decision, since it accounts for the total agency and user costs for the period through which the alternatives are being compared (FHWA, 2002).

The National Highway System (NHS) Designation Act in 1995 mandates that states conduct LCCA on all high-cost projects, more than $25 million, constructed with Federal funding (FHWA, 2002). However, this requirement was removed in 1998 through the Transportation Equity Act for the 21st Century, since states had difficulty addressing this requirement (ASCE, 2014). Currently, the federal LCCA policy is more advisory, attentive to create guidance and assistance for states to implement their own LCCA programs. Under the current federal legislation "Moving Ahead for Progress in the 21st Century" modest economic analysis is mandatory for states and localities to receive federal funds for their programs. Despite that several agencies have implemented LCCA in their programs and saved substantial amount of money, there are still many challenges to adopt the use of LCCA. Some obstacles include lack of consistent data, training and incentives (ASCE, 2014).

2.4.2 Main Steps of Life Cycle Cost Analysis

The LCCA steps are summarized according to FHWA (2002) as:

1. Establish design alternatives: the alternatives should be developed to accomplish the objectives of the project, and level of service and benefits provided by them should be equivalent. Moreover, alternatives should be compared over equivalent analysis periods. Both procedures yield fair comparisons of life cycle costs.

2. Determine activity timing: the initial and future activities involved for each alternative should be identified and scheduled.
3. Estimate costs: agency and user costs should be included. It is not required by LCCA to calculate all costs related to each alternative, but only those that shows the differences between alternatives.
4. Compute life cycle costs: the schedule of activities and their related agency and user costs compose the life cycle cost (LCC) of an alternative. All the costs should be converted into present dollar values and summed for each alternative, so they can be directly compared. It is appropriate to express future costs in constant dollars and then discount them to the present at a discount rate.
5. Analyze the results: the most cost-effective alternative is chosen in this step. It is important to highlight that the lowest LCC alternative may not be the most feasible due to higher risk, political and environmental concerns.

While the economic concepts and steps abovementioned utilized in LCCA are straightforward, the application of this analysis may impose some challenges due to uncertainties and assumptions (FHWA, 2002). For instance, a survey conducted by ASCE about the use of LCCA by governmental entities across the U.S. (from town to federal spheres) that are responsible for transportation planning showed that only 59% of them applies some form of LCCA. In addition, more than two-thirds said their LCCA needs improvement. Nevertheless, almost all participants agreed that LCCA should be used for decision-making process. Thus, better tools, data and coordination would facilitate the LCCA implementation. (ASCE, 2014)

2.4.3 Main Components of Life Cycle Cost for Bridges

Despite of the limitations and challenges in implementing a LCCA, the understanding of the costs involved over the entire life cycle of an infrastructure or a component of it can offer better subsidies to decide on the most cost-effective alternative (ASCE, 2014). The main costs during the life service of bridges are gathered in the chart of Figure 2.8 (Hawk, 2003).

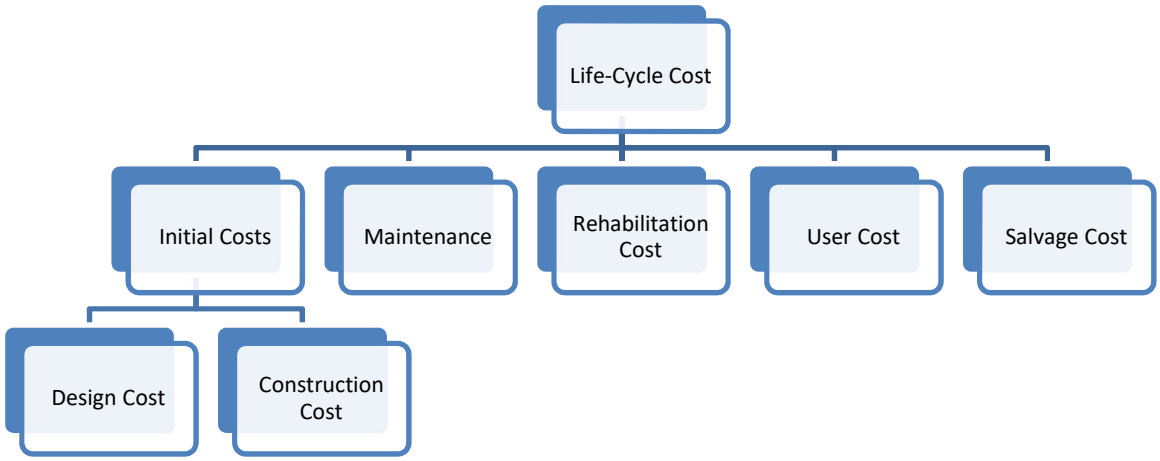

Figure 2.8 – Main components for bridge life cycle cost

The initial costs comprise mainly of the design and construction costs. They are characterized by small uncertainties since they are one-time cost at the beginning of the life cycle of the bridge. It is important to highlight that the construction cost will influence the user cost due to establishing work zones that will influence the traffic in surrounding areas. (Kelly, 2017)

The maintenance cost is related to activities to maintain the condition of the asset. In the case of bridges with expansion joints, cleaning and replacement of expansion joints are examples of critical maintenance costs, since they are prone to being clogged by debris and deteriorate due to weather and traffic loads. If those activities are not performed periodically and in an effective manner, major deterioration and structural problems can arise. In addition, maintenance costs affect user costs due to traffic control and detours.

Rehabilitation cost is related to major work to restore the integrity of the structure and correct safety defects (FHWA, 2018a). Similar to construction and maintenance, rehabilitation also impacts the user cost.

User costs of primary interest are vehicle operating costs, travel time costs and crashes costs. They result from work zones during construction, maintenance, and rehabilitation of bridges that cause speed changes, stops, delays, detours and incidents (FHWA, 2002). They also constitute an important parcel of the cost in LCCA since they impact the public, and as such the variabilities in these costs are relatively large (Kelly, 2017).

Salvage Cost is an end cost, generally the net value from the recycling of materials of the asset at its project life end. Moreover, as presented further in this study, some LCCA alternatives may involve the replacement of the whole bridge. In this case, another end cost to be accounted in the LCC of the asset is the cost of demolition (and the respective user costs).

Besides allowing for the comparison of alternatives and identification of the most cost-effective option, the application of LCCA in the present study is utilized to quantify the cost of three distinct climate change scenarios over the maintenance of SSSG bridges in the U.S.

3. DATA COLLECTION

3.1 National Bridge Inventory Data

This study is focused on the analysis of simply supported steel girder (SSSG) bridges. Thus, relevant information of each one of the approximately 80,000 SSSG bridge assessed was obtained after processing the whole tabular data from the 2017 NBI (FHWA, 2017). The available data are: geographic coordinates, state code, type of route, year built, average daily traffic, type of design and material, length and number of spans, deck width, status classification as deficient or obsolete, among others. Further details as principal characteristics of the bridges analyzed are presented in Chapter 4.

The data utilized to conduct structural analysis was mainly extracted from the 2017 NBI. However, additional geometric information not available in the NBI database regarding superstructure cross sections was estimated using the relationships given in AASHTO (2012) and Ruddy and Ioannides (2004) as described in Chapter 4.

3.2 Temperature Data

In order to evaluate the vulnerability of SSSG bridges due to induced thermal stresses when the expansion movement is restrained by clogged joints, it is necessary to determine the corresponding temperature range to which the superstructure might be subjected. This temperature variation ΔT (°C) is calculated using equation (3.1):

$$\Delta T = T - T_o \tag{3.1}$$

Where T (°C) is the daily maximum projected temperature for future years and T_o (°C) is the base temperature at the stage of construction when the joints are installed. During the construction, in order to obtain the desired structural performance when T_o is near the mid-range (average of maximum and minimum expected temperatures during the service life), the joint can be set at mid movement range.

However, if T_o is above or below this mid-range, the joint gap needs to be reduced and increased, respectively (Childs, 2018). For the sake of simplicity, this study considers the temperature variation ΔT to be constant along the bridge superstructure depth and length.

3.2.1 NOAA Regional Time Series Temperature Data

The temperature during construction of each bridge, at the stage in which the expansion joints were installed, is estimated based on the geographical position of the bridge and the year of completion of its construction – both information were extracted from 2017 NBI (FHWA, 2017).

First, each bridge is tied to one of the nine U.S. climate regions: Northwest, Northern Plains and Rockies, Upper Midwest, Ohio Valley, Northeast, West, Southwest, South, and Southeast as shown in Figure 3.1.

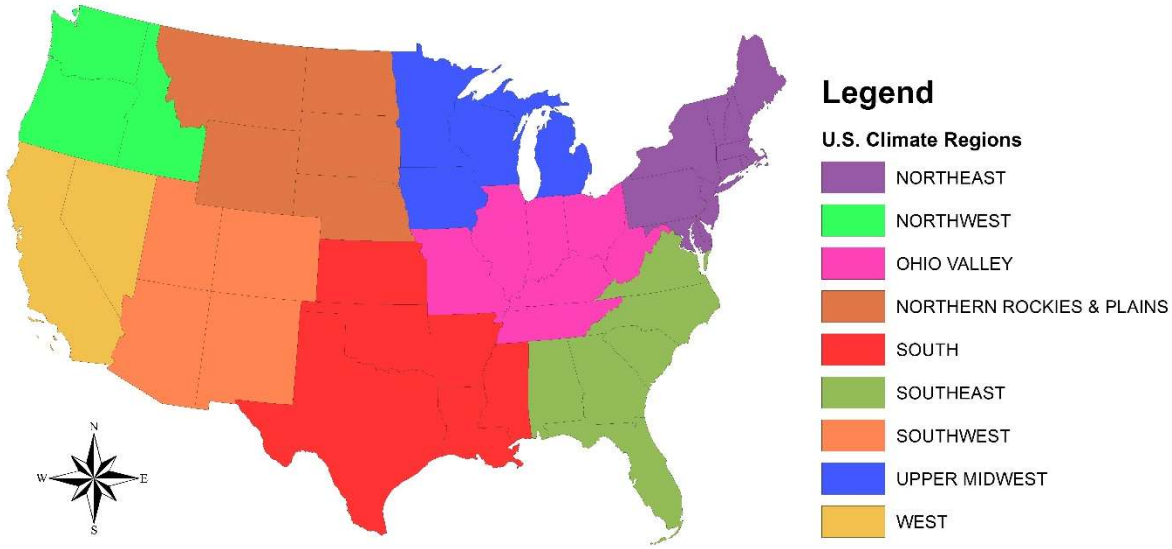

Figure 3.1 – U.S. climate regions

Since, only the year of construction completion is available in the inventory, four possible scenarios to account for the seasonal temperature variation during construction are considered – construction during winter (Scenario 1), spring (Scenario 2), summer (Scenario 3) and fall (Scenario 4).

Thus, each bridge is assessed under all these four possible scenarios, where each scenario can be interpreted as a hypothetical temperature condition: Scenario 1 (winter) is the worst case – the range from low temperatures that occurs in the winter until projected daily maximum temperatures for future years provides the greatest amplitudes, Scenario 3 (summer) is the most optimistic – since this is the warmest season, the variation until the projected daily maximum temperatures for future years presents the smallest amplitudes, and Scenarios 2 and 4 (spring and fall) have intermediate ranges of temperature. While Scenario 1 is included in the analysis, it is recognized that it is not a very realistic scenario, particularly for states residing in colder climates since those states enforce construction activities in the warmer part of the year.

Once the bridge climate region is defined, the temperature of construction for each scenario (for the respective year of construction conclusion) is assigned using the NOAA Regional Time Series (NOAA, 2018) as schematically illustrated in Figure 3.2.

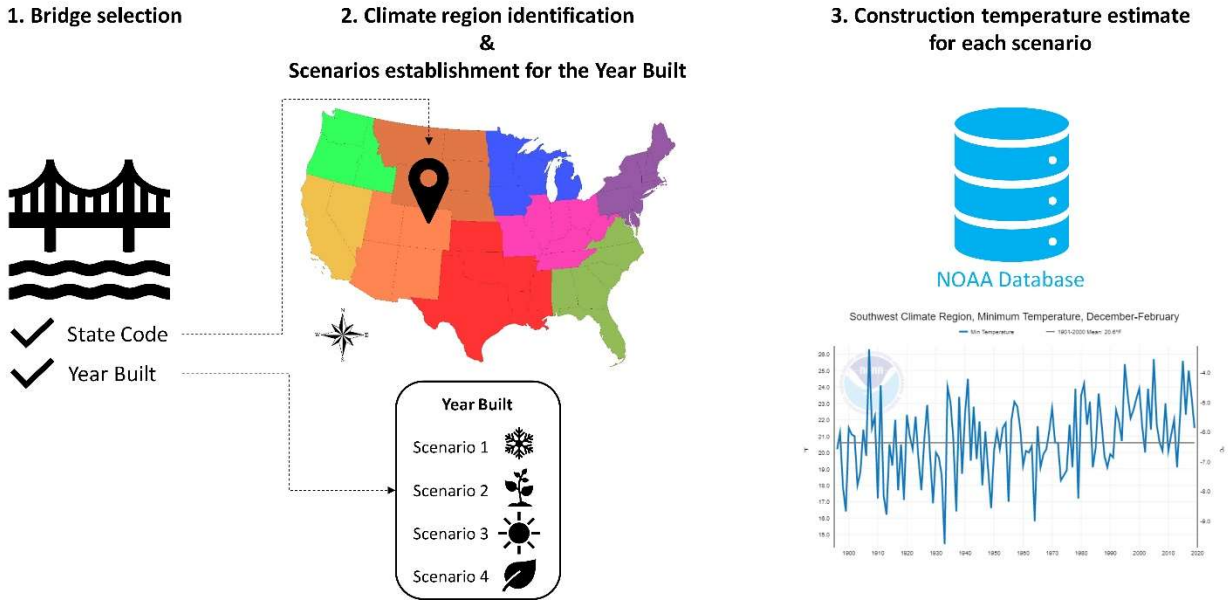

Figure 3.2 – Steps to estimate the construction temperature for each scenario of each bridge

The NOAA database contains historical records along the U.S. climate regions. Conservatively, the temperature for each scenario is taken as the average of minimum temperatures of each season. The option for taking this average of minimum temperatures (instead the average) is because it provides a larger temperature range to calculate the maximum thermal stress into the structures in analysis. Bridges built prior to 1895 were not analyzed since temperature data for this period is not available.

3.2.2 Coupled Model Intercomparison Project (CMIP5) Future Temperature Data

The projected daily maximum temperature throughout the U.S. for years 2040, 2060, 2080 and 2100 are obtained from GFDL CM3 coupled climate model from the National Oceanic Atmospheric Administration (NOAA) Geophysical Fluid Dynamics Laboratory, which follows the Coupled Model Intercomparison Project Phase 5 (CMIP5) protocol. The present analysis accounts for three of the Representative Concentration Pathway (RCP) scenarios, which are named for the approximate radiative forcing in year 2100: the lower forcing scenario RCP 2.6, a moderate scenario RCP 6.0 and the higher forcing scenario RCP 8.5.

The downscaled data have 1/8° resolution, which corresponds to approximately 12.5 km. MATLAB version R2018a was used to read and export the data into ArcMap version 10.5.1, where the projected daily maximum temperature of each bridge location for years 2040, 2060, 2080 and 2100 were extracted as detailed in Chapter 4. It is important to note that data for Alaska, Hawaii, and Puerto Rico were not available. Figure 3.3 presents the evolution of global mean annual surface temperature changes (in ℃) over future years, simulated by GFDL CM3 coupled climate, under four scenarios: RCP 2.6, 4.5, 6.0 and 8.5. Each scenario leads to a distinct trend in global temperature, since they consider different greenhouse gas concentrations in the atmosphere.

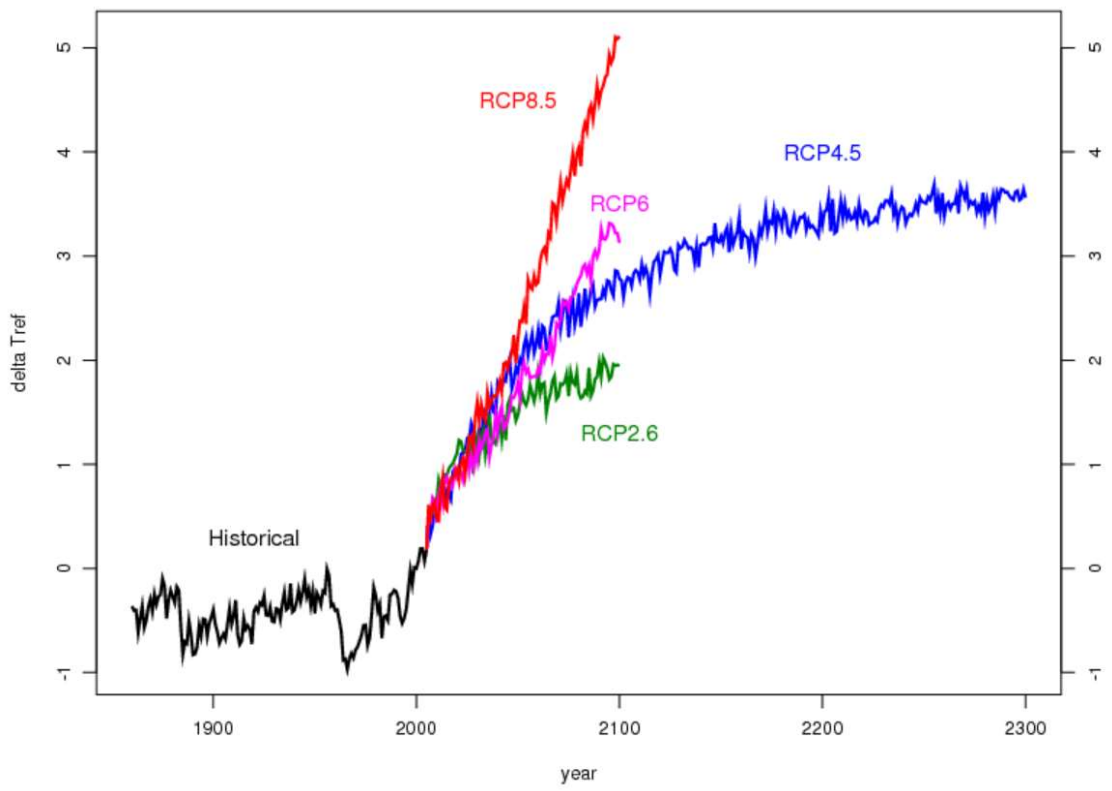

Figure 3.3 – Global mean annual surface temperature changes (℃) simulated by GFDL CM3 coupled climate model for historical conditions (1860-2005) and four projected future RCP scenarios (GFDL, 2019)

4. DATA ANALYSIS

4.1 National Bridge Inventory Analysis

The processing of the 2017 NBI tabular data allowed for analysis of the relevant characteristics of U.S. bridges and the particular class of bridges – simply supported steel girder bridges (SSSG), which is the focus of the present study, as outlined in sections 4.1.1 and 4.1.2.

4.1.1 Main Characteristics of US Bridges

According to the 2017 NBI (FHWA, 2017) the U.S. highway bridges belong mainly to County, followed by State, and then U.S. and Interstate routes, as presented in Figure 4.1.

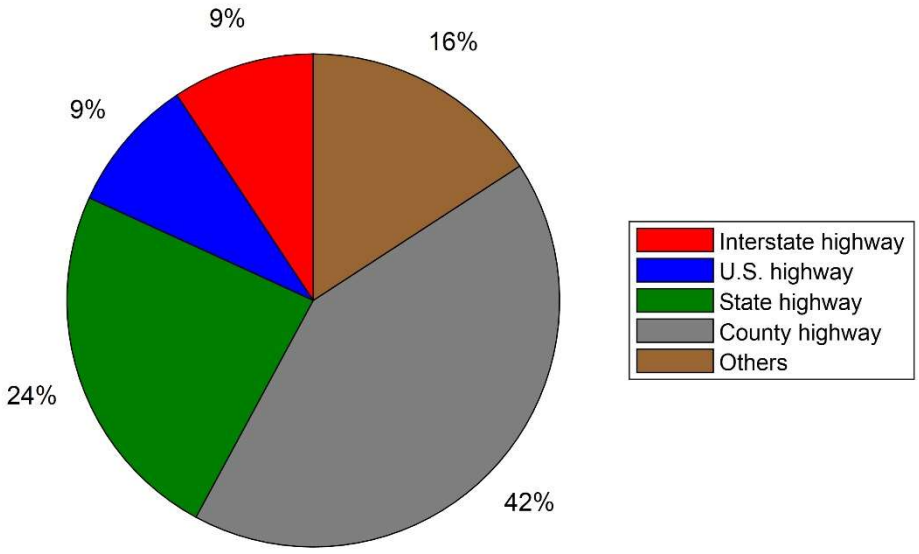

Figure 4.1 – USA highway bridges distribution for each route jurisdiction

Analysis of the 2017 NBI also shows that four in ten bridges are 50 years or older, reaching or even exceeding their design life. The average age of bridges in America is 45 years old (FHWA, 2017). Aging causes bridges to lose part of or the whole functionality; that is, it prevents their ability to serve their intended purpose.

As an example, 14% of bridges in America were considered functionally obsolete in 2017 (FHWA, 2017). This reduction in functionality is defined for example on the basis of having narrow lanes or low load-carrying capacity for the present traffic demand. Consequently, they do not attend to the current engineering standards anymore (ASCE, 2017a).

In addition, it is noted that 54,560 bridges in U.S. were characterized as structurally deficient in 2017 (FHWA, 2017), where 'deficient' implies that elements of the bridge structure were found in poor conditions due to deterioration or damage (ASCE, 2017a). Despite the poor conditions of these bridges, there were approximately 188 million trips across them each day in 2016 (ASCE, 2017a).

Figure 4.2 shows that the design type "Girder" is the most abundant on highways. It corresponds to 245,957 out of 615,002 highway bridges in the nation (~40%). In addition, this group has the largest number of functionally obsolete and structurally deficient bridges: 41,610 and 29,094 respectively.

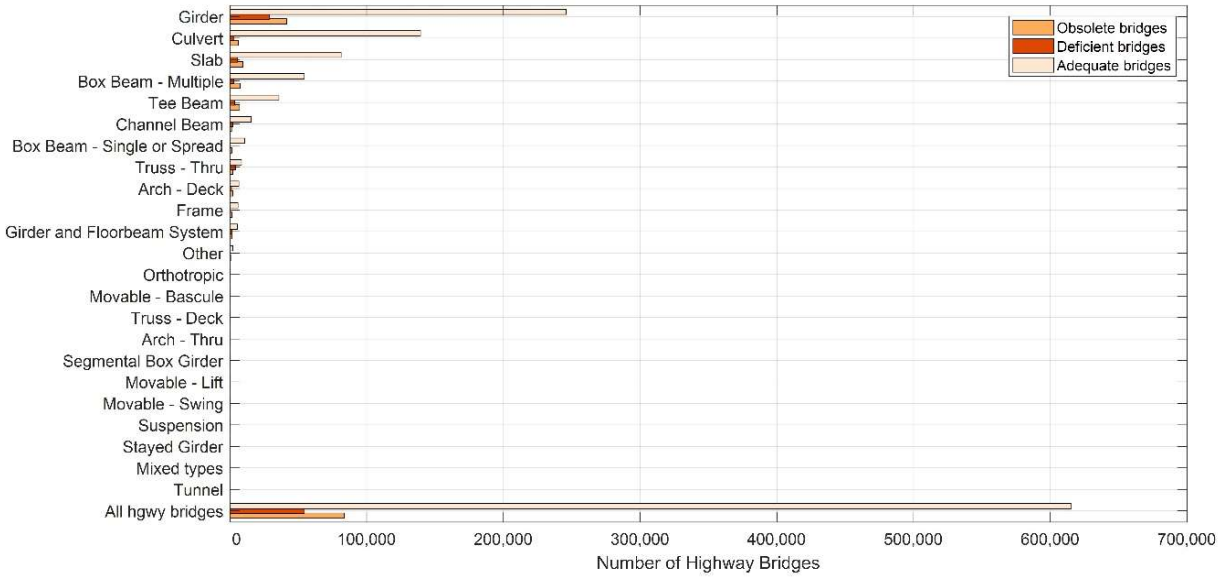

Figure 4.2 – U.S. highway bridges distribution including all types of design

4.1.2 Main Characteristics of U.S. Steel Simply Supported Girder Bridges

There are approximately 97,000 (FHWA, 2017) SSSG bridges along the U.S. highways. Their geographic distribution is illustrated in the map of Figure 4.9. A closer look into deficient bridges as illustrated in Figure 4.3, reveals that girder-type bridges correspond to 53% of deficient highway bridges in the national inventory, with most of them being SSSG (approximately one third of the U.S. deficient highway bridges). Moreover, half of all obsolete bridges are girder type and SSSG bridges represent about a quarter of the total obsolete bridges, as one can note in Figure 4.4.

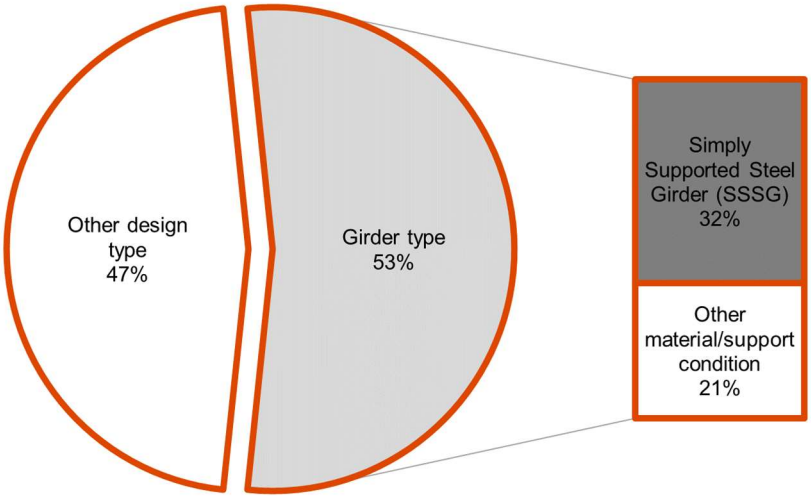

Figure 4.3 –U.S. structurally deficient highway bridges

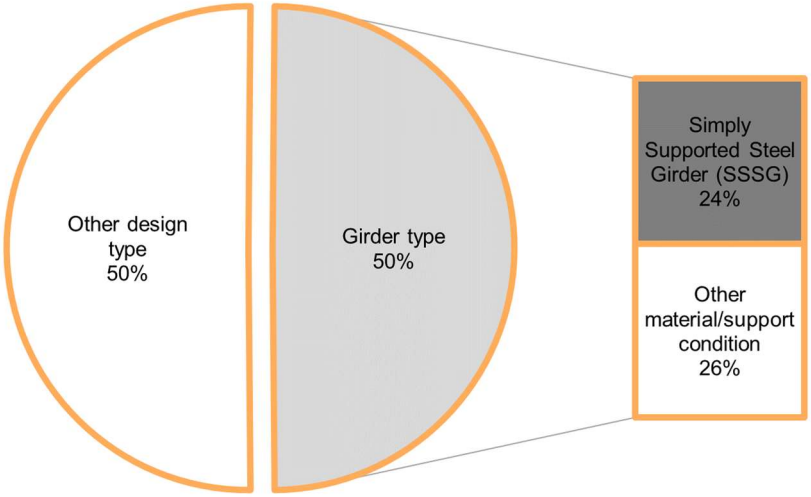

Figure 4.4 –U.S. functionally obsolete highway bridges

Another pertinent information is the age distribution of the SSSG bridges in U.S. From the pie chart in Figure 4.5 one can observe that this particular class of bridges is aging, with more than half of the structures exceeding 50 years. This average age (50 years old) exceeds the national average bridge age of 45 years.

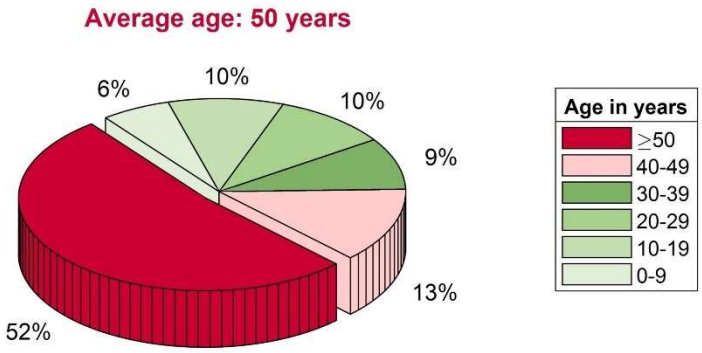

Figure 4.5 – Relative age distribution and average age of SSSG bridges in U.S.

In addition to the vulnerability to deterioration of expansion joints, one can observe from the previous data analysis that there are also other issues involving SSSG bridges which can potentially compromise the safety and serviceability of those bridges, such as deficiency and obsolescence. It is important to highlight that a substantial parcel of the deficient and obsolete bridges in the U.S. comprises of SSSG bridge type. Moreover, the average age of these bridges (50 years old) call for immediate attention to be given to this particular class of bridges since aging clearly can aggravate the deterioration processes.

4.2 Temperature Analysis

4.2.1 NOAA Regional Time Series Temperature Analysis

The construction temperatures of each bridge, at the time of expansion joints installation under the hypothetical Scenarios 1, 2, 3 and 4 (winter, spring, summer and fall respectively) are estimated according to the methodology presented in section 3.2.1. A summary of the historical temperatures for each of the nine U.S. climate regions is illustrated in Figure 4.6 from the year of 1895 to the year of 2017.

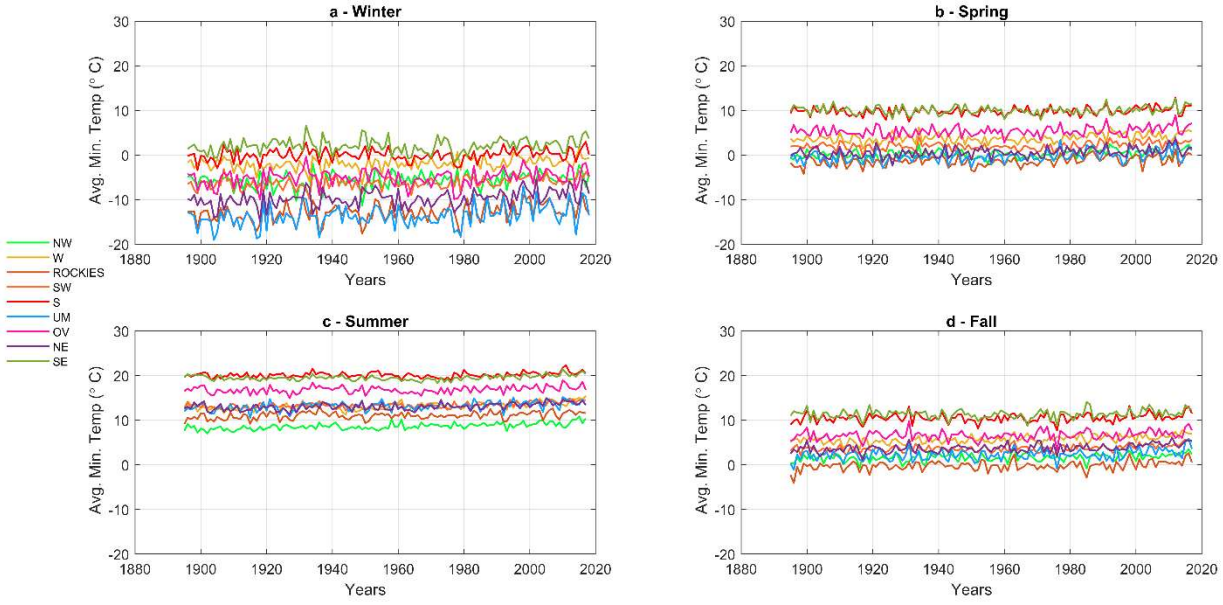

Figure 4.6 – Historical average minimum temperature along the years for each region evaluated in the a) winter, b) spring, c) summer and d) fall

One can observe that Scenario 1 (winter) is the most severe scenario, since it provides the maximum temperature variations to which bridges can be subjected in future years. This ranges vary from the lowest absolute temperatures at the time of bridge construction, around -15℃ in the Upper Midwest or 0℃ in the Southeast until the maximum daily temperatures projected for future years presented in section 4.2.2. In contrast, Scenario 3 (summer) is the most optimistic, presenting the highest construction temperatures about 10℃ in Northwest and 20℃ in South, which generates the mildest projected variations toward future years. Scenarios 2 (spring) and 4 (fall) are intermediate scenarios, showing similar temperatures of construction – approximately 0℃ in Northern Rockies & Plains and 10℃ in Southeast.

Table 4.1 presents an example of historical temperature data that is processed in order to account for the temperature of construction of a specific bridge (B-16-FM) in Colorado.

Table 4.1 – Example of historical temperature data processing procedure to account for the temperature of construction for bridge B-16-FM

Data Available in NBI			Data Processed				
Structure Number	State Code	Year Built	U.S. Climate Region	Avg. Min. Temp. (°C) Winter Scenario 1	Avg. Min. Temp. (°C) Spring Scenario 2	Avg. Min. Temp. (°C) Summer Scenario 3	Avg. Min. Temp. (°C) Fall Scenario 4
B-16-FM	8	1966	Southwest	-7	2	14	4

The first three columns in Table 4.1 are specific for each bridge as provided by the NBI (FHWA, 2017). The Structure Number is provided in item 8 of the NBI data and it is represented by a unique code for each bridge. The State Code is given by item 1 of NBI and corresponds to the Federal Information Processing Standards (FIPS) code for States. The Year Built comprises the item 27 of NBI and it represents the year of construction completion (FHWA, 1995).

For this example, the bridge identified as B-16-FM is located in the State of Colorado (FIPS code 8) and had its construction completed in 1966. With that information, this particular bridge is classified to belong to the Southwest climate region and the average minimum temperature of each season for the year 1966 (shown in Table 4.1) is extracted from the historical records from NOAA database (NOAA, 2018). Thus, the four proposed scenarios that simulates the construction of the bridge during each season can be evaluated.

4.2.2 Coupled Model Intercomparison Project (CMIP5) Future Temperatures Analysis

The projected daily maximum temperature for the future years 2040, 2060, 2080 and 2100 are obtained from GFDL CM3 coupled climate model from the National Oceanic Atmospheric Administration (NOAA) Geophysical Fluid Dynamics Laboratory. This study analyzes three Representative Concentration Pathway (RCP) scenarios: the lower forcing scenario RCP 2.6, a moderate scenario RCP 6.0 and the higher forcing scenario RCP 8.5.

For each RCP scenario, the abovementioned data provides the projected daily maximum temperature for approximately seventy-six thousand geographic coordinates along the U.S. main territory. The data are provided in blocks of 5 years.

Thus, five main blocks of data were processed (end of 20 years): 2036-2040, 2056-2060, 2076-2080 and 2096-2100. MATLAB version R2018a was used to read and process these temperature data. As a result, a daily maximum temperature grid was generated for future years 2040, 2060, 2080, 2100. The points of the grid take the highest daily temperature reached during the 5 years interval.

Then, the grids of daily maximum temperature for 2040, 2060, 2080 and 2100 were processed in ArcMap version 10.5.1. The respective maps for each RCP scenario are illustrated in Figure 4.7.

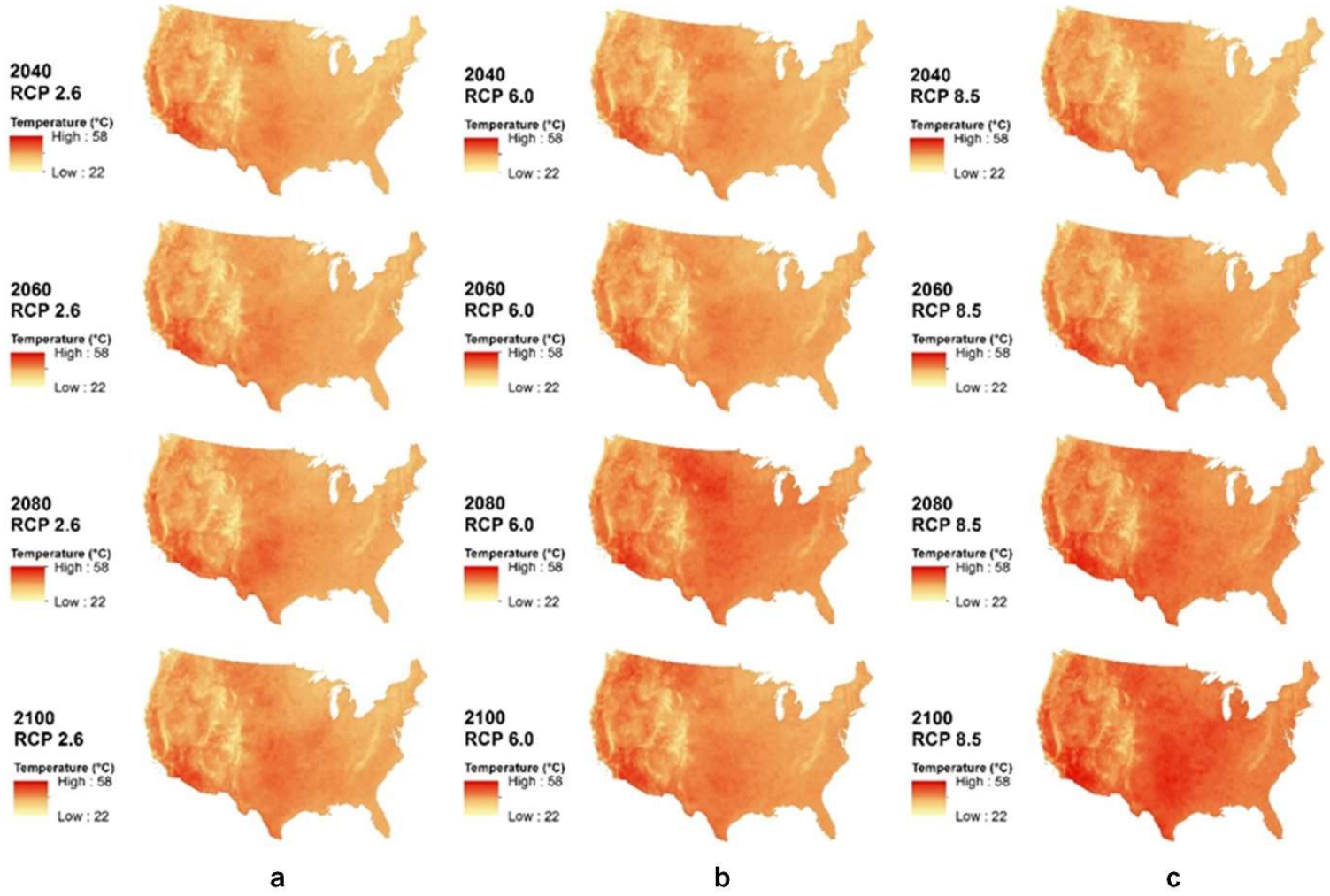

Figure 4.7 – Projected daily maximum temperatures along U.S. for 2040, 2060, 2080 and 2100 from NOAA climate model GFDL CM3 for a) RCP 2.6 b) RCP 6.0 and c) RCP 8.5

As one can observe in Figure 4.7, each RCP scenario shows a distinct trend of projected daily maximum temperatures in the U.S. along the future years. For the lower forcing scenario RCP 2.6, the projected temperatures tend to remain constant, while being slightly augment in the South region in 2080. In contrast, the higher forcing scenario RCP 8.5 clearly presents a gradual and overall increase in temperature as the years progress, especially in the central portion of the country. The moderate scenario RCP 6.0 displays an intermediate behavior between the other two extreme scenarios, with a pronounced temperature increase in Northern Rockies and Plains region in 2080. In summary, the maps of future temperatures in the U.S. along the years for each RCP scenario plotted in Figure 4.7 depicts the expected behavior in which the magnitude of the temperatures increases in accordance to the level of radiative force of the scenario.

In order to offer a general magnitude of the temperatures, Table 4.2 summarizes the upper, lower and average projected daily maximum temperature for U.S. in future years from NOAA climate model GFDL CM3 for three different RCP scenarios – 2.6, 6.0 and 8.5.

Table 4.2 – Upper, lower and average projected daily maximum temperature in the U.S. for 2040, 2060, 2080 and 2100 from NOAA climate model GFDL CM3 for RCP 2.6, 6.0 and 8.5

RCP 2.6	2040	2060	2080	2100
Upper temperature (℃)	53.9	52.8	52.8	52.5
Lower temperature (℃)	21.3	22.3	23.6	24.1
Avg temperature (℃)	**38.3**	**39.3**	**39.9**	**39.9**
Std. Dev.	4.1	3.6	3.9	3.9

RCP 6.0	2040	2060	2080	2100
Upper temperature (℃)	53.1	52.9	56.9	56.2
Lower temperature (℃)	20.8	23.7	24.3	25.2
Avg temperature (℃)	**39.0**	**39.6**	**43.2**	**41.6**
Std. Dev.	3.8	3.4	4.0	3.7

RCP 8.5	2040	2060	2080	2100
Upper temperature (℃)	53.9	54.3	57.0	60.2
Lower temperature (℃)	23.4	23.4	26.7	29.2
Avg temperature (℃)	**39.1**	**40.8**	**43.5**	**45.6**
Std. Dev.	3.8	3.8	3.9	4.1

An overview of the average projected daily maximum temperature along future years in the U.S. can be observed in the bar graph of Figure 4.8 under different RCP scenarios. As expected, scenario RCP 2.6, which is related to efforts to reduce greenhouse emissions, shows a slight temperature increase (about 1.6℃) from 2040 to 2080 and then it stabilizes. Scenario RCP 6.0 presents a temperature peak in 2080, but in 2100 it declines approximately 1.6℃. Finally, the higher forcing scenario RCP 8.5 shows a trend of increasing temperature over the future years. For this last scenario the variation between 2040 to 2080 is around 6.5℃.

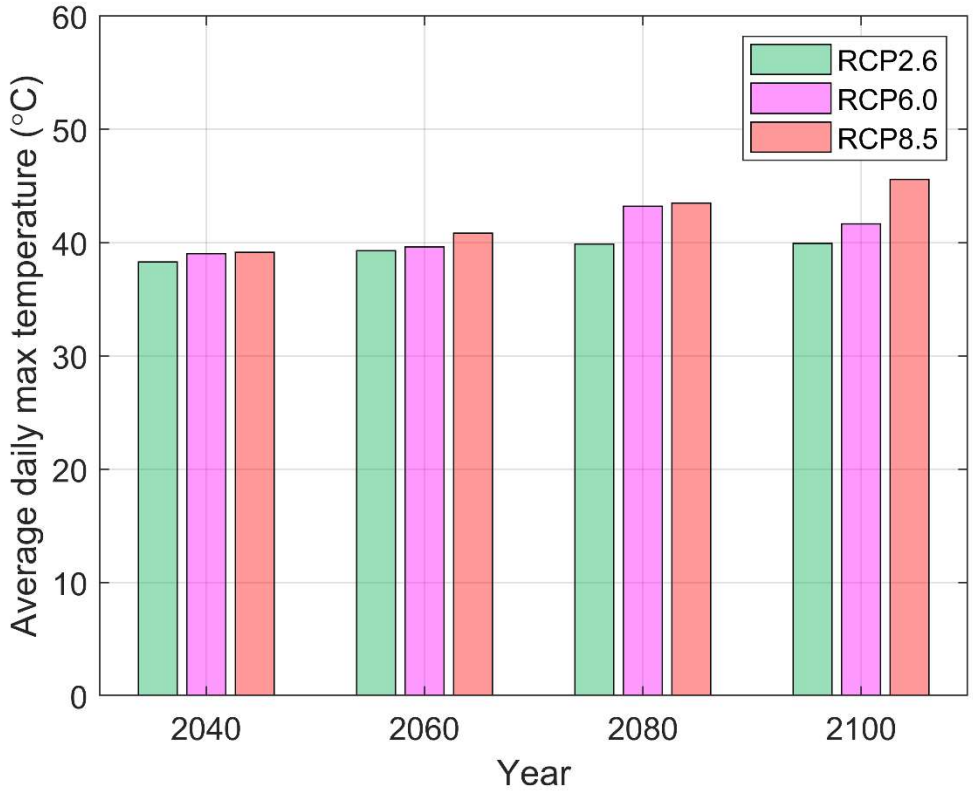

Figure 4.8 – Average of projected daily maximum temperatures in the U.S. for 2040, 2060, 2080 and 2100 from NOAA climate model GFDL CM3 for RCP 2.6, 6.0 and 8.5

After combining the spatial temperature information with the location of the bridges (available in NBI 2107), the extraction of the projected daily maximum temperature for future years of each SSSG bridge under analysis was possible. To illustrate this procedure, Figure 4.9 shows the projected temperatures for 2100 under RCP 8.5 and all SSSG bridges.

These future temperatures (in association with the temperatures during bridge construction) are the temperature inputs to assess the aggravated effect of clogged joints.

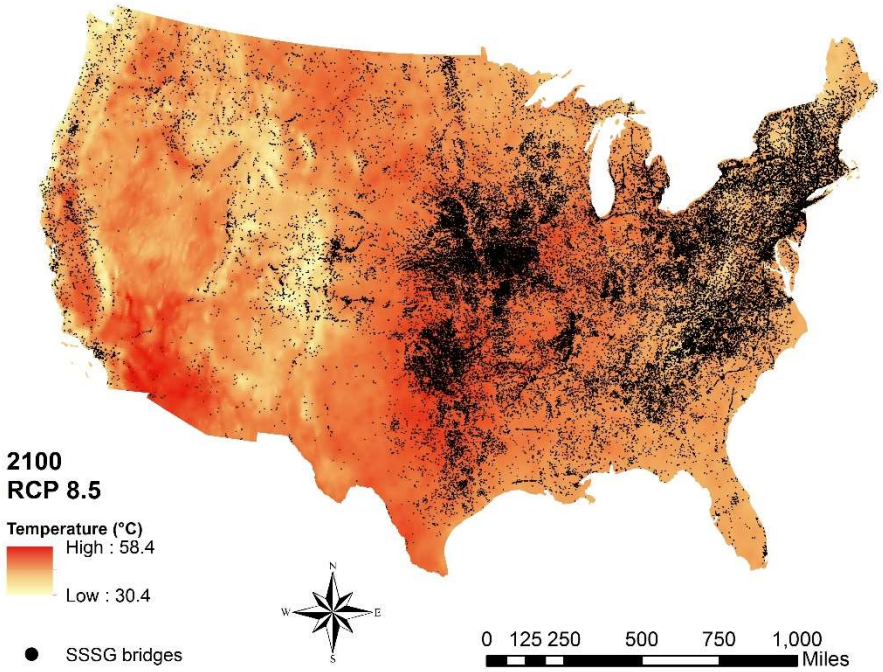

Figure 4.9 – Projected daily maximum temperatures for 2100 under RCP 8.5 and location of SSSG bridges

The next chapter presents details of the analytical method used to quantify the potential impact of a changing climate on deteriorated SSSG bridges in the U.S.

5. ANALYTICAL METHOD

Herein, an analytical method comprised of a structural assessment and a posterior life cycle analysis is developed to evaluate the impact of projected temperatures on the U.S. simply supported steel girder (SSSG) bridges, with approximately 80,000 structures. The first part of this method is presented in section 5.1 on Assessment of Interaction Equation, and pertain to quantifying the level of vulnerability of each bridge in terms of the interaction equation value (IEV) due to the simultaneous effect of clogged joint condition and temperature rise. The second part of the methodology is described in section 5.2 on Life Cycle Cost Analysis Models and it uses the IEV outcomes from the structural assessment as inputs to conduct the life cycle analysis for SSSG bridges maintenance alternatives. The application of the framework aims to offers insights on establishing a priority order for maintenance and replacement of SSSG bridges in the U.S., while taking into account the climate scenarios.

5.1 Assessment of Interaction Equation

Unaccounted for during the design process, the effect of clogged joints associated with projected temperature rise due to climate warming results in undesired demand on the slab-girder composite superstructure of SSSG bridges as well as other components of the bridge. Herein, this effect is quantified in terms of the interaction equation.

It is critical to note that historically bridge girders are only evaluated for their moment and shear capacity without the inclusion of the effect of the axial load because it is assumed that the expansion joints will always be functional. In the case of clogged joints, it is imperative to evaluate the bridge superstructure against their ability to not only carry bending moment but also the axial load as it interacts with the bending moment.

The interaction equation accounts for the demand-to-capacity ratio under axial loading and bending moment and it has long been recognized as a design limit state for main load carrying elements (AISC, 2017; Salmon & Johnson, 1996). As such, to ensure adequate structural performance of the bridge superstructure, this ratio should not exceed unity. The ramifications of the interaction equation exceeding a value of unity, which implies failure, will depend on the level of exceedance. This could entail substantial deformations in the bridge girders, slab concrete crushing (in case of composite sections), and subsequent failures in other main load-carrying elements and secondary elements (Vasdravellis et al., 2015a).

Before applying the interaction equation technique, it is important to identify if the superstructure cross-section is composite or not. Figure 5.1 (a) illustrates a typical steel-concrete composite cross-section, where the composite action is provided by the shear connectors, while Figure 5.1 (b) and (c) illustrates the difference in the behavior of a non-composite and a composite steel-concrete section, respectively. In the latter, there is no relative slip between the concrete slab and steel I-girder and consequently the entire cross section deflects as a single unit. In a non-composite girder, the flange is typically embedded in concrete slab but no shear connectors are used.

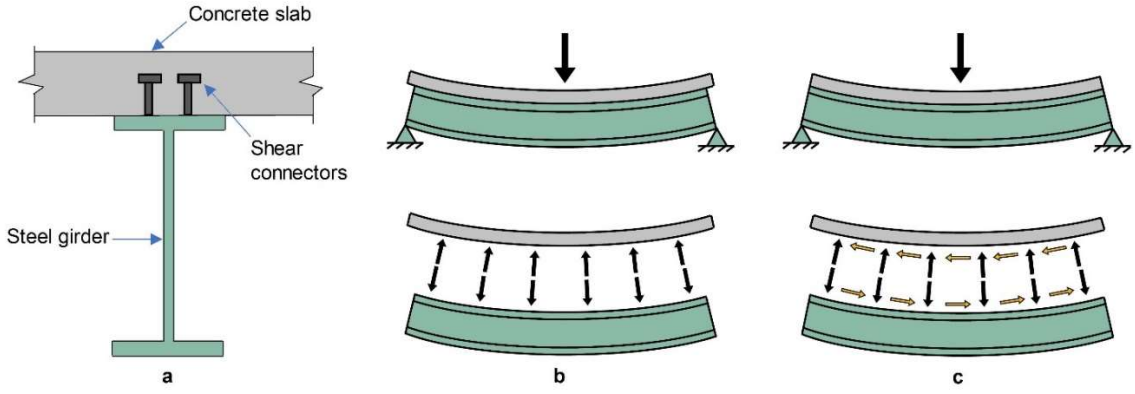

Figure 5.1 – a) Steel-concrete composite section and a comparison between b) non-composite and c) composite steel-concrete beam

This study assumes that the superstructure of the bridges is comprised of steel-concrete composite sections due to their common use, this type of section in bridge construction began in the early 1930's (Salmon & Johnson, 1996). Although the existence of non-composite bridges is very limited, even if the bridge is non-composite field tests and monitoring of bridges have shown that these types of bridges behave in almost a composite way (i.e. about 80% composite) (Connor et al., 2005). Furthermore, the adoption of composite steel systems became routine during the interstate era, with the construction of bridges after World War II (Chen & Duan, 2000). The usage of steel-concrete composite increases the speed of construction of bridge decks or building floors. In addition, safe, robust, and economic structures result from the optimal combination of the individual structural properties of steel and concrete. Nevertheless, current structural provisions (e.g. AISC 360-10, AS2327.1 and Eurocode 4) do not establish a method of design for composite beams subjected to the simultaneous action of bending moment and axial load. Current design codes refer to procedures utilized for bare steel sections instead. (Vasdravellis et al., 2015b).

In a recent study, Vasdravellis et al (2015b), proposed a moment-axial compression interaction formulation for steel-concrete composite beams under the concomitant action of sagging bending and axial compression based on experimental and numerical results, according to the equation (5.1). The proposed equation is intended to cover actual gap in codes and allow for a more efficient design of composite structures.

$$(1-\Gamma)\frac{\Sigma\gamma M}{M_n}+\frac{\gamma P}{P_n}=1\ (for\ P>\Gamma P_n) \tag{5.1}$$

Where P (kN) is the induced thermal axial compressive load when the superstructure of the bridge is restrained from expansion by clogged joints and M (kN.m) is the bending moment due to dead load (weight of the materials), live load HL-93 (traffic) and the thermal load (due to the eccentricity of the thermal axial load); γ is the load factor for the limit state Service II (AASHTO, 2012). Γ is a factor varing from 0.3 to 0.4. M_n is the plastic moment resistance and P_n is the compression capacity of the composite section calculated according to equation (5.2).

$$P_n = 0.85 f_c' A_c + A_s f_y \quad (5.2)$$

Where A_c and A_s are the cross-section areas of the concrete and steel girder respectively, f_y is the steel yielding strength and f_c' is the compressive strength of the concrete slab.

Depending on the level of axial load application, three modes of failure of the specimens (simply supported composite beams) were observed during the tests: concrete crushing of the slab, shear connection failure and buckling of the steel girder, as shown in Figure 5.2.

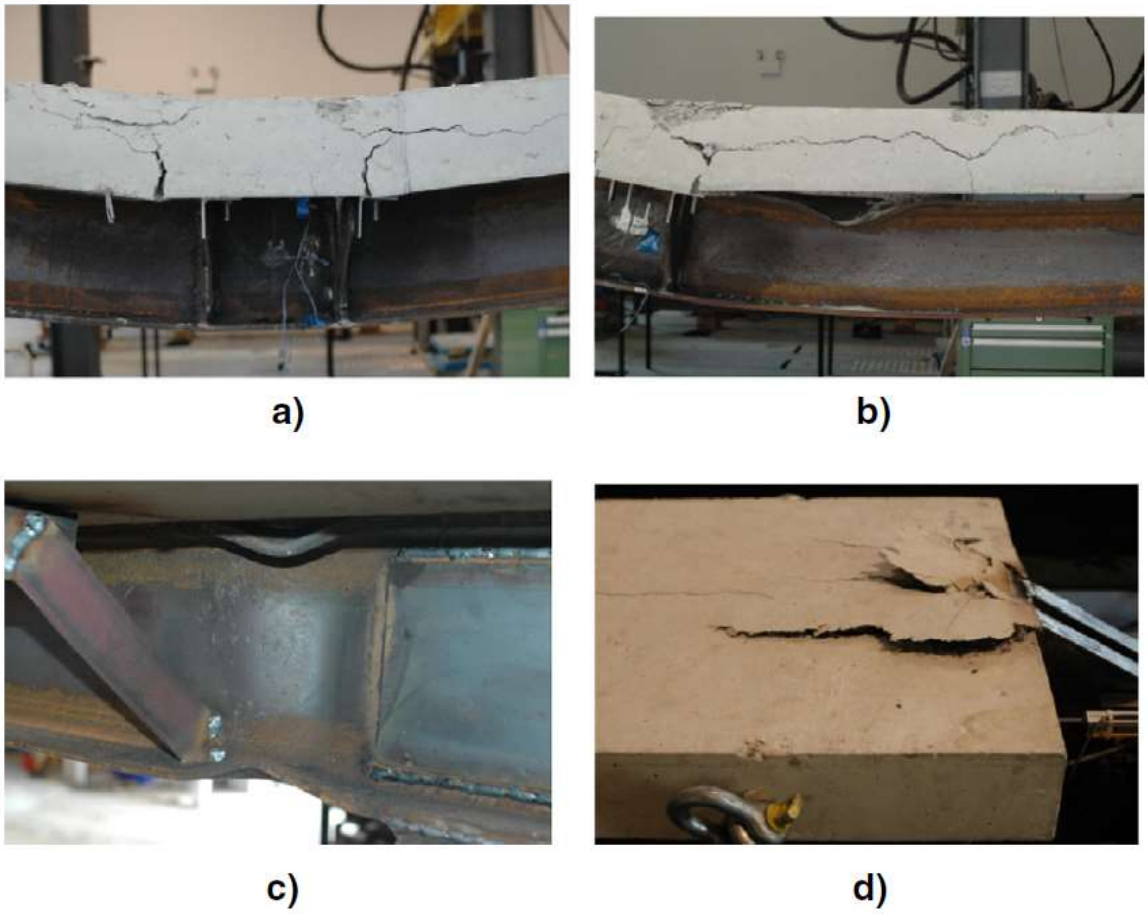

Figure 5.2 – Failures in composite beams specimens: a) concrete crushing and cracking of the slab at midspan; b) shear connection failure; c) local buckling of the steel girder; d) concrete crushing at the zone of axial load application (Vasdravellis et al., 2015b)

5.1.1 Estimate of Girder and Slab Geometry

From the data available at National Bridge Inventory, the dimensions of the steel girder bridges could be estimated using the design equations in S.I. system (Ruddy & Ioannides, 2004). Initially, an approximation for girder depth d (mm):

$$d = \frac{L}{24} \times 1000 \tag{5.3}$$

The weight per length is:

$$w_t = \frac{78.5M}{0.32F_y d} K \tag{5.4}$$

Where w_t is the weight (kN/m), M is the demanded bending moment (kN.m), F_y is the steel yield stress (kN/m^2), d is the girder depth (m) and K is a dimensionless reduction factor, approximately equal to 0.7 for composite sections (concrete and steel).

The cross-section area of the steel girder A_S (mm^2) is calculated as:

$$A_S = \frac{w_t}{78.5} \times 1000^2 \tag{5.5}$$

In addition, the moment of inertia I_x (mm^4) can be calculated as:

$$I_x = \frac{0.16d^2 w_t}{78.5} \times 1000^4 \tag{5.6}$$

From the equation above one can obtain the elastic section modulus S_x (m^3):

$$S_x = \frac{0.32dw_t}{78.5} \tag{5.7}$$

For the slab, a commonly used concrete deck with thickness (t_s) of 0.2 m and 28-day compressive strength $f'_c = 25$ MPa is assumed (Caltrans, 2015). Considering the evolution of the mechanical properties of the structural steel for bridges, the inventory is divided into three groups, in order to differentiate the steel strength: bridges built before 1901 with yield strength of 26 ksi, from 1901 to 1965 with yield strength of 36 ksi, and 1966 to 2017 with yield strength of 50 ksi (Ferris, 1954; Hatfield, 2001).

The abovementioned parameters are used to estimate the capacity of the composite section as further presented in section 5.1.4 on Capacity of the Composite Section and to account for the dead and thermal loads.

5.1.2 Restriction to the longitudinal expansion of the superstructure of the bridge

The effect of the clogged joints filled by sand and gravel, which restricts the longitudinal movement of expansion of the composite steel slab-concrete girder, is taken in account through the linear springs coefficients of the soil $\mathrm{k_{soil}}$ (kN/m) given by equation (5.8).

$$k_{soil} = \frac{E_{soil} A_{clogged}}{\Delta L_{joint}} \tag{5.8}$$

Where $\mathrm{E_{soil}}$ $(\mathrm{kN/m^2})$ is the modulus of elasticity of the soil; $\mathrm{A_{clogged}}$ $(\mathrm{m^2})$ is the cross sectional area of the joint clogged by debris; and $\Delta \mathrm{L}_{joint}$ (m) is the design thermal movement range of the bridge superstructure (AASHTO, 2012).

The modulus of elasticity of sand, gravel and a combination of sand and gravel is assumed respectively as 50,000 $\mathrm{kN/m^2}$, 150,000 $\mathrm{kN/m^2}$ and 100,000 $\mathrm{kN/m^2}$ (Rager, 2016). Then, the effective stiffness $\mathrm{k_{eff}}$ $(\mathrm{kN/m^2})$ of the steel-concrete composite considering the stiffness of the soil is computed according to equation (5.9).

$$k_{eff} = \left(\frac{1}{k_{composite}} + \frac{1}{k_{soil}} \right)^{-1} \tag{5.9}$$

5.1.3 Thermal Loads

Once the expansion joints are clogged and the bridge is exposed to a temperature variation, the superstructure is restrained from expanding. As a result, thermal stresses not predicted in the original design, are induced onto the girders and slab.

Thus, the corresponding thermal load P (kN) required to restrain the expansion movement of the superstructure, is accounted for in the first term of the interaction equation and can be computed according to equation (5.10).

$$P = k_{eff}\varepsilon L \tag{5.10}$$

Where $\mathrm{k_{eff}}$ (kN/m) is the effective stiffness of the steel-concrete composite considering the effect of the stiffness of the soil according to equation (5.9); ε is the strain of the steel-concrete composite; and L (m) is the length of the steel-concrete composite. Since the steel girder and the concrete slab act as a unit, the strain in the concrete is equal to the strain in the steel. Thus, the actual strain of the steel-concrete composite ε is presented in equation (5.11).

$$\varepsilon = \alpha_c \Delta T + \frac{1}{E_c}\frac{\Delta T(\alpha_s - \alpha_c)}{\left(\frac{1}{E_c} + \frac{A_c}{A_s E_s}\right)} = \alpha_s \Delta T - \frac{1}{E_s}\frac{A_c}{A_s}\frac{\Delta T(\alpha_s - \alpha_c)}{\left(\frac{1}{E_c} + \frac{A_c}{A_s E_s}\right)} \tag{5.11}$$

Where α_c and α_s ($^oC^{-1}$) are the coefficient of thermal expansion of concrete and steel; $\mathrm{A_c}$ and $\mathrm{A_s}$ $(\mathrm{m^2})$ are the cross sectional areas of the concrete slab and steel girder, respectively; and $\mathrm{E_c}$ and $\mathrm{E_s}$ are the modulus of elasticity $(\mathrm{kN/m^2})$ of the concrete and steel, respectively. In addition, the bending moment $\mathrm{M_T}$ (kN.m) due to the eccentric nature of the thermal axial load is calculated according to equation (5.12).

$$\mathrm{M_T = P.e} \tag{5.12}$$

Where P (kN) is the thermal load required to restrain expansion of the superstructure; and e (m) is the distance from the point of application of P, that is, half of the depth of the clogged joint to the center of gravity of the composite section.

5.1.4 Capacity of the Composite Section

The nominal strength M_n is based on plastic stress distribution on the composite sections and it is calculated according to equations (5.13) and (5.14). Tension in the concrete slab is neglected when the plastic neutral axis is in the slab since the tension resistance of concrete is low (Salmon & Johnson, 1996).

$$M_n = A_s F_y \left(\frac{d}{2} + t_s - \frac{a}{2}\right) \; for \; Plastic \; neutral \; axis \; (PNA) in \; the \; slab \qquad (5.13)$$

$$M_n = C_c d_2' + C_c d_2'' \; for \; Plastic \; seutral \; axis \; (PNA) \; in \; the \; steel \; beam \qquad (5.14)$$

Where A_s is the cross-section area of the steel girder; F_y is the steel girder yield stress and d, t_s, a, C_c (compressive force in the slab); d_2' and d_2'' (moment arms) are indicated in Figure 5.3. The geometric and resistances parameters are calculated according to sections 5.1.1 on Estimate of Girder and Slab Geometry.

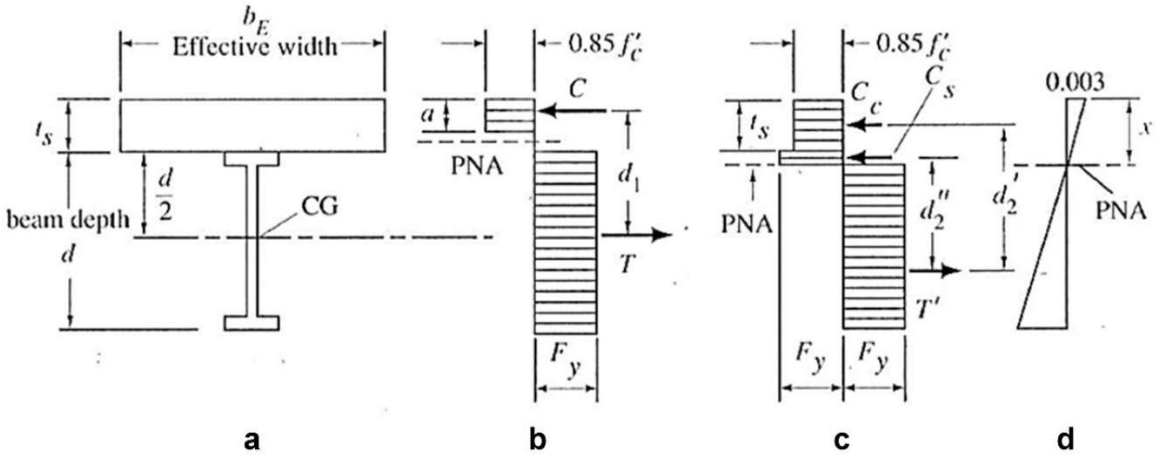

Figure 5.3 – a) Composite cross-section, b) Plastic stress distribution at nominal strength M_n when the plastic neutral axis is in the slab, c) Plastic stress distribution at nominal strength M_n when the plastic neutral axis is in the steel beam and d) Strain when nominal strength M_n is reached (Salmon & Johnson, 1996)

For the calculation of the compression capacity P_n of the composite section, the cross-sectional area of the concrete slab and the steel girder, and their respective resistances, compressive strength $0.85f'_c$ (MPa) of the concrete and yield stress F_y (MPa) of the steel, are considered.

5.1.5 IEV-Stress Relationship

The correlation between the maximum service stress levels on the composite cross-section at the extreme fibers and the IEV was developed. This relationship follows the equation (5.15).

$$\frac{\sigma}{\sigma_{allowed}} = \alpha \times \mathrm{IEV} + \beta \times \mathrm{L} + \rho \quad (5.15)$$

Where $\sigma_{allowed}$ is equal f_c' to determine σ_{top} and F_y for σ_{bottom}; σ_{top} is the maximum compression in service on the top of the concrete slab and σ_{bottom} is the maximum tension in service on the bottom of the steel girder. The coefficients α, β and ρ for concrete slab compressive strength of f_c'=25MPa are given in Table 5.1.

Table 5.1 – Coefficients α, β and ρ

Fy	Stress (kN/m^2)	α	β	ρ
50ksi (345MPa)	σ_{top}	1.14	-0.0063	0.0422
	σ_{bottom}	0.34	0.0167	0.2399
36ksi (248MPa)	σ_{top}	1	-0.0052	0.0245
	σ_{bottom}	0.36	0.0182	0.2104
26ksi (179MPa)	σ_{top}	0.88	-0.004	0.0127
	σ_{bottom}	0.41	0.0163	0.2381

5.1.6 Finite Element Model

An additional numerical finite element analysis was conduct in order to compare the numerical results with the analytical calculation (Salmon & Johnson, 1996) of service stresses on the composite cross-section at the extreme fibers. To that end, a bridge with known geometry and material resistances is selected from NBI and the finite element model is developed using SAP 2000 to simulate the behavior of the superstructure under uniform thermal load when the expansion joints are completely clogged. The temperature varies from the temperature at construction (Scenario 1 – average of minimum temperatures of winter for the location and year of construction of the particular bridge) to the projected temperature for 2100 (projected daily maximum temperature for the chosen bridge). The numerical model accounts for the stages of construction and service of the bridge as illustrated by Figure 5.4. Small geometry approximations necessary to conduct the analysis are applied and indicated in Table 5.2. The compressive strength of the concrete slab is 25 MPa and the yield strength of the steel girder is 50 ksi.

In the first stage, the girder is subjected to the action of dead loads – self-weight of girders and concrete slab (the absence of shoring is considered). Thus, initially only the girder is modeled, being discretized into 8-noded solid elements with appropriate steel properties assigned to them. The weight of the slab is applied as distributed load along the steel girder. In order to simulate the simply supported condition of the beam, vertical translation is restrained at both ends and also horizontal movement of one of the supports.

For the second stage, the concrete slab is modeled on the top flange of the girder and is also discretized with *solid* elements. *Spring* elements of type *gap* (active only under compression) are applied at both ends of the slab to simulate the clogged joints with stiffness of $10^{10}\,kN/m^2$. Then, live load in the form of an HL-93 truck plus lane load, and thermal loads corresponding to ΔT=52℃ are applied.

Table 5.2 – Geometry of the concrete slab and steel girder

Geometric Parameter	Dimension
Slab thickness	0.2m
Girder depth	1,118mm
Web thickness	8mm
Flanges width	44mm
Flanges thickness	356mm

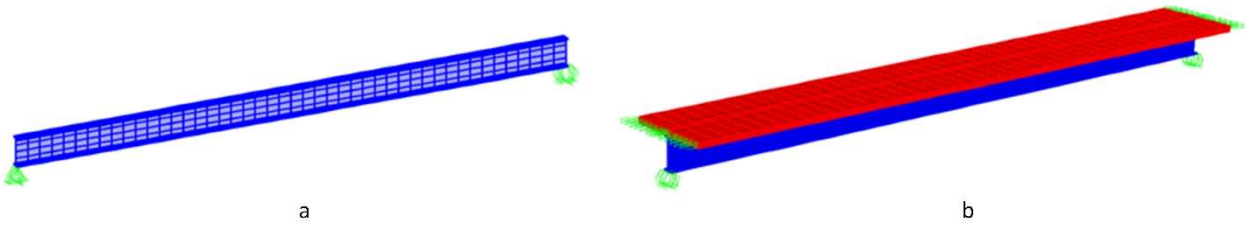

Figure 5.4 – Finite element model for the stages of a) construction and b) service of B-16-FM bridge

Table 5.3 shows the total service stresses (summation of first and second stage stresses) along the cross-section of the composite, obtained by the numerical model and analytical calculation.

Negative values mean compression while positive values imply tensile stress. The stresses obtained from the numerical model presents small variations when compared to the analytical calculation.

Table 5.3 – Total service stresses in the composite cross section from numerical model and analytical calculation

Stress	Analytical Calculation	Numerical Model	Variation
$\sigma_{slab,top}\ (kN/m^2)$	-28,468	-29,890	5%
$\sigma_{girder,bottom}\ (kN/m^2)$	261,867	258,054	-1%

5.2 Life Cycle Cost Analysis Models

5.2.1 Conventional Maintenance Practices

Effective maintenance is essential to keep the expansion joints clean and consequently functional to ensure serviceability and potentially safety of the bridges. Herein, a life cycle cost analysis of maintenance alternatives is conducted to select the approach that offer the best economic results without compromising structural safety in the management of the entire inventory of U.S. SSSG bridges.

The main direct costs related to maintenance used in this study are the cost of cleaning expansion joints C_c [twice a year (Kelly, 2017)] to avoid excessive clogging by debris and the cost of replacing the expansion joints C_r [every 3.5 years (Kelly, 2017)] due to deterioration caused by weather and traffic condition along the years. In addition, indirect costs resulting from bridge closure during maintenance are also computed. This type of cost is calculated as a percentage of the direct cost, using a factor γ, and function of the average daily traffic (ADT) obtained for each bridge from the NBI database. The assumed relationship between the ADT and γ is shown in Table 5.4. The reason for linking the indirect social and economic losses to ADT and for the direct relationship between the factor γ and the ADT is due to the obvious reason that the higher the ADT the higher the losses.

However, in that formulation, it is assumed that the indirect losses will be lower than or equal (in few cases) the direct losses, which will not always be true. It is realized that this is just a crude approximation of indirect social and economic losses and as such much more refined analysis is needed for more accurate assessment. However, this was outside of the scope of this study.

Table 5.4 – Factor γ as function of ADT

ADT	γ
50	0.2
500	0.4
5,000	0.6
50,000	0.8
>50,000	1

Thus, the total cost for the current practices of maintenance can be calculated as follows for each bridge.

$$C_{CP} = (C_c \times f_c \times L_{j,total} + C_r \times f_r \times L_{j,total}) \times (1 + \gamma) \quad (5.16)$$

Where, C_{CP} is the total cost (direct plus indirect costs) of the current maintenance practice; C_c is the cost of cleaning expansion joints; and C_r is the cost of replacing expansion joints. f_c and f_r are the frequecies of cleaning and replacing expansion joints, respectively. γ is a factor to calculate the indirect cost caused by parcial or total bridge closure when cleaning and replacing expansion joints, and in relation to ADT. $L_{j,total}$ is calculated according to expression (5.17):

$$L_{j,total} = L_j \times N_j \quad (5.17)$$

Where, L_j and N_j are the length and number of the expansion joints of the bridge, respectively, processed from the NBI. The present value cost due to maintenance is therefore calculate using a uniform series as given by equation (5.18).

$$P_V = C_{CP} \frac{(1+r)^n - 1}{r(1+r)^n} \quad (5.18)$$

Where, r is the interest rate; and n is the number of periods (years). Table 5.5 summarizes the constant parameters and the values used in this analysis.

Table 5.5 – Constant parameters used in the life cycle cost analysis (FHWA, 2002; Kelly, 2017)

Parameter	Value	Description
C_c	\$66/m	cost of cleaning expansion joints
C_r	\$1,148/m	cost of replacing expansion joints
f_c	0.5 years	frequency of cleaning expansion joints
f_r	3.5 years	frequency of replacing expansion joints
r	5%	interest rate

According to FHWA (2002), typical interest rates utilized in life cycle cost analysis varies from 3% to 5%. In this study, an interest rate of 5% was adopted, nevertheless, using different rates can lead to results different than those presented here.

Other parameters such as $L_{j,total}$ and ADT (this last is used to calculate γ) vary for each bridge and are obtained from NBI.

Initially, the costs associated with the abovementioned conventional maintenance practice are calculated to establish a cost reference. However, one should note that this approach neither accounts for climate scenarios for future years nor prioritize the most critical bridges in the national inventory. This current practice, named “A0” herein, represents the maintenance procedures in which the same treatment is given to all the bridges.

5.2.2 Alternative Maintenance Approaches and Assumptions

Alternatively, two new bridge maintenance approaches are proposed considering climate scenarios and the vulnerability of each structure (quantified by the IEVs) to establish a priority order of bridge maintenance to optimize financial resources. Therefore, the outcomes of the previous structural assessment presented in section 6.2 serve as inputs for the present economic analysis.

Alternative 1 (A1) considers performing cleaning of expansion joints twice a year only after the IEV equals to or exceeds 0.85 (this is checked for every bridge in the inventory independently).

While it is acknowledged that a bridge is more prone to develop a structural failure related to the combined loading effect when this value is unity, the reason for using a threshold value of 0.85 is to provide a safety margin. The replacement of expansion joints every 3.5 year is always considered, because the deterioration of expansion joints components is not function of the IEV. Thus, the cost of Alternative A1 for each U.S. SSSG bridge can be calculated according to equation (5.19).

$$C_{A1} = \begin{cases} if\ IEV \leq 0.85 \rightarrow (C_r \times f_r \times L_{j,total}) \times (1+\gamma) \\ if\ IEV > 0.85 \rightarrow (C_c \times f_c \times L_{j,total} + C_r \times f_r \times L_{j,total}) \times (1+\gamma) \end{cases} \quad (5.19)$$

The present value can be calculated according to equation (5.20).

$$P_V = C_{A1} \frac{(1+r)^n - 1}{r(1+r)^n} \quad (5.20)$$

The second alternative, Alternative 2 (A2), is a combination of maintenance and replacement of old bridges, i.e. demolition and construction of new ones. When a bridge under analysis meets the criteria of being 70 years in service and the IEV equals to or exceeds 0.9 this structure is replaced. However, up to the date of demolition regular replacement of expansion joints every 3.5 years is considered. After demolition, it is assumed that a new type of bridge design is adapted in which climate change effects are considered (e.g. expansion joints are not used). For other bridges that are not demolished, the cost of maintenance is the same as that of Alternative A1. Thus, the cost of alternative A2 for each bridge is given by the expression (5.21).

$$C_{A2} = \begin{cases} if\ IEV > 0.9\ and\ age \geq 70 \rightarrow (C_{br}) \times (1+\gamma) + (C_r \times f_r \times L_{j,total}) \times (1+\gamma) \\ else \rightarrow C_{A1} \end{cases} \quad (5.21)$$

Where, C_{br} is the cost of bridge replacement calculated by expression (5.22).

$$C_{br} = C_{dc} \times A_b \quad (5.22)$$

Where, C_{dc} is the unit cost per meter square of demolition and construction of a new bridge, estimated as \$2,895/m^2 using national average data (FHWA, 2019; MDOT, 2018) and A_b is the bridge deck area processed from the NBI. For the particular cost of bridge replacement, the present value is calculated according to equation (5.23), since it is a single cost event.

$$P_V = \frac{C_{br}(1+\gamma)}{(1+r)^n} \tag{5.23}$$

The present value of joint replacement which occurs prior to bridge demolition, is calculated using a uniform series.

The Alternative A1 and A2 are evaluated under each climate scenario separetely (RCP 2.6, 6.0 and 8.5) and considering the construction temperature scenario of fall. Moreover, the analysis uses the time intervals of 2020-2040, 2020-2060, 2020-2080 and 2020-2100, with 2020 the reference year for the present value. The interaction equation values for each year is obtained through a linear interpolation. Lastly, it is assumed a mix of gravel and sand as the material accumulated in the joints. All three maninance alternatives are listed in Table 5.6.

Table 5.6 – Summary of maintenance alternatives and respective costs involved

Alternative	Cost of expansion joints cleaning	Condition	Cost of expansion joints replacement	Condition	Cost of Bridge replacement	Condition
A0	✓	from 2020	✓	from 2020	-	-
A1	✓	if IEV≥0.85	✓	from 2020	-	-
A2	✓	if IEV<0.9 and/or age<70	✓	if IEV<0.9 and/or age<70	✓	if IEV≥0.9 and age≥70

6. ANALYSIS OF RESULTS

6.1 Introduction

Analysis of the results are presented in two main sections: 6.2 on Structural Assessment and 6.3 on Life Cycle Cost Analysis. The first section assesses the vulnerability of the bridges due to the coupled effect of clogged joints and temperature rise, in terms of the interaction equation. Moreover, the main variables expected to affect the integrity of the bridges are: the construction temperatures, type of material present in the clogged joints and projected temperatures for future years. Therefore, a sensitivity analysis is conducted to evaluate the impact of each one of those parameters on the results, which are later employed as inputs for the life cycle cost analysis.

The second part presents the life cycle cost analysis of the three expansion joints maintenance alternatives. The initial alternative mimics the conventional maintenance practices. The two other alternatives address the effect of climate scenarios and utilize the interaction equation value to prioritize maintenance of the most vulnerable bridges, which could ultimately aid in optimizing allocation of financial resources.

6.2 Structural Assessment

6.2.1 Sensitivity Analysis and Temperature Scenarios

The intensity of thermal stresses developed into the bridge superstructure when expansion joints are clogged does not depend on future temperature only, but also on the temperature at the time of construction of the bridge. Hence, the induced thermal stress is a function of the temperature range [equation (3.1)] and not of the absolute temperature value for which the bridge is subjected.

In order to determine these temperature ranges, there are two different types of scenarios to take into account: construction temperature scenarios and climate scenarios. The former one is associated with four seasonal temperature possibilities during bridge construction (winter, spring, summer, and fall), while the latter is related to the temperature for future years projected according to three different greenhouse gas concentration pathways (RCP 2.6, 6.0 and 8.5). Both types of scenarios are introduced in detail in Chapters 3 and 4.

To conduct the analysis, construction temperature scenarios and climate scenarios are combined as illustrated in Table 6.1. Each climate scenario (RCP 2.6, 6.0 and 8.5) is analyzed separately, considering four seasonal construction temperature possibilities (winter, spring, summer, fall) to obtain the temperature range for 2040, 2060, 2080, 2100, for each bridge

Table 6.1 – Scenarios matrix for temperature range

Temperature Range (ΔT) Combinations		Future Temperature → Climate Scenarios (RCP 2.6, 6.0, 8.5)			
		T_{2040}	T_{2060}	T_{2080}	T_{2100}
Construction Temperature Scenarios	T_{Winter} (1)	**$\Delta T = T_{2040} - T_{Winter}$**	**$\Delta T = T_{2060} - T_{Winter}$**	**$\Delta T = T_{2080} - T_{Winter}$**	**$\Delta T = T_{2100} - T_{Winter}$**
	T_{Spring} (2)	**$\Delta T = T_{2040} - T_{Spring}$**	**$\Delta T = T_{2060} - T_{Spring}$**	**$\Delta T = T_{2080} - T_{Spring}$**	**$\Delta T = T_{2100} - T_{Spring}$**
	T_{Summer} (3)	**$\Delta T = T_{2040} - T_{Summer}$**	**$\Delta T = T_{2060} - T_{Summer}$**	**$\Delta T = T_{2080} - T_{Summer}$**	**$\Delta T = T_{2100} - T_{Summer}$**
	T_{Fall} (4)	**$\Delta T = T_{2040} - T_{Fall}$**	**$\Delta T = T_{2060} - T_{Fall}$**	**$\Delta T = T_{2080} - T_{Fall}$**	**$\Delta T = T_{2100} - T_{Fall}$**

The most optimistic scenario is obtained combining the lower forcing climate scenario RCP 2.6 with the construction temperature during the summer season (Scenario 3), which gives the smallest temperature range. In contrast, the largest temperature range is obtained by the most conservative higher forcing climate scenario RCP 8.5 and construction temperature during winter (Scenario 1). Intermediate scenarios are given by RCP 6.0 and considering either, construction temperature during spring or fall (Scenarios 2 or 4, respectively). Nevertheless, other possible combinations that lead to other temperature range outcomes such as RCP 2.6 or RCP 8.5 and fall are also evaluated. In these cases, the purpose is to simulate future temperatures ranges given by these two extreme climate scenarios (lowest and highest forcing), although considering midway construction temperatures. Furthermore, once the construction and future temperatures depends on the geographic position of the bridges, a spatial analysis throughout the U.S. territory is also conducted.

Another variable considered is the modulus of elasticity of the soil accumulated in the bridge joints. Different types of debris such as sand or gravel for instance, can lead to different levels of movement restriction and stresses into the superstructure. Thus, a sensitivity analysis of all these main variables abovementioned is presented in the next sections.

6.2.2 Construction Temperature

Since the temperature at the time of installation of the expansion joints is unknown, the construction temperature of each bridge is estimated based on its year of construction conclusion (data available in the NBI) and the climate region. As a result, four possible temperature construction scenarios are proposed: winter (Scenario 1), spring (Scenario 2), summer (Scenario 3) and fall (Scenario 4), as described previously in Chapter 3.

For the investigation of the effect of each temperature construction scenario on the response of U.S. SSSG bridges under clogged condition associated with temperature rise, other variables such as climate scenarios and the type of debris material were kept fixed. Thus, the intermediate climate scenario RCP 6.0 and a mix of sand and gravel were selected to conduct this initial analysis. The results for 2100 (long-term), as an example, are presented as histograms shown in Figure 6.1. and Table 6.2.

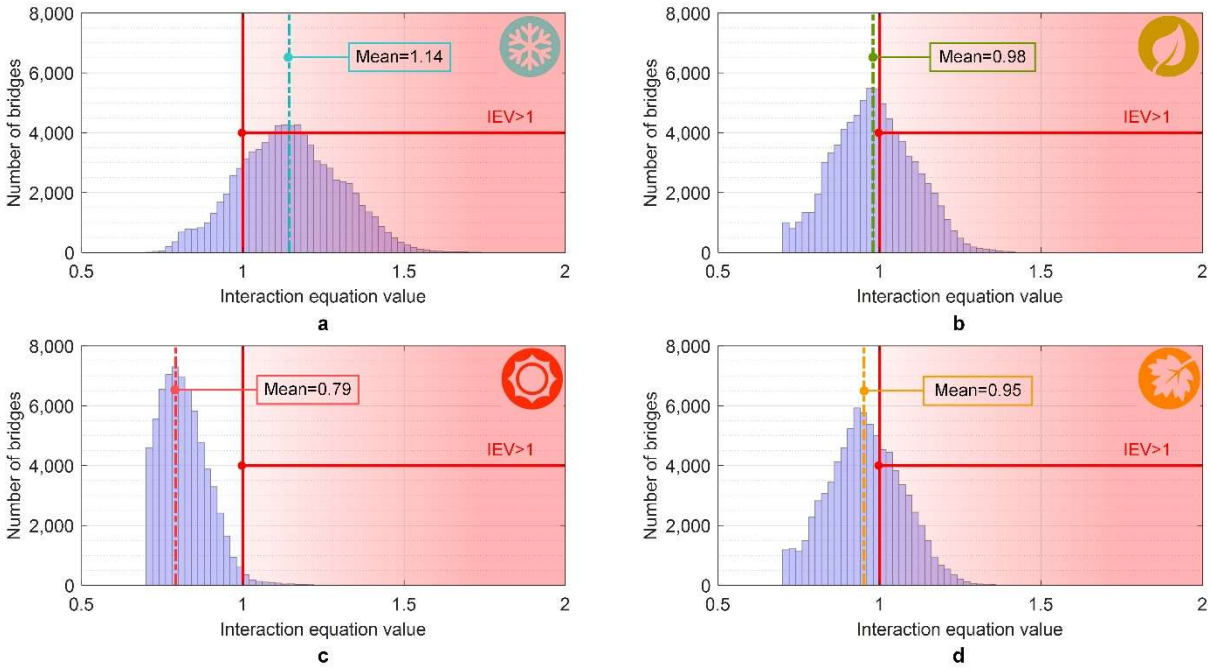

Figure 6.1 – Histograms of the interaction equation value (IEV) for 2100 and RCP 6.0 considering a) Scenario 1 (winter), b) Scenario 2 (spring), c) Scenario 3 (summer) and d) Scenario 4 (fall)

Table 6.2 – Comparison of temperature ranges, percentage of bridges with IEV>1, and national average IEV for different construction temperature seasonal scenarios (results for year 2100)

Parameter Range	winter (Scenario 1)	spring (Scenario 2)	summer (Scenario 3)	fall (Scenario 4)
ΔT Min (℃)	29	22	13	22
ΔT Avg (℃)	47	37	26	35
ΔT Max (℃)	66	52	44	51
ΔT SD (℃)	5.5	4.4	3.6	4.1
IEV>1 (%)	82	43	1	34
IEV Avg	1.14	0.98	0.79	0.95

As expected, the largest temperature ranges occur when bridges are built during winter and lowest for summer. For instance, as shown in Table 6.2, the average ΔT for bridges built in winter (47℃) is 81% percent higher than average ΔT for those built in summer (26℃). Also, the winter construction scenario results in the largest standard deviation, which means a larger variation of ΔT along the country. The consequence is a more spread histogram as illustrated in Figure 6.1.

In addition, the long-term analysis for projected temperatures in 2100 shows that 82% of the SSSG bridges in the U.S. have above 1 the value for the interaction equation, for the most severe construction scenario – “Scenario 1” (assumption of bridges being built during the winter), followed by 43%, 1% and 34% for Scenario 2 (spring), Scenario 3 (summer) and Scenario 4 (fall) respectively, as presented in the histograms of Figure 6.1. The portion of the histograms in the red region corresponds to bridge failures.

These percentages indicate the amount of bridges in which the demand-to-capacity ratio would be beyond the structural design limits, if no intervention is made. The larger percentage of bridges failures (82%) occur for the hypothesis in which the bridges construction took place during the winter, because it provides the larger ranges of temperatures, varying from the lowest seasonal temperatures to the projected temperatures for 2100. For the assumption of construction in spring or fall, the failures reduce approximately by half (43% and 34% respectively) compared to the winter scenario. Finally, failures projection for 2100 drop to 1% if summer construction scenario is considered, characterizing it as the most optimistic scenario. In addition, Figure 6.1 indicates the projection of the average interaction equation value (IEV) for each construction scenario: 1.14 (winter), 0.98 (spring), 0.79 (summer) and 0.95 (fall). Therefore, one can clearly observe the significance of construction temperatures in the evaluation of bridges vulnerability to the coupled effect of clogged joints and thermal load.

6.2.3 Types of Debris Material

The interaction equation values shown in Figure 6.1 assume that the accumulated debris between the joints comprises of a mix of gravel and sand. However, these values are expected to change if different material is used in the analysis. Therefore, in this second stage of the analysis, the year (2100) and RCP (6.0) remain fixed, while the temperature construction scenarios vary (winter, spring, summer and fall) and now different materials are simulated such as gravel, sand, mix of gravel and sand, and the pinned condition as summarized in Table 6.3. The pinned condition is an idealization of the presence of incompressible materials in the joints.

Table 6.3 – Average interaction equation value (IEV) and percentage of bridges failure for 2100 and RCP 6.0 as function of type of joint debris and construction scenario

	Pinned		Gravel		Mix of Gravel and Sand		Sand	
Scenario	Avg IEV	IEV≥1	Avg IEV	IEV≥1	Avg IEV	IEV≥1	Avg IEV	IEV≥1
Winter (1)	1.51	99%	1.24	91%	1.14	82%	0.96	36%
Spring (2)	1.27	92%	1.05	63%	0.98	43%	0.83	3%
Summer (3)	0.99	46%	0.84	7%	0.79	1%	0.69	0%
Fall (4)	1.23	90%	1.02	56%	0.95	34%	0.81	1%

Since the pinned case reflects a severe condition where the girders are completely restricted from expansion, it results in the largest IEV for all construction scenarios and consequently, the greater incidence of bridge failures, which can be considered a very conservative assumption. On the other hand, sand debris, which have the lowest modulus of elasticity and so the spring coefficient, result in the smallest interaction equation values and percentage of failures. Mix of gravel and sand considers the existence of different size of materials in the debris composition, which is more representative of field conditions, and as such provides intermediate IEVs. Thus, further analysis was carried out considering a mix of gravel and sand to simulate realistic joint debris.

6.2.4 Climate Scenarios

To extend the analysis to the other two climate scenarios RCP 2.6 and 8.5, the fall construction scenario (Scenario 4) was selected by the fact that it accounts for intermediary temperatures during construction, instead of extreme temperatures. Moreover, now the assessment of years 2040, 2060 and 2080 were included to simulate the structural bridge conditions considering the interaction equation value. The evolution of the mean interaction equation value over future years for each RCP is compared in Figure 6.2 and Table 6.4.

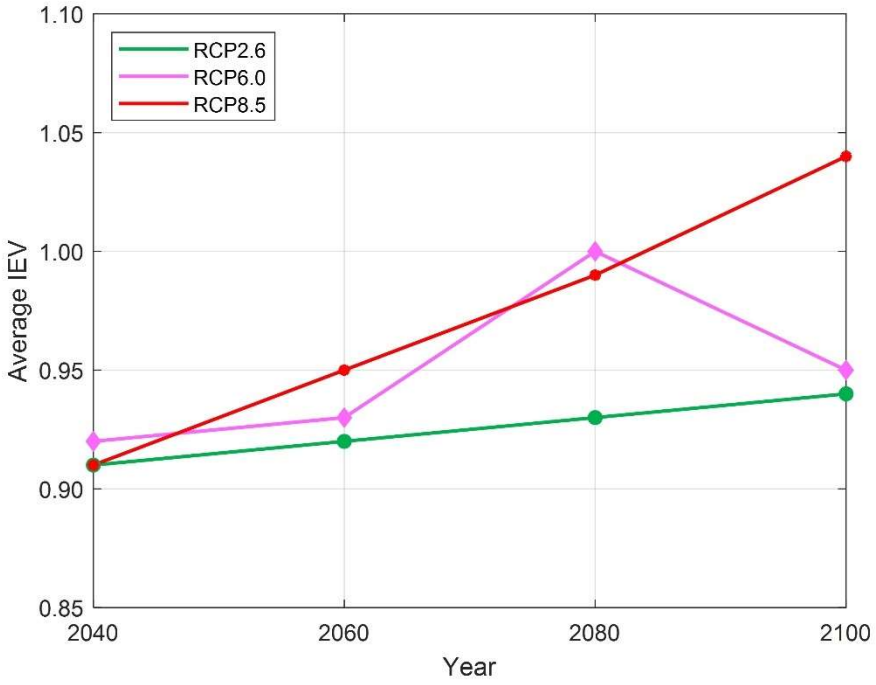

Figure 6.2 – Comparison of average IEV between different RCP scenarios over future years (for fall construction temperatures scenario and mixed gravel and sand debris)

Table 6.4 – National average IEV and IEV≥1 for each RCP over future years (for fall construction temperatures scenario and mixed gravel and sand debris)

Climate Scenario	2040	IEV≥1	2060	IEV≥1	2080	IEV≥1	2100	IEV≥1
RCP 2.6	0.91	21%	0.92	25%	0.93	30%	0.94	31%
RCP 6.0	0.92	24%	0.93	28%	1.00	49%	0.95	34%
RCP 8.5	0.91	22%	0.95	34%	0.99	46%	1.04	62%

For climate scenario RCP 2.6, there is a discrete increase of average IEV from 0.91 in 2040, 0.92 in 2060, 0.93 in 2080 and 0.94 in 2100. In the case of RCP 6.0, the average IEV also slightly increases from 2040 to 2060 (0.92 to 0.93), reaching a peak value of 1 in 2080, which equals the limit value. Then, in 2100 the IEV decreases to 0.95. RCP 8.5 shows an average IEV of 0.91 in 2040, and it gradually rises until 1.04 in 2100, surpassing the unity limit.

Since a single construction scenario was set (Scenario 4 - Fall) to evaluate the average IEV along future years under three distinct climate scenarios, one can clearly realize that the behavior of the IEV follows the pattern of the future temperature trend previously described in Figure 4.8.

Another interesting finding is that the average IEV increases linearly with the average temperature range (ΔT) projected for 2040, 2060, 2080 and 2100 regardless the climate scenario (RCP's). Specifically, each 1°C increment added to ΔT (difference between the future temperature and the base temperature of bridge construction) increases the interaction equation by approximately 2% according to the equation indicated in Figure 6.3. This trend line signalizes a continuous reduction of bridge integrity throughout the country over future years, if the issue concerning clogging of joints of SSSG bridges is not properly addressed.

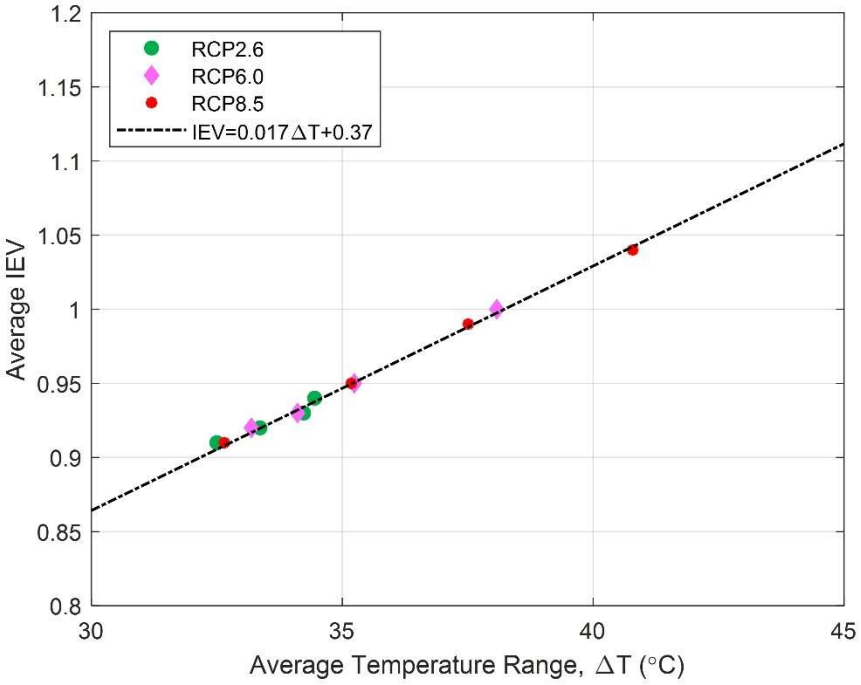

Figure 6.3 – Average IEV as function of average temperature range

In addition, the interaction equation value of each bridge can be translated to relative service stress on the top of the concrete slab or bottom of steel girder (most demanded regions) according to equation (5.15). Figure 6.4 shows the plots of relative stress of each U.S. SSSG bridges considering the RCP 6.0 over future years. These plots show the ratio of actual tensile stress on girder bottom to steel yielding stress $(\sigma_{girder,bottom}/F_y)$ on the x-axis and the corresponding ratio of compressive stress on slab top to concrete compressive strength $(\sigma_{slab,top}/fc')$ on the y-axis. When one of these relative ratios exceed unity, it represents failure (not implying system collapse but rather failure of the cross section). Thus, the points coinciding or laying outside the horizontal and vertical boundary lines represents bridges demanded beyond their capacity.

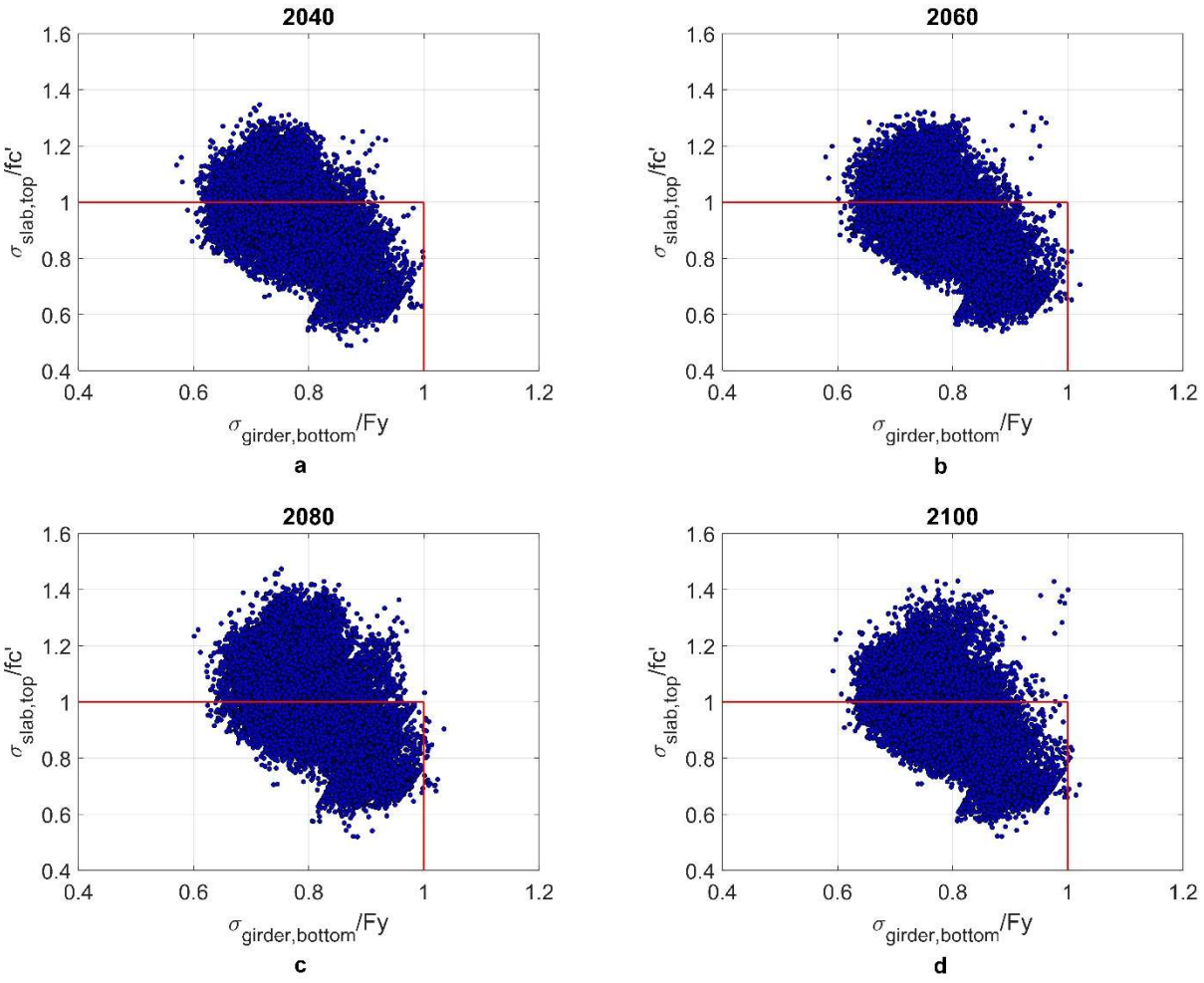

Figure 6.4 – Relative stresses in the girders of U.S. SSSG bridges for RCP 6.0 and Scenario 4 (fall) over future years

One can realize the evolution of possible failure along future years, where crushing concrete ($\sigma_{slab,top}/fc' \geq 1$) prevails over failures in steel. The number of bridges that surpasses its capacity for intermediate forcing scenario RCP 6.0 is approximately 27,000 (2040), 31,000 (2060), 46,000 (2080) and 36,000 (2100). The same analysis was carried out for the other RCP's and the results are summarized in Table 6.5 and Figure 6.5.

Table 6.5 – Number and percentage of bridges that exceed the structural capacity

Scenario	2040		2060		2080		2100	
	Total	Percent.	Total	Percent.	Total	Percent.	Total	Percent.
RCP 2.6	23,608	29%	27,774	34%	31,602	38%	33,027	40%
RCP 6.0	26,829	33%	31,293	38%	46,163	56%	35,864	43%
RCP 8.5	24,178	29%	35,845	43%	45,039	55%	55,186	67%

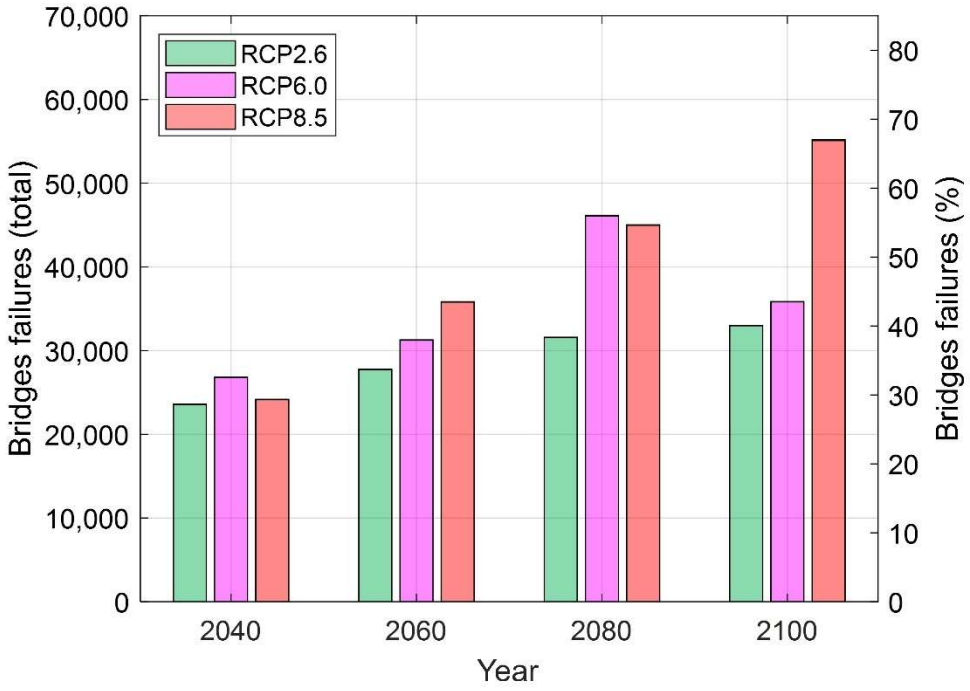

Figure 6.5 – Number of bridges failures over the years for each RCP, considering Scenario 4 (fall)

One should note that the difference in the number of bridges damaged, considering the different RCP's becomes more expressive after 2060. For instance, in 2100 the results diverge dramatically from one climate scenario to another, from 40% of bridges for RCP 2.6 to almost 70% for RCP 8.5, showing that the climate change impacts are more pronounced in long-term periods.

6.2.5 Geographic Analysis

A geographic analysis is conducted for three scenarios:

1. Optimistic scenario: future temperatures projected under lower forcing scenario RCP 2.6 and construction temperatures of summer (Scenario 3);
2. Intermediate scenario: future temperatures projected under intermediate forcing scenario RCP 6.0 and construction temperatures of fall (Scenario 4);
3. Conservative scenario: future temperatures projected under higher forcing scenario RCP 8.5 and construction temperatures of winter (Scenario 1).

For all scenarios it was assumed that the accumulated debris in the joints comprises of a mix of gravel and sand.

Figure 6.6 indicates that the average IEV of most states increases with the amplification of RCP. RCP 2.6 allows for the lowest IEVs in a way that the totality of states range from 0.5-1.0 along the future years. For the intermediate climate scenario RCP 6.0, one can observe the most affected regions are the Northwest, Northern Rockies & Plains, Upper Midwest and West, where the average IEV gradually increases from 0.5-1.0 to 1.0-1.5 over the years. The peak is reached in 2080 where 14 states exceeds the limit of one (double of the states in 2040), followed by a slight decrease in 2100 where 12 states are in the 1.0-1.5 range. One can note the substantial influence of projected temperatures on the progress of IEV. Finally, as expected, RCP 8.5 provides the higher IEV ranges. In 2040, almost 90% of the states already presents the average IEV in the 1.0-1.5 range (critical condition). These observations indicate the significant sensibility of the bridges to a potential changing climate.

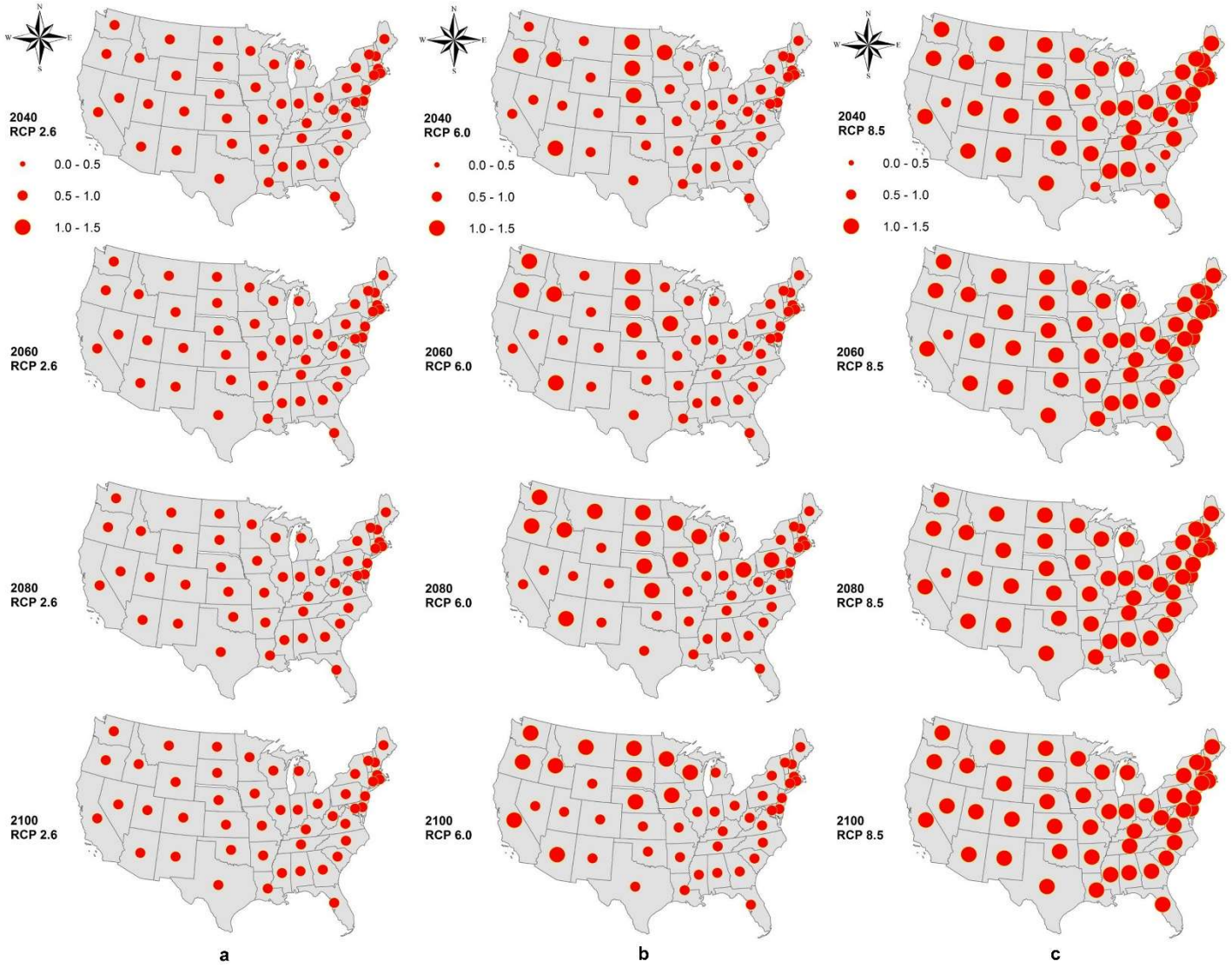

Figure 6.6 – Ranges of interaction equation value by state over the years for a) RCP 2.6 and Scenario 3 (summer), b) RCP 6.0 and Scenario 4 (fall) and c) RCP 8.5 and Scenario 1 (winter)

Another result of this spatial analysis is the evolution of the average of interaction equation value over the years for U.S. bridges per climate region, as shown in Figure 6.7. Such analysis highlights the progressive increase of the undesirable thermal demand imposed on the bridges over the years when there is insufficient maintenance.

Regardless of the RCP used in the analysis, the most critical regions in descending order are: Northern Rockies & Plains, Northwest, Upper Midwest and West. In contrast, the less susceptible regions are the Southeast followed by the Northeast. The regions of Southwest, South and Ohio Valley present intermediate level of vulnerability.

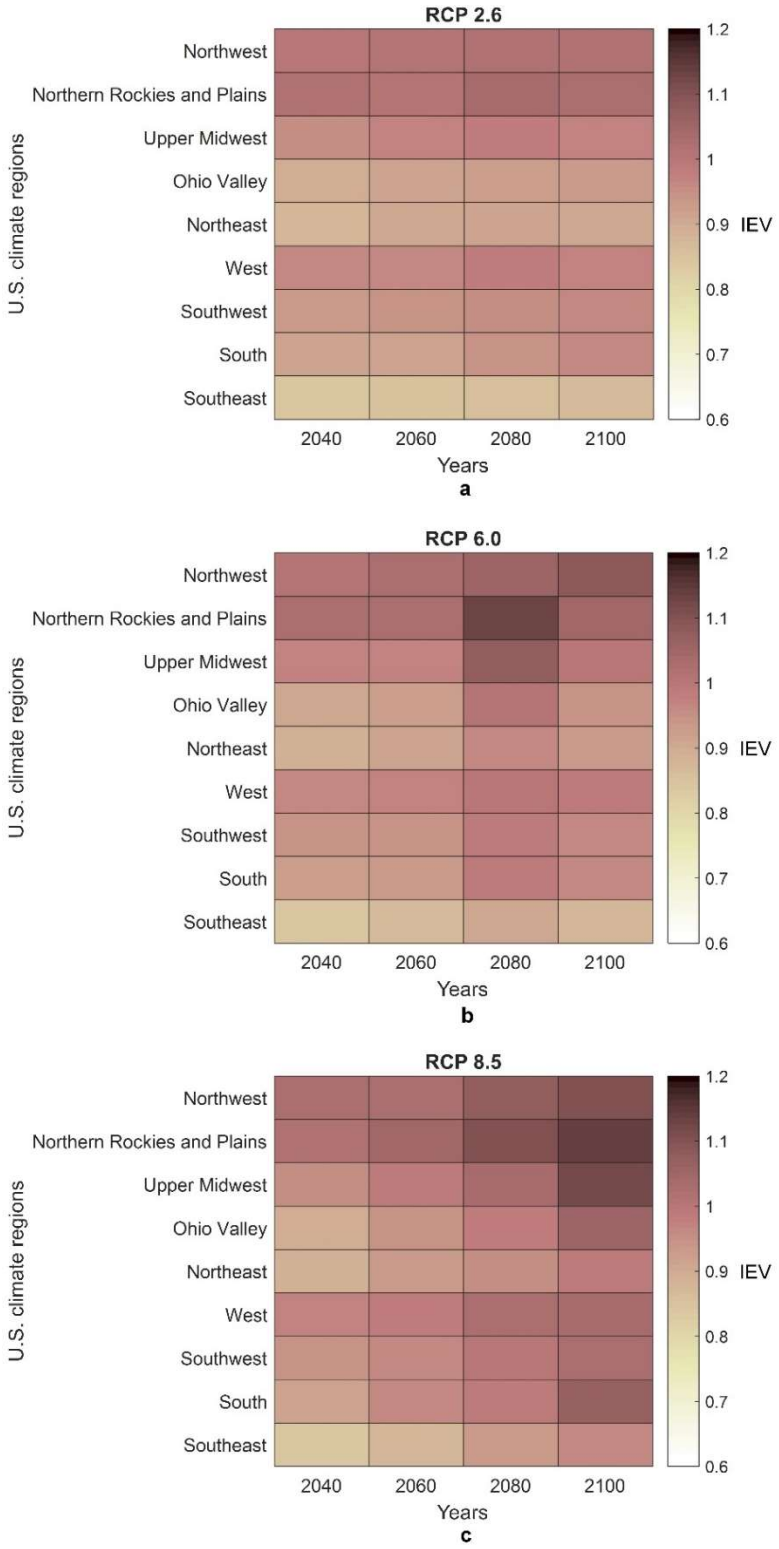

Figure 6.7 – Variation of average interaction equation value (IEV) projected over future years for each U.S. climate region considering a) RCP 2.6, b) RCP 6.0, c) RCP 8.5

6.3 Life Cycle Cost Analysis

Herein, the results of the life cycle cost analysis for alternatives A0, A1 and A2 are presented considering the three climate scenarios RCP 2.6, 6.0 and 8.5. The purpose is to define the alternative that presents the low cost yet preserving the structural safety and serviceability of the SSSG bridges inventory. Moreover, an assessment per state is conducted. In overall, the objective of the analysis is to allow for provide insight on prioritizing allocation of financial resources and quantify potential impact of climate change over management practices in bridge maintenance at state and national level.

6.3.1 Results for Alternative A0

Alternative A0 represents current maintenance practices costs. The results for this alternative consider equation (5.18) and parameters of Table 5.4 and Table 5.5 and are shown in Table 6.6. These results are further used as a reference for comparison with other alternatives.

Table 6.6 – Present Values for alternative A0 for U.S. SSSG bridges

Year	Present Values (US$x10^6)
2040	20,503
2060	28,231
2080	31,143
2100	32,241

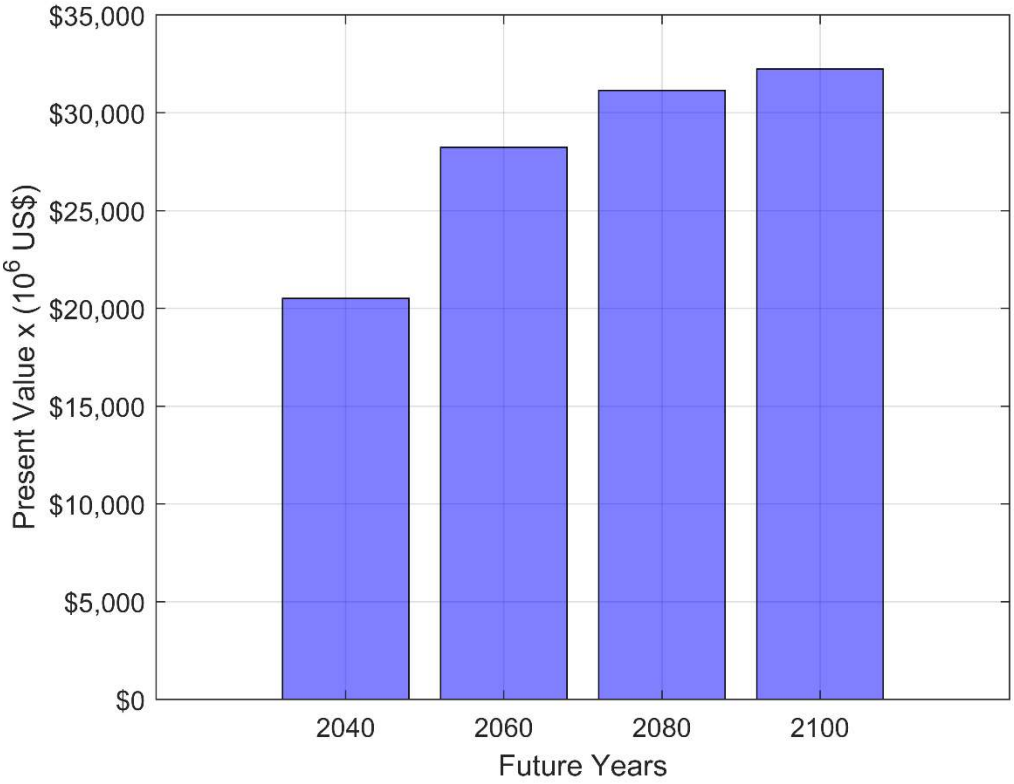

Figure 6.8 – Present values for time intervals 2020-2040, 2020-2060, 2020-2080 and 2020-2100 of alternative A0 for U.S. SSSG bridges

The graph of Figure 6.8 presents the maintenance cost of alternative A0 for the time intervals 2020-2040, 2020-2060, 2020-2080 and 2020-2100 brought to present values (2020 as reference year). This alternative does not account for climate scenarios nor the degree of expansion joints deterioration due clogging by debris but applies the same maintenance treatment to each bridge. Therefore, the cost variation is attributed exclusively to the interest rate parameter.

6.3.2 Results for Alternative A1

Alternative A1 introduces the IEV from the structural assessment into the life cycle cost model to consider the vulnerability of each bridge and thus establish a priority order of maintenance.

Therefore, bridges with IEV less than the threshold of 0.85 at the year under analysis are exempt of expansion joints cleaning cost. Since the projected IEV varies with the climate scenarios, this alternative is examined for RCP 2.6, 6.0 and 8.5. It is important to highlight that the costs of joints replacement every 3.5 are in included in the analysis, regardless of the computed IEV. The results for this alternative consider equation (5.20) and parameters of Table 5.4 and Table 5.5 and are shown in Table 6.7 and Figure 6.9.

Table 6.7 – Present Values for alternative A1 for each climate scenario

Present Values (US$x10^6)	2040	2060	2080	2100
RCP 2.6	16,454	22,656	24,994	25,875
RCP 6.0	16,840	23,188	25,581	26,482
RCP 8.5	17,518	24,344	26,937	27,915

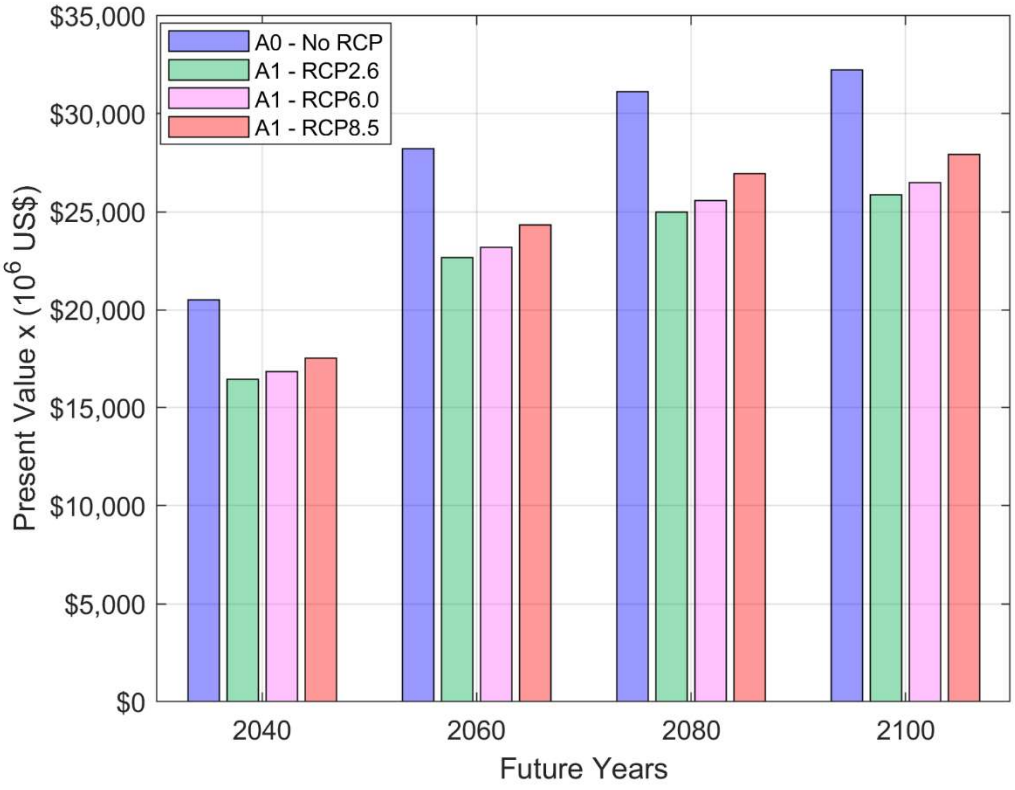

Figure 6.9 – Present values for time intervals 2020-2040, 2020-2060, 2020-2080 and 2020-2100 of alternative A1 under RCP 2.6, 6.0 and 8.5

As expected, the cost of maintenance varies with the climate scenarios where the smallest, medium and largest costs result respectively from RCP 2.6 (lower forcing scenario),

RCP 6.0 (intermediate forcing) and RCP 8.5 (higher forcing) in all time intervals analyzed. As an example, for a long-term analysis as 2020-2100, the projected costs for alternative A1 under RCP 2.6, 6.0 and 8.5 are respectively 25.9, 26.5 and 27.9 billion of dollars. One can also note that the costs of alternative A1 are always lesser than A0, even for the worst-case scenario RCP 8.5. The reason is attributed to savings associated with costs of cleaning expansion joints as discussed further in 6.3.4.

6.3.3 Results for Alternative A2

Alternative A2 combines the maintenance procedures of A1 with a bridge replacement approach. For each year under analysis, this model identifies the structures that are old (70 years or older) and prone to structural failure (IEV≥0.9) to be replaced. The results for this alternative consider equations (5.21) to (5.23) and parameters of Table 5.4 and Table 5.5 and are shown in Table 6.8.

Table 6.8 – Present Values for alternative A2 for each climate scenario

Present Values (US$x10^6)	2040	2060	2080	2100
RCP 2.6	22,964	28,145	30,045	30,759
RCP 6.0	25,200	30,339	32,228	32,938
RCP 8.5	23,673	30,831	33,110	33,678

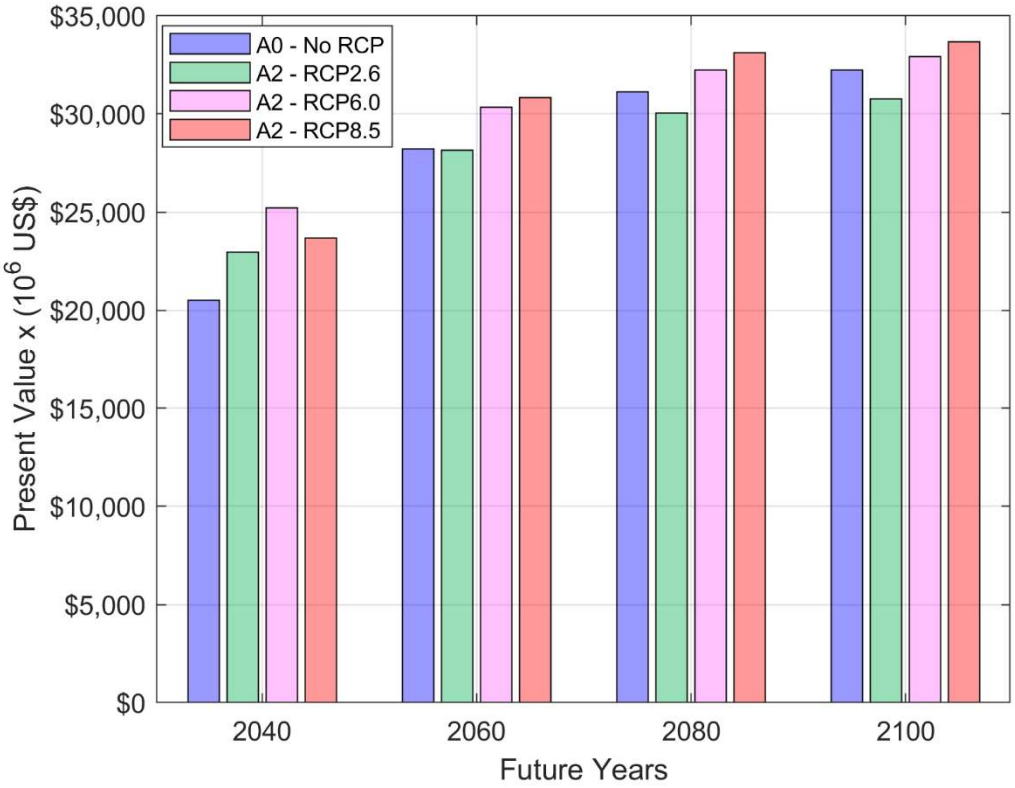

Figure 6.10 – Present values for time intervals 2020-2040, 2020-2060, 2020-2080 and 2020-2100 of alternative A2 under RCP 2.6, 6.0 and 8.5

The bar graph of Figure 6.10 shows that for medium to long-term analysis (2060, 2080,2100), RCP 2.6 generates the lowest costs, RCP 6.0 intermediate costs and RCP 8.5 the highest costs. Moreover, one can observe that for RCP 2.6 alternative A2 is more economical (even involving costs of bridges replacement) than A0 (2060, 2080,2100). However, for RCP 6.0 and RCP 8.5, A0 is less costly and as such is considered a better option. The main reason is because the number of bridges eligible for demolition and reconstruction for climate scenario RCP 2.6 is less than for RCP 6.0 and 8.5 as presented further in section 6.3.4.

6.3.4 Discussion and Comparison of Alternatives

Table 6.9 summarizes the life cycle cost (in present values) of alternatives A0, A1 and A2 for the climate scenarios RCP 2.6, 6.0 and 8.5. One can observe that the present values of alternative A0, which represents conventional maintenance practices, are not affected by potential climate scenarios (different from A1 and A2).

The best alternative is A1, which presents the lowest present values for all time intervals analyzed and under all climate scenarios. The reason for the economic savings provided by this alternative is the fact that in this alternative the IEV is used in the life cycle cost model to identify bridges that require cleaning of expansion joints. While some bridges in the national inventory will exhibit a higher IEV as soon as year 2040 hits, others will reach the limit value of one in years later or even after 2100. In these last cases there is no need to address the cost of cleaning expansion joints, since the bridges present an IEV below the threshold.

Comparing the other two alternatives, A0 with A2, one can observe that A0 prevails over A2 for RCP 6.0 and 8.5, since under these intermediate and higher forcing scenarios more old bridges (70 years or older) reach the IEV threshold for replacement of the structure in comparison to the lower forcing RCP 2.6, which leads to significant costs associated to demolition and construction. Table 6.9 summarizes the cost of the alternatives for the different RCP's scenarios.

Table 6.9 – Summary of present values for alternatives A0, A1 and A2 for each climate scenario

Climate Scenario	Present Values (US$x10^6)	2040	2060	2080	2100
RCP 2.6	A0	20,503	28,231	31,143	32,241
	A1	16,454	22,656	24,994	25,875
	A2	22,964	28,145	30,045	30,759
RCP 6.0	A0	20,503	28,231	31,143	32,241
	A1	16,840	23,188	25,581	26,482
	A2	25,200	30,339	32,228	32,938
RCP 8.5	A0	20,503	28,231	31,143	32,241
	A1	17,518	24,344	26,937	27,915
	A2	23,673	30,831	33,110	33,678

6.3.5 Economic Impact of Climate Scenarios on U.S. SSSG Bridges

One overview about the total cost associated with climate change scenarios can be obtained observing the difference between the cost of RCP 8.5 and 2.6 or RCP 6.0 and 2.6 for the chosen alternative A1, as illustrated in Figure 6.11. The RCP 2.6 is taken as reference since it provides the lowest cost (among the climate scenarios) along the years.

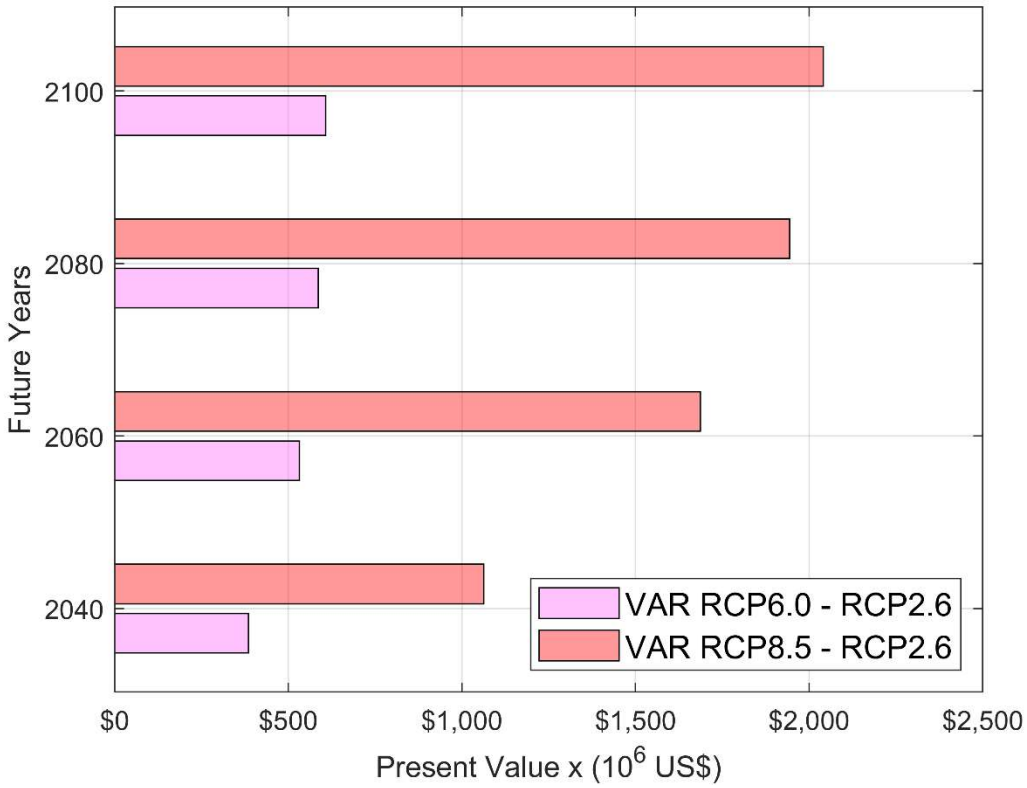

Figure 6.11 – Cost variations for alternative A1.

Observing the present values in Figure 6.11 one can realize that for a long-term analysis the intermediate scenario (RCP 6.0) results in an additional maintenance cost of $600 million while the projection for the most unfavorable scenario (RCP 8.5) results in an extra expenditure of $2 billion.

It is important to note that these projected costs of climate change are related to maintenance of expansion joints of SSSG bridges. Other potential costs associated with other changes in climate such as flooding, scour of pier and abutment foundation are not considered in this study.

6.3.6 Life Cycle Cost Analysis by State

Once alternative A1 was identified as the best alternative for providing the lowest maintenance costs, an analysis at state level is carried out. The cost related to expansion joint replacement was excluded because it does not depend on climate scenarios. Figure 6.12 to Figure 6.14 shows the unit cost of maintenance (cleaning) by bridge area for each state under RCP 2.6 to 8.5. The costs refer to present value considering the year 2100.

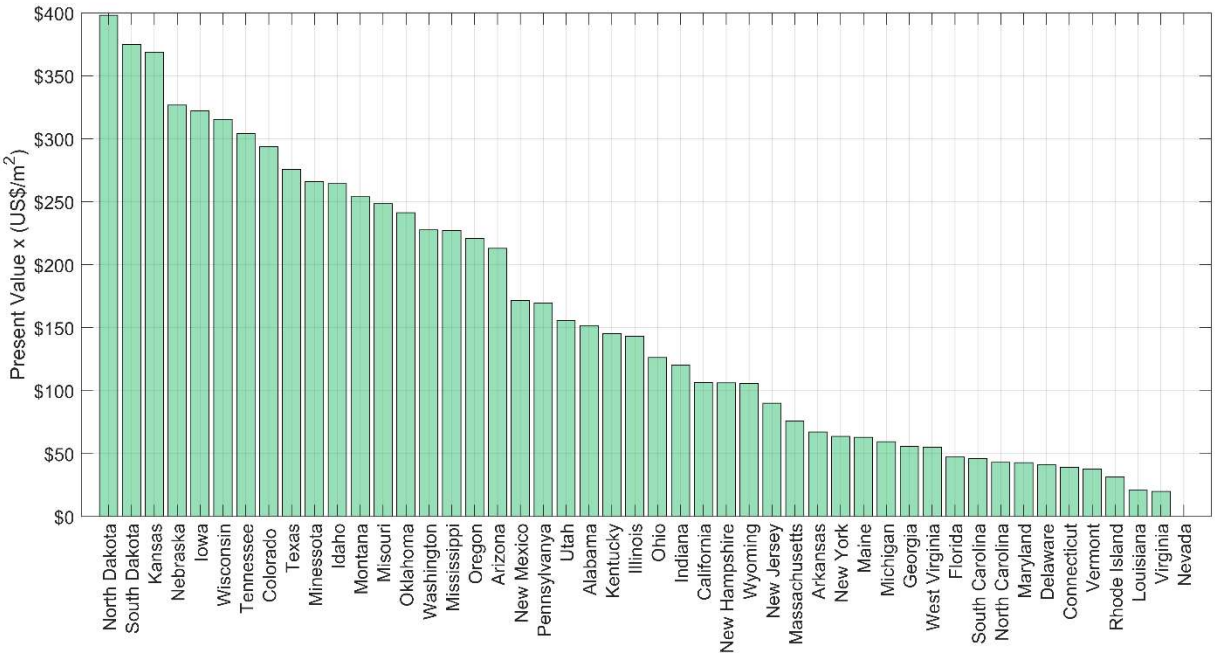

Figure 6.12 – Alternative A1 costs (present values) of expansion joints cleaning per area for states projected to 2100 under RCP 2.6

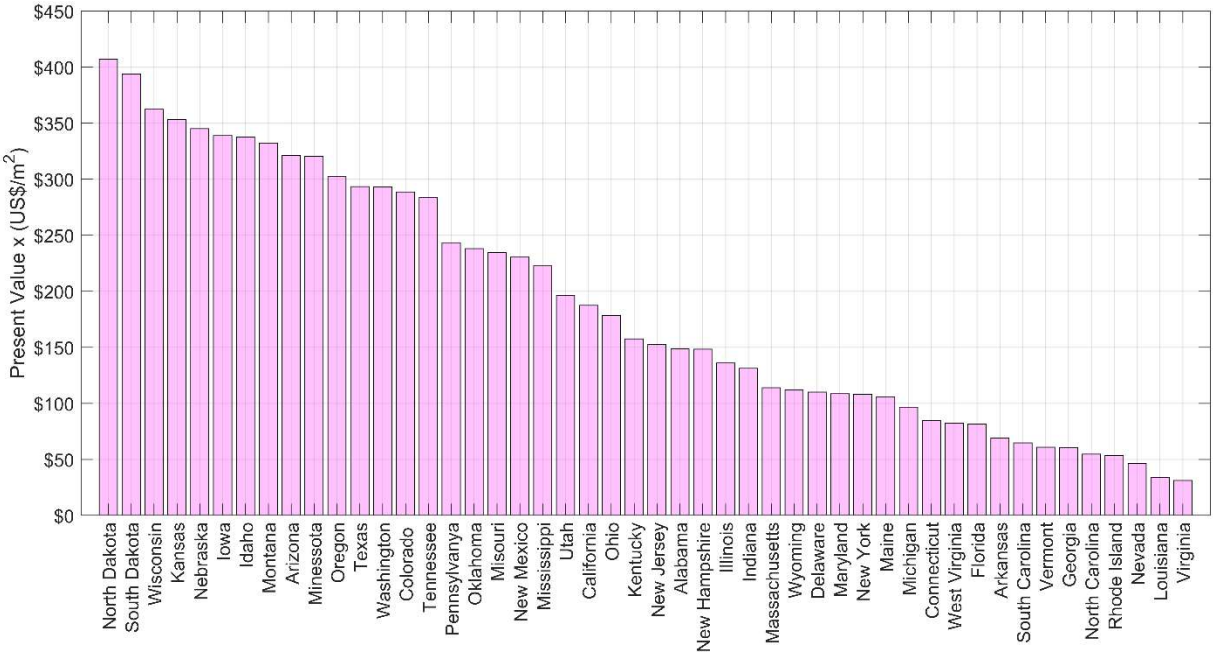

Figure 6.13 – Alternative A1 costs (present values) of expansion joints cleaning per area for states projected to 2100 under RCP 6.0

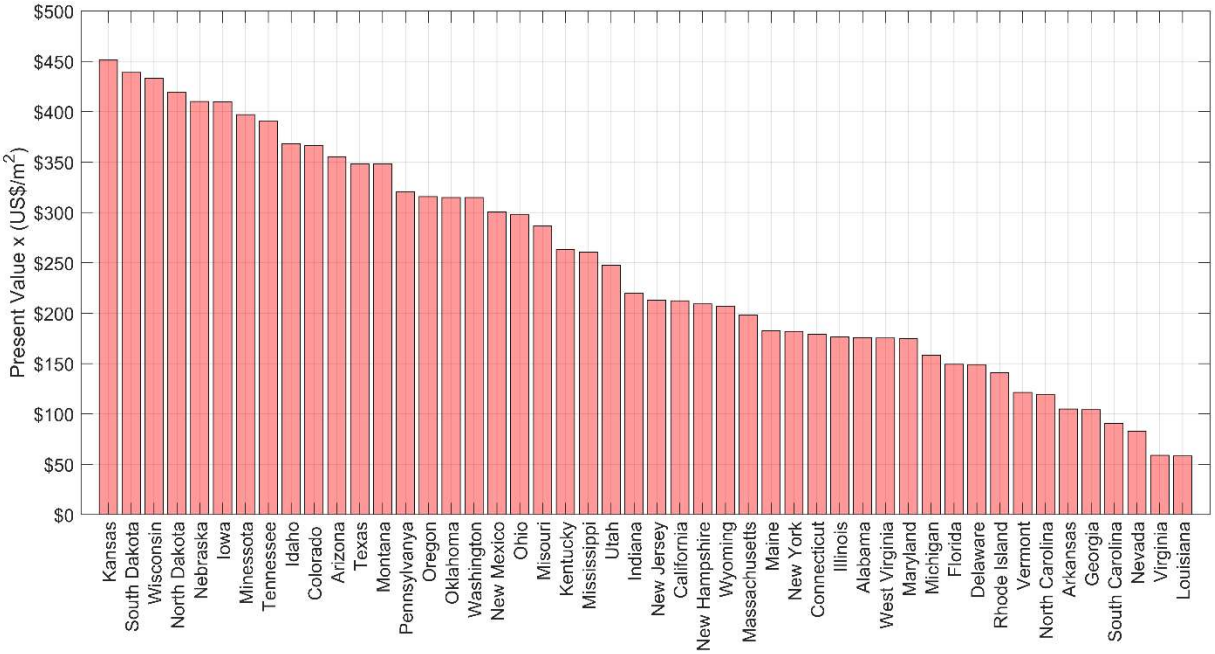

Figure 6.14 – Alternative A1 costs (present values) of expansion joints cleaning per area for states projected to 2100 under RCP 8.5

As one can observe, the unit cost ranges from \$0 (Nevada) to \$398/m^2 (North Dakota) for RCP 2.6; \$31 (Virginia) to \$407 (North Dakota) for RCP 6.0; and \$58 (Louisiana) to \$452 (Kansas) RCP 8.5.

The left half of the graphs (most costly) contains states that are located particularly in the north, central and west regions of the U.S., while the right half includes most states on the east coast. Finally, North Dakota, South Dakota, Kansas, Nebraska, Wisconsin, Iowa are the costliest states regardless the climate scenario (RCP 2.6, 6.0, 8.5).

7. SUMMARY, CONCLUSION, AND FUTURE WORK

7.1 Summary and Concluding Remarks

In this study, a new framework was developed to assess the structural vulnerability and estimate maintenance costs over an extensive inventory of approximately 80,000 SSSG bridges in the U.S., considering potential climate change effects over future years. The IEV was utilized to quantify the level of susceptibility of the bridges to the effects of projected temperature ranges associated with malfunction of expansion joints due to clogging by road debris. The focus was on the load carrying capacity of the superstructure, comprised of girder-slab composite. This assessment allowed for a quick identification of the most critical structures. In order to consider the thermal stresses induced into the structures, projected daily maximum temperatures for the future years 2040, 2060, 2080 and 2100 were obtained from the coupled climate model GFDL CM3 from the National Oceanic Atmospheric Administration Geophysical Fluid Dynamics Laboratory. This study analyzed three distinct climate scenarios, known as Representative Concentration Pathway (RCP): the lower forcing scenario RCP 2.6 (more optimistic), a moderate scenario RCP 6.0 and the higher forcing scenario RCP 8.5 (worst case scenario). Following the structural assessment, an economic analysis involving different maintenance alternatives was conducted through a life cycle cost model that accounts for climate scenarios and the respective structural condition of the bridges. Maintenance cost savings were obtained through the implementation of IEV thresholds, since this approach addresses maintenance activities for bridges in need only (with IEV equal or greater than the established threshold), instead of applying the same treatment for all bridges. Therefore, this approach can be used in a preliminary assessment of SSSG bridges, considering climate change effects, to aid in establishing a priority order for bridge maintenance and planning for better allocation of funds, especially under budget constraints. The following conclusions can be drawn from the study:

- The impacts of climate change scenarios RCP 2.6, 6.0 and 8.5 are more distinguished after 2060. Thus, for a long-term analysis such as year 2100, the projected percentage of bridges failures are: 40% (RCP 2.6), 43% (RCP 6.0) and 67% (RCP 8.5).

- The analysis of SSSG bridges in the U.S. shows that the national average IEV increases linearly with the national average temperature range (ΔT) projected for 2040, 2060, 2080 and 2100, regardless the climate scenario (RCP's). Specifically, each 1°C increment added to ΔT (difference between the future temperature and the base temperature of bridge construction) increases the interaction equation by approximately 2%. Therefore, if expansion joints of SSSG bridges are not kept clean and thus functional, a continuous reduction of bridge integrity throughout the country over future years may occur.

- The most critical regions which present highest average IEV, regardless the RCP, are: Northern Rockies & Plains, Northwest, Upper Midwest and West. In contrast, the less susceptible regions are the Southeast followed by the Northeast. The regions of Southwest, South and Ohio Valley present intermediate level of structural vulnerability.

- A priority maintenance cost is proposed considering expansion joints cleaning only after a bridge presents IEV>0.85. This alternative presents savings on the order of $4.5 billion when compared with conventional maintenance practice, which does not consider climate scenarios and employ the same frequency of maintenance for all bridges.

The reason for the economic savings provided for any time-period and climate scenario is because the costs of expansion joints cleaning are applied only on bridges that have this necessity (determined by IEV), that is, those that exceed the selected threshold.

- Considering the best cost-effective alternative in long term analysis, the states that show the highest projected unit cost of maintenance (cleaning joints) are in general located in north, central and west regions of the country. Kansas ($452/m^2 for RCP 8.5), South Dakota ($439/m^2 for RCP 8.5), Wisconsin ($433/m^2 for RCP 8.5), North Dakota ($420/m^2 for RCP 8.5), Nebraska and Iowa ($410/m^2 for RCP 8.5) are the costliest states for all climate scenarios. In contrast, most of those states that present the lowest unit cost are in the east coast.

- One can note that there is in fact expected additional costs associated with climate change scenarios related to none or moderate actions to reduce emissions. The projected maintenance cost of the most cost-effective alternative (A1) for the time period 2020-2100 in present value under the climate scenario RCP 2.6 is $25.9 billion. Since RCP 2.6 simulates major actions to limit anthropogenic climate change, this is the most optimistic scenario. In case of moderate interventions, represented by RCP 6.0, the projected maintenance cost augments to $26.5 billion. Otherwise, for the worst-case scenario RCP 8.5, in which emissions continue to rise rapidly along the years, the projected maintenance cost increases to $27.9 billion.

Since the cost of RCP 2.6 hypothetically means the lowest cost of maintenance, this cost is taken as reference to calculate the costs difference between this and

the two other scenarios (RCP 6.0 and 8.5). Therefore, moderate actions over emissions implies an increase in $600 million, while no intervention at all results in an additional amount of $2 billion.

7.2 Recommendations for Future Studies

Complementary study is necessary to adapt and extend the proposed framework to the assessment of simply supported reinforced and prestressed concrete girder bridges. In addition, more refined analysis is needed to account for the indirect social and economic losses, which involve large variability of parameters such as required days for replacement, length of affected roadway, hourly driver cost, among others, in order to obtain a more comprehensive and precise assessment.

To address the uncertainties associated with climate models, further research might be conducted in order to create an ensemble of them. Also, future research on potential impacts of climate change can be extrapolated to other types of bridge design or regarding different nature of the impact such as increased floods frequency, that may cause scour on pier and abutment foundations.

REFERENCES

AASHTO. (2012). *LRFD Bridge Design Specifications* (Sixth). Washington, DC: American Association of State Highway Transportation Officials.

AISC. (2017). *Steel Construction Manual* (15th ed.). AISC.

ARTBA. (2018). Frequently Asked Questions—The American Road & Transportation Builders Association (ARTBA). Retrieved June 10, 2018, from https://www.artba.org/about/faq/

Asam, S., Bhat, C., Dix, B., Bauer, J., & Gopalakrishna, D. (2015). *Climate Change Adaption Guide for Transportation Systems Management Operations and Maintenance* (p. 86). Washington, DC: U.S. Department of Transportation - Federal Highway Administration. Retrieved August 8, 2018, from https://ops.fhwa.dot.gov/publications/fhwahop15026/index.htm

ASCE. (2014). *Maximizing the Value of Investiments Using Life Cycle Cost Analysis* (p. 25).

ASCE. (2017a). *Infrastructure Report Card 2017—Bridges* (Infrastructure Report Card) (pp. 1–4). ASCE. Retrieved June 10, 2018, from https://www.infrastructurereportcard.org/cat-item/bridges/

ASCE. (2017b). Report Card History. Retrieved August 20, 2018, from https://www.infrastructurereportcard.org/making-the-grade/report-card-history/

ASCE. (2019). COMMITTEE ON ADAPTATION TO A CHANGING CLIMATE.

Caltrans. (2015). Bridge Design Practice Manual BDP. Caltrans. Retrieved from http://www.dot.ca.gov/des/techpubs/manuals/bridge-design-practice/page/bdp-preface.pdf

Carroll Chris, & Juneau Andrew. (2015). Repair of Concrete Bridge Deck Expansion Joints Using Elastomeric Concrete. *Practice Periodical on Structural Design and Construction*, *20*(3), 04014038.

Chen, Q. (2008). Effects of thermal loads on Texas steel bridges. Retrieved July 30, 2018, from https://repositories.lib.utexas.edu/handle/2152/17802

Chen, W.-F., & Duan, L. (Eds.). (2000). *Bridge Engineering Handbook* (2 edition). CRC Press.

Childs, D. (2018). Temperature Effects in Bridge Decks [Tutorial for Temperature Effects in Bridge Decks]. Retrieved August 29, 2018, from http://www.bridgedesign.org.uk/tutorial/temptut.html#diag2i

Chinowsky, P., Helman, J., Gulati, S., Neumann, J., & Martinich, J. (2017). Impacts of climate change on operation of the US rail network. *Transport Policy*. Retrieved August 8, 2018, from http://www.sciencedirect.com/science/article/pii/S0967070X16308198

Connor, R. J., Hodgson, I. C., Mahmoud, H., & Bowman, C. (2005). *Field Testing and Fatigue Evaluation of the I-79 Neville Island Bridge Over the Ohio River—Final Report* (No. ATLSS 05-02). Bethlehem, PA: National Center for Engineering Research on Advanced Technology for Large Structural Systems.

CTT. (2017). Center for Technology & Training. Retrieved July 9, 2019, from http://ctt.mtu.edu/

Dunker, K. F., & Rabbat, B. G. (1993). Why America's Bridges Are Crumbling. *Scientific American*, *268*, 66–72.

Ferris, H. W. (1954). *Historical Record Dimension and Properties ROLLED SHAPES, Steel and Wrought Iron Beams & Columns, As Rolled in U.S.A., Period 1873 to 1952 With Sources as Noted*. American Institute of Steel Construction.

FHWA. (1995). *Recording and Coding Guide for the Structure Inventory and Appraisal of the Nation's Bridges* (No. FHWA-PD-96-001) (p. 124).

FHWA. (2002). Life-Cycle Cost Analysis Primer.

FHWA. (2017). National Bridge Inventory 2017—Bridge Inspection—Safety—Bridges & Structures—Federal Highway Administration. Retrieved July 23, 2018, from https://www.fhwa.dot.gov/bridge/nbi/ascii2017.cfm

FHWA. (2018a, Spring). Bridge Preservation Guide—Maintaining a Resilient Infrastructure to Preserve Mobility. FHWA. Retrieved from https://www.fhwa.dot.gov/bridge/preservation/guide/guide.pdf

FHWA. (2018b). Questions and Answers on the National Bridge Inspection Standards 23 CFR 650 Subpart C - National Bridge Inspection Standards—Bridge Inspection—Safety—Bridges & Structures—Federal Highway Administration. Retrieved September 7, 2018, from https://www.fhwa.dot.gov/bridge/nbis/index.cfm

FHWA. (2019). Bridge Replacement Unit Costs 2018. Retrieved June 28, 2019, from https://www.fhwa.dot.gov/bridge/nbi/sd2018.cfm

GFDL. (2019). Coupled Physical Model, CM3 [Text]. Retrieved August 8, 2018, from https://www.gfdl.noaa.gov/coupled-physical-model-cm3/

Hatfield, F. J. (2001). Engineering for Rehabilitation of Historic Metal Truss Bridges, (3), 6.

Hawk, H. (2003). *Bridge life-cycle cost analysis*. Washington, D.C: Transportation Research Board, National Research Council.

IPCC. (2014). *Climate Change 2014 Synthesis Report Summary for Policymakers*.

Kelly, A. L. (2017). *LIFE CYCLE COST ANALYSIS FOR JOINT ELIMINATION RETROFITS AND THERMAL LOADING ON COLORADO BRIDGES*. Colorado State University.

Lichtenstein, A. G. (1993). The Silver Bridge Collapse Recounted. *Journal of Performance of Constructed Facilities*, *7*(4), 249–261.

Mahmoud, H. N. (2017). Upgrading our infrastructure: Targeting repairs for locks, dams and bridges. Retrieved June 9, 2018, from http://theconversation.com/upgrading-our-infrastructure-targeting-repairs-for-locks-dams-and-bridges-69748

Mahmoud, H. N., Chulahwat, A., & Irfaee, M. (2018). Inspection Intervals for Fracture-Critical Steel Bridges Based on Fatigue and Fracture Life-Cycle Cost Assessment. In *Proceedings of World Steel Bridges Symposium 2018* (p. 10). National Steel Bridge Alliance.

Marques Lima, J., & de Brito, J. (2009). Inspection survey of 150 expansion joints in road bridges.

MDOT. (2018). Michigan.gov. Retrieved from https://search.michigan.gov/AppBuilder/search?utf8=%E2%9C%93&id=&type=&ctx=SO

M&q=2017_BRIDGE_SCOPING_COST_ESTIMATE_WORKSHEETS_550685_7_1_607073_7&button=search

NASA. (2019). The Causes of Climate Change. Retrieved from https://climate.nasa.gov/causes/

National Academy of Engineering. (2018). NAE Grand Challenges for Engineering. Retrieved from http://www.engineeringchallenges.org/9136.aspx

NOAA. (2018). Climate at a Glance | National Centers for Environmental Information (NCEI). Retrieved July 24, 2018, from https://www.ncdc.noaa.gov/cag/regional/mapping/-1/tavg/201706/12/value

NOAA. (2019). Climate Modeling.

Olsen, J. R. (2015). Adapting Infrastructure and Civil Engineering Practice to a Changing Climate—Committee on Adaptation to a Changing Climate. ASCE.

Peduzzi, P. (2017). Flooding: Prioritizing protection? *Nature Climate Change*, *7*(9), 625–626.

Rager, K. (2016). *Thermal Loading Analysis in Plate Girder Bridge Using Health Monitoring And Finite Element Simulations*. Colorado State University, Fort Collins, CO.

Rogers, C. E., Bouvy, A., & Schiefer, P. (2012). *Alleviating the Effects of Pavement Growth on Structures* (Region Bridges Support Unit) (p. 14). Michigan Department of Transportation (MDOT).

Ruddy, J. L., & Ioannides, S. A. (2004). Rules Of Thumb For Steel Design (pp. 1–7). American Society of Civil Engineers. Retrieved July 31, 2018, from http://ascelibrary.org/doi/abs/10.1061/40700%282004%29173

Salmon, C. G., & Johnson, J. E. (1996). *Steel Structures: Design and Behavior* (Fourth). New York: Harper Collins. Retrieved July 22, 2018, from https://www.amazon.com/Steel-Structures-Design-Behavior-Fourth/dp/B001KY7VP2

TRB. (2008). *Potential Impacts of Climate Change on U.S. Transportation* (No. Special Report 290) (p. 280). Washington, DC: Committee on Climate Change and U.S Transportation - Transportation Reserach Board - Division on Earth and Life Studies.

Underwood, B. S., Guido, Z., Gudipudi, P., & Feinberg, Y. (2017). Increased costs to US pavement infrastructure from future temperature rise. *Nature Climate Change*, *7*(10), 704–707.

Vasdravellis, G., Uy, B., Tan, E. L., & Kirkland, B. (2015a). Behaviour and design of composite beams subjected to sagging bending and axial compression. *Journal of Constructional Steel Research*, *110*, 29–39.

Vasdravellis, G., Uy, B., Tan, E. L., & Kirkland, B. (2015b). Behaviour and design of composite beams subjected to sagging bending and axial compression. *Journal of Constructional Steel Research*, *110*, 29–39.

Wardhana, K., & Hadipriono, F. C. (2003). Analysis of Recent Bridge Failures in the United States, 7.

Wells, D., Meade, B. W., Hopwood, T., & Palle, S. (2017). A Programmatic Approach to Long-Term Bridge Preventive Maintenance.

Wuebbles, D. J., Fahey, D. W., Hibbard, K. A., Dokken, D. J., B.C. Stewart, & Maycock, T. K. (2017). *Climate Science Special Report: Fourth National Climate Assessment, Volume I* (p. 470). Washington, DC, USA: USGCRP.